Molecular Characterization of NFAT Transcription Factors in Experimental Mouse Models

Molekulare Charakterisierung von NFAT-Transkriptionsfaktoren in experimentellen Mausmodellen

PhD thesis submitted as a partial fulfillment of requirements for the PhD degree at the Graduate School of Life Sciences, Julius-Maximilians- Universität Würzburg,
Section Infection and Immunity

Submitted by
Hani Gouda Alsaid Alrefai
from
El-Mansoura, Egypt

Würzburg, 2014

„Gedruckt mit Unterstutzung des Deutschen Akademischen Austauschdienstes“

Submitted on: ……..……..

Office stamp

Members of the *Promotionskomitee*:

Chairperson:

Primary Supervisor: Prof. Dr. Edgar Serfling

Supervisor (Second): Prof. Dr. T. Müller

Supervisor (Third): Prof. Dr. A. Müller

Date of Public Defence:

Date of receipt of Certificates:

Affidavit

I hereby declare that my thesis entitled "**Molecular Characterization of NFAT Transcription Factors in Experimental Mouse Models**" is the result of my own work. I did not receive any help or support from commercial consultants. All sources and / or materials applied are listed and specified in the thesis.

Furthermore, I verify that this thesis has not yet been submitted as part of another examination process neither in identical nor in similar form.

Würzburg……

Date Signature

Eidesstattliche Erklärung

Hiermit erkläre ich an Eides statt, die Dissertation „**Molekulare Charakterisierung von NFAT-Transkriptionsfaktoren in experimentellen Mausmodellen**" eigenständig, d.h. insbesondere selbstständig und ohne Hilfe eines kommerziellen. Promotionsberaters, angefertigt und keine anderen als die von mir angegebenen Quellen und Hilfsmittel verwendet zu haben.

Ich erkläre außerdem, dass die Dissertation weder in gleicher noch in ähnlicher Form bereits in einem anderen Prüfungsverfahren vorgelegen hat.

Würzburg……

Datum Unterschrift

"Among Allah's worshipers, those who have the most knowledge, fear him the most"

Surat Fater, Vers 28, The Holly Qurraan.

Acknowledgments

I would like to thank my supervisor, Prof. Dr. Edgar Serfling, for his advice and guidance. His availability at all time made it possible to go through my work, knowing that he got my back. I enjoyed working with him side by side on the bench. His famous question –with a full smile on his face- 'Why not do it today?', kept me running and was needed to get me where I am standing today. I would also like to thank my other supervisors, Prof. Dr. T. Müller and Prof. Dr. A. Müller for their valuable time and input. I am much obliged to Prof. Dr. Thomas Hünig for the excellent learning experience he provides in the graduate college GK520 "Immunomodulation" I am grateful to all the GSLS members, especially Gabriele, Bianca, Jennifer, Susanne and Rose for their friendly help and support.

I am very grateful to Doris and Ilona for their help with the cells and mice. I would like to thank Rhoda, Ron and Amiya, for introducing me to FACS. I cannot forget to acknowledge Jolly and Sankar for taking my hand into establishing my own WB protocol. I thank Khaled for his help and support. I would like to thank Stefan for his advice on EMSA and helping me with the 'Zusammenfassung'. I thank Andris for his continuous support in primer design. I enjoyed my scientific and social talks with Martin and for this I am thankful to him. I want to extend my regards to Rike, Lena, Tobi and Duong for being there as a pushing force. It would have been more difficult for me without Angelika, our department secretary, helping me in all the formal paper work. I sincerely thank Dr. Puppe –for IT support-, Mr. Ralf –for Immunohistochemistry support- and Mr. Schmitt –for his lovely clear pictures-.

I am very much indebted to the Egyptian government and DAAD (Egypt and Germany teams) for providing the funds and the support that gave me the chance to conduct my PhD studies in Germany.

No words can describe my deep gratitude to Shereen, my wife. Her endless caring carried me every step of the way and whom without I could never had came this far. I thank my children: Ahmed, Hesham and Malak for always painting a smile on my heart.

Most of all, I would like to acknowledge my debt to my parents. Their vision and love always paved the way and their prayers blessed my life.

Contents

List of Figures:

Summary

In this work we wanted to investigate the role of NFATc1 in lymphocyte physiology and in pathological conditions (eg. psoriasis). NFATc1 is part of the signal transduction pathways that regulates B cells activation and function. NFATc1 has different isoforms that are due to different promoters (P1 and P2), polyadenylation and alternative splicing. Moreover, we tried to elucidate the points of interactions between the NFAT and the NF-κB pathways in activated B-cell fate. NFAT and NF-κB factors share several properties, such as a similar mode of induction and architecture in their DNA binding domain. We used mice which over-express a constitutive active version of NFATc1/α in their B cells with -or without- an ablated IRF4. IRF4 inhibits cell cycle progression of germinal center B cell-derived Burkitt's lymphoma cells and induces terminal differentiation toward plasma cells. Our experiments showed that a 'double hit' in factors affecting B cell activation (NFATc1 in this case) and late B cell differentiation (IRF4 in this case) alter the development of the B cells, lead to increase in their numbers and increase in stimulation induced proliferation. Therefore, the overall picture indicates a link between these 2 genes and probable carcinogenic alterations that may occur in B cells.

We also show that in splenic B cells, c-Rel (of the NF-κB canonical pathway) support the induction of NFATc1/αA through BCR signals. We also found evidence that the lack of NFATc1 affects the expression of Rel-B (of the NF-κB non-canonical pathway). These data suggest a tight interplay between NFATc1 and NF-κB in B cells, influencing the competence of B cells and their functions in peripheral tissues.

We also used IMQ-induced psoriasis-like inflammation on mice which either lack NFATc1 from B cell. Psoriasis is a systemic chronic immunological disease characterized primarily by abnormal accelerated proliferation of the skin keratinocytes. In psoriasis, the precipitating event leads to immune cell activation. Our experiments showed that NFATc1 is needed for the development of psoriasis. It also showed that IL-10 is the link that enables NFAT from altering the B cell compartment (eg Bregs) in order to affect inflammation. The important role of B cell in psoriasis is supported by the flared up psoriasis-like inflammation in mice that lack B cells. Bregs is a special type of B cells that regulate other B cells and T cells; tuning the immunological response through immunomodulatory cytokines.

Zusammenfassung

Diese Arbeit befasst sich mit der Regulation und der Funktion des Transkriptionsfaktors NFATc1 (“nuclear factor of activated T-cells c1) in B-Lymphozyten. Hierzu wurde zum einen die transkriptionelle Kontrolle des *Nfatc1*-Gens in aktivierten B-Lymphozyten und zum anderen die Bedeutung dieses Faktors für die Wachstumskontrolle und Autoimmunität anhand verschiedener Modellsysteme analysiert.

Sechs verschiedene NFATc1-Isoformen können in B-Lymphozyten durch die Nutzung zweier verschiedener Promotoren, zweier Polyadenylierungsstellen und eines alternativen Splicings generiert werden. Wir zeigen hier, dass insbesondere die NF-kB Faktoren c-Rel und p50 eine essentielle Bedeutung für die starke Induktion des Promoters P1 und damit der Expression der kurzen Isoform NFATc1αA in B-Zell-Rezeptor-stimulierten B-Zellen spielen. Interessanterweise zeigen NFATc1-defiziente B-Lymphozyten eine geschwächte Aktivierung der NF-kB-Faktoren, was auf eine enge Verknüpfung dieser zwei Signalwege hindeutet.

NFATc1-defiziente B-Lymphozyten weisen eine Aktivierungs- und Wachstumsschwäche auf (Bhattacharyya S., et.al.). Hier zeigen wir, dass die Überexpression von konstitutiv aktivem NFATc1αA in B-Lymphozyten, insbesondere wenn dies im Kontext einer IRF4-Defizienz geschieht, zu einer verstärkten Expansion der B-Zellpopulation, insbesondere nach deren Aktivierung, führt. Dies belegt die kritische Bedeutung, die der wohldosierten Expressions- und Aktivierungskontrolle der NFATc1-Faktoren in B-Lymphozyten zukommt.

Dies zeigt sich auch in einem Imiquimod-induziertem Psoriasis Mausmodell. Hier wird durch Applikation von Imiquimod auf die Haut eine der Schuppenflechte ähnelnde entzündliche Reaktion ausgelöst, die insbesondere durch eine stark verstärkte Proliferation der Keratinozyten gekennzeichnet ist. Wir können zeigen, dass die NFATc1-Faktoren in B-Lymphozyten kritisch an dieser Reaktion beteiligt sind. Fehlt den B-Lymphozyten das NFATc1-Gen, so produziert eine Subpopulation, die sogenannten regulatorischen B-Zellen, verstärkt das immunmodulatorischen Zytokins IL-10, wodurch die entzündliche Reaktion fast komplett unterdrückt wird. Dies ähnelt vorhergehenden Beobachtungen, in denen wir zeigen konnten, dass auch in einem Mausmodell der Multiplen Sklerose (EAE) die Immunreaktion durch den Verlust von NFATc1 in B-Zellen erheblich gelindert werden kann (Bhattacharyya S., et.al.).

1. Introduction

1.1. Nuclear factors of activated T lymphocytes (NFATs)

1.1.1. Family and structure

The name of NFAT comes from its first discovery in T cells as a transcription factor (TF) that binds to the IL-2 DNA promoter region following the activation of the TCR (Serfling et al., 1989; Shaw et al., 1988). This name was sustained, although, studies have shown that this TF family is expressed in many cell types other than T cells. NFAT gained more interest after discovering that it is negatively regulated by Cyclosporin A (CsA). At that time, CsA was the new "dream drug" for improvement of transplantation medicine as an immune suppressor against organ rejection. The identification of the NFAT family and their isoforms was followed giving rise to 5 NFAT members, but only 4 of them are considered typical and are part of the Ca-Calcineurin pathway (NFATc1, c2, c3 and c4). NFATc5 is regulated by osmotic stress and is considered a kind of evolutionary link between the NFAT family and the NF-κB family. The typical NFAT members have different isoforms that come from different promoters (P1 and P2), polyadenylation and alternative splicing, differing in the C or/and N terminals. The Rel-Similarity domain (RSD) is the DNA binding domain and its name comes from its similarity to the DNA binding site in the older NF-κB family. The NFAT similarity Domain (NSD) contains the regulatory domain (REG) that is rich of serine residues. There is about 70% similarity in the RSD among the typical NFAT members that falls to only 40% with the NFATc5. NFATc5 lacks the REG domain (Chen et al., 1998; Chuvpilo et al., 1999; Lopez-Rodriguez et al., 1999).

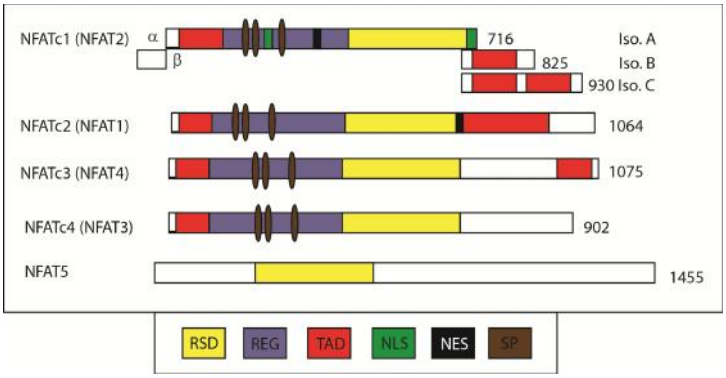

Figure 1.1: NFAT family members.
All five NFAT family members are shown with their different structures. NFATc1 is shown with its diffrent isoforms. Ca2+-dependent regulatory domain (REG) is in violet. The highly conserved Rel-similarity domain ,RSD, is in yellow. The transactivation domains (TADs) are marked in red. Brown ellipses mark the serine-pro(SP) 1-3 motifs. Nuclear localization signal (NLS) domains are in green. Nuclear export signal (NES) domains are in white. Modified from (Serfling et al., 2006b).

1.1.2. Activation

At the basal state, NFAT factors are located in an inactive form in the cytoplasm. The rise of the intracellular calcium is the corner stone of the NFAT activation cascade. The engagement of the BCR or TCR or other surface receptors in the immune cells (eg. Toll like receptors (TLR)) leads to activation of the phospholipase C (PLC) enzymes (eg. PLCγ). PLC cleaves phosphoinositoidbiphospate (PIP2) into diacylglycerol (DAG) and inositoltriphosphate (IP3). IP3 binds to its specific receptors in the endoplasmic reticulum (ER) leading to release of the intracellular calcium stores. The depletion of these stores stimulates ER stromal interaction molecules (STIM1 & STIM2) which induce a conformational change in the calcium-release activated calcium channels (CRAC) protein Orai1, opening of the channel and leading to influx of calcium from the extracellular compartment (Hogan et al., 2010). Calcium binds to calmodulin, then the Ca++/calmodulin complex activates calcineurin (serine/threonine specific phosphatase).

Activation of calcineurin is rate-limiting for NFAT activation in all cells. Calcineurin dephosphorylates the serine pro motifs (SP) that are mainly located in the REG domain (18 out of the 20 identified), exposing the NLS domain leading to nuclear transfer of the NFAT. NFAT bind to specific DNA sequence and promote transcription in association with other transcription factors. When Calcineurin is inhibited , nuclear kinases re-phosphorylate NFAT leading to its transfer back to the cytoplasm. Different scaffold proteins have been shown to interact with NFAT proteins and to be involved in the regulation of their activity (Li et al., 2011).

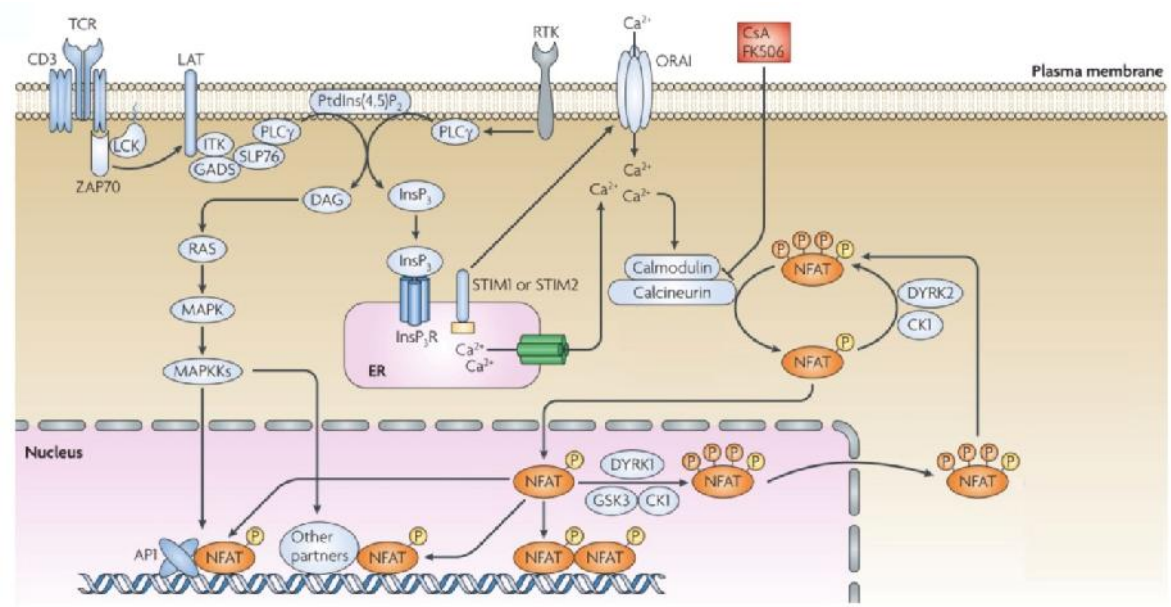

Figure 1.2: NFAT Activation cascade
Immunoreceptors and receptor tyrosine kinases (RTKs) bind to their ligands and activate the phospholipase Cγ (PLCγ). Inositol-1,4,5-trisphosphate (InsP3) binds to the InsPR on the endoplasmic reticulum (ER) membrane and induces the efflux of Ca^{++}. Stromal interaction molecules (STIMs) communicate with the calcium-release activated calcium (CRAC) channel protein ORAI in the plasma membrane. Ca^{++} binds to the calcium sensor protein calmodulin, which in turn activates calcineurin. Calcineurin dephosphorylates and activates NFAT transcription factors, which then translocate to the nucleus, where they can cooperate with multiple transcriptional partners (for example, activator protein 1 (AP1)) to regulate gene expression. NFAT proteins are rephosphorylated and inactivated by multiple NFAT kinases. Adapted from (Muller and Rao, 2010).

1.1.3. Genetics of NFATc1

The murine and human NFATc1 genes are highly conserved. The NFATc1 genes span 110-140kb long, extending over 11 exons. The transcription of Nfatc1 genes are controlled by two different promoters (P1 and P2). The P1 promoter is an inducible promoter that comes in action with engagement of the immune receptors (e.g. TCR, BCR …etc.). The P2 promoter is a constitutively active promoter that is serving under resting conditions. The products of these two promoters are further processed by alternative splicing and polyadenylation machinery giving six known different isoforms with individual functions (Serfling et al., 2012). Specific for the NFATc1/A, is the autoregulation that is exhibited by the binding of the NFAT factors to the κB/NFAT site (at position −720 within the distal homology of P1) and NFAT−90 (within the proximal P1 promoter region). It was suggested that binding of the NFATc1 to this site produces positive regulatory effects while binding of the NFATc2 produces a negative regulatory effect on NFATc1/αA expression (Chuvpilo et al., 2002).

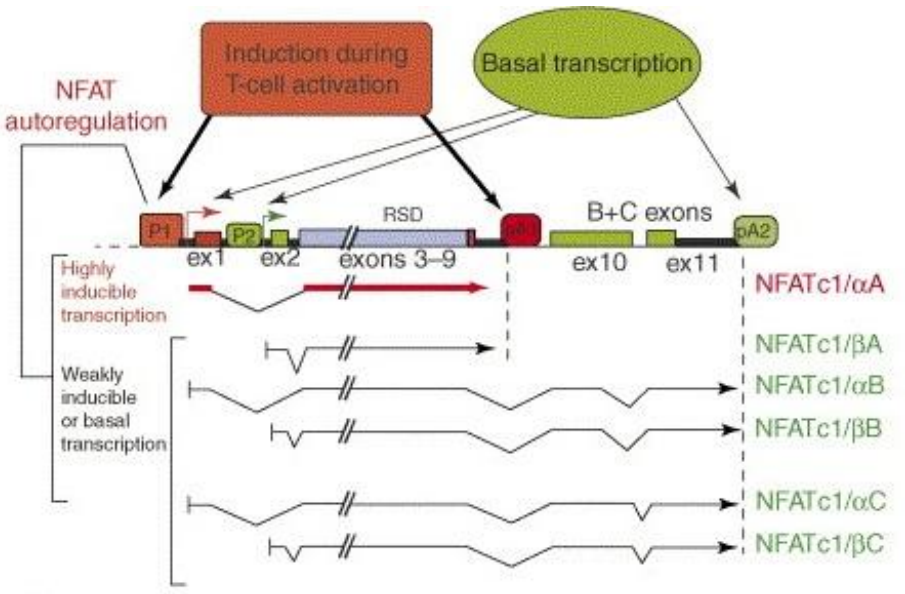

Figure 1.3: Illustration of the Nfatc1 gene and its expression products
The transcription of *Nfatc1* is directed by two alternative promoters, the inducible P1 promoter and the relatively constitutive P2 promoter, which together with alternative splicing and polyadenylation events are giving rise to six known different isoforms. pA1 is a weak polyadenylation site, which is used to terminate the short isoforms α/A and β/A. pA2 is a strong polyadenylation site, which is used to terminate the long isoforms B and C. Based on (Chuvpilo et al., 2002).

1.1.4. Functions

NFATc1 and NFATc2 regulates FOXP3 expression in iTReg cells by binding regulatory elements in the Foxp3 gene (Zheng et al., 2010). Constitutive NFATc1 is important to sustain the expression of IL-17A in CD4+ T cells (Gomez-Rodriguez et al., 2009). NFATc2 is preferentially required for CD8 peripheral tolerance, although it is not required for CD4 tolerance or their regulatory effect on CD8 T cells functions (Fehr et al., 2010). NFATc1 is one of the prerequisites for the B-1a cells development (Berland and Wortis, 2003). NFATc1 is part of the signal transduction pathways that regulates B cells activation and function (Haylett et al., 2009; Winslow et al., 2006). NFATc2 is important for the function of dendritic cells (DCs) and megakaryocytes (Crist et al., 2008; Zanoni et al., 2009). NFATs are essential in the development of muscles (cardiac , skeletal and smooth) nervous system, vascular system , skeleton and skin (Hogan et al., 2003; Horsley et al., 2008; Negishi-Koga and Takayanagi, 2009).

1.2.NF-κBs

1.2.1. Family and structure

The first description of this family of TFs was for B cells (Sen and Baltimore, 1986). The family members are the Rel proteins: RelA (p65), RelB, c-Rel and NF-κB1(p50) and NF-κB2(p52). The p50 and the p52 proteins are the processing products of the p105 and p100 precursor proteins respectively. This activation is mediated by the ubiquitin/proteasome pathway (Nabel and Verma, 1993). The NF-κB factors are present in a functional dimeric unit which maybe a homodimeric or a heterodimeric complex. All NF-κB members can form homodimers, except RelB (Ghosh et al., 1998). The most common pairs of active NF-κB are RelA-p50 (canonical pathway) and RelB-p52 (non canonical pathway). All five NF-κB proteins contain the Rel homology domain (RHD) which is responsible for DNA binding, dimerization and nuclear translocation. The RHD spans 300-amino-acids and is highly conserved. The Rel family members also contain a transactivation domain that is responsible for the activation of promoters and enhancers of numerous other genes (Li and Verma, 2002).

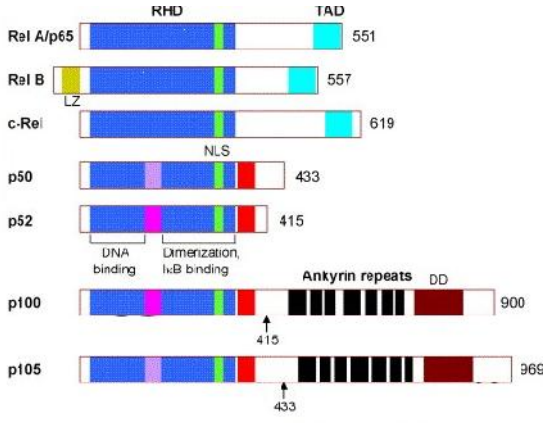

Figure 1.4: NF-κB family members
Schematic representation of members of NF-κB family. The processing sites for p100 and p105 are also indicated by an arrow. The numbers of amino acids spanning each protein are listed on the right. The abbreviations used are: RHD, rel homology domain; TAD, transactivation domain; NLS, nuclear localization sequences; NES, nuclear export sequences; DD, death domain, also dubbed as PID, processing inhibitory domain; LZ, leucine zipper adapted from (Xiao et al., 2006).

1.2.2. Activation

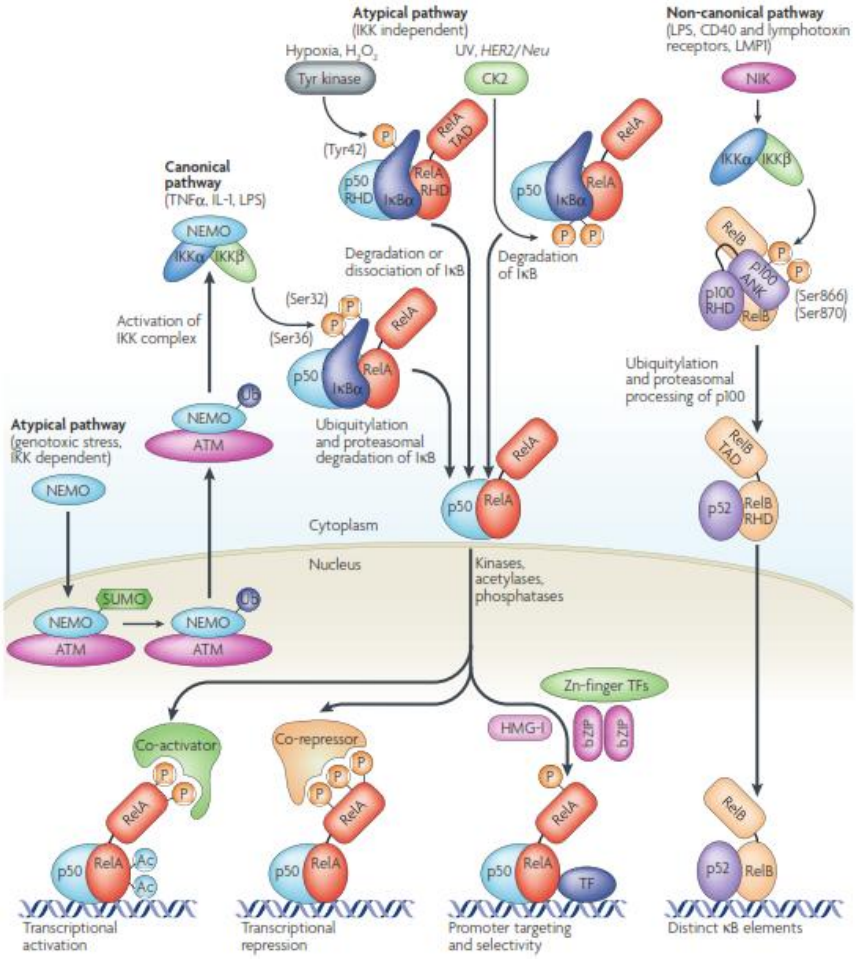

Figure 1.5: Pathways leading to the activation of NF-κB

The figure illustrates the different activation pathways for NF-κB in response to different stimuli. The canonical (atypical and typical) and non canonical pathways are shown. Abbreviations: Ac, acetylation; bZIP, leucinezipper-containing transcription factor; HMG-I, high-mobility-group protein-I; IκB, inhibitor of κB; IKK, IκB kinase; LMP1, latent membrane protein-1; LPS, lipopolysaccharide; NF-κB, nuclear factor-κB; RHD, Rel-homology domain; TAD, transcriptional activation domain; TF, transcription factor; UV, ultraviolet; Zn-finger TF, zinc-finger-containing transcription factor. Adapted from: (Perkins, 2007)

The most common activation pathway of NF-κB is the canonical pathway. This is due to the fact that it can be induced through different external stimuli and receptors leading to highly variable forms of NF-κB subunits with various functions. The typical activation is IKK dependent and starts by TNFα, TCR, BCR or TLRs. These receptors when engaged lead to activation of NEMO (NF-κB essential modifier) in the IKK complex and causes phosphorylation of the IκBα at Ser23 and Ser36 and their subsequent ubiquitylation and degradation. At the end several forms of the NF-κB dimers are formed based on the contribution of all NF-κB members (Perkins, 2006).

Another atypical, though IKK dependent, activation of the canonical pathway is that in response to genotoxic stress. NEMO is shuttled into the nucleus and is sumoylated and then ubiquitylated under the control of the ataxia telangiectasia mutated checkpoint kinase (ATM). After that, the NEMO-ATM complex is shuttled back to the cytoplasm where it activates the IKK complex. The atypical IKK independent pathways relies on two players to induce the degradation of IκBα: CK2 (casein kinase-II) and TyrK (tyrosine dependent kinase) (Krappmann and Scheidereit, 2005). The non-canonical pathway is stimulated through CD40 ligands, TLRs, lymphotoxin receptors and others. These stimuli leads to activation of the IKKα through NIK (NF-κB inducing kinase). The active IKKα leads to 26S proteosome-mediated modification of p100. At the end the active p52-RelB dimmer is formed which binds to distinct κB DNA motifs (Moorthy et al., 2006).

1.2.3. Function and dysfunction

The NF-κB family is widely distributed in many cells of the body. Studies have shown that they are important for embryogenesis and normal development of tissues (Carrasco et al., 1994). They control and share in regulating many fundamental processes of the body; as cell survival, cell proliferation, immunity (adaptive and innate) and memory (Lai et al., 2010; Mao et al., 2009). Also, they act as mediators of cellular responses against stress of different nature: chemical (eg. free radicals), physical (UV) and biological stress (bacteria and virus) (Kim et al., 2008; Murley et al., 2001; Muthusamy and Piva, 2010). The NF-κB pathway is integrated into other signal transmission pathways in the cell and performs many interactions to finely tune cell homeostasis. Cell survival is moderated by fine tuning the activity of the NF-κB versus the JNK pathway (Resch et al., 2009). Cell response to genotoxicity is a product of cross talk between the NF-κB and the p53 pathways (Heyne et al., 2013). Hormonal mechanisms of action are affected by collobaration of the NF-κB pathway with nuclear receptors (Greene et al., 2010). In B cells, NF-κB mediate signals initiated through the BCR that contribute to their final stages of maturity as well as early developmental stages (Balkhi et al., 2012). Therefore, its easily predictable that dysfunction of the NF-κB pathway leads to severe defects in B cell development and to B cell oncogenesis (Staudt, 2010).

1.3.B cells

1.3.1. B cells development and activation

The development of B cells starts in fetal life in the fetal liver. It continues postnatal in the bone marrow and peripheral lymphoid organs (PLO), like the lymph nodes (LN) and spleen (LeBien, 2000). The B cells pass through two main stages of development: antigen-independent (Pro B cell, Pre B cell, immature B cell and naïve B cell; in the BM) and antigen-dependent (B cell activation, Memory B cell and plasma B cell; in the PLO) (LeBien and Tedder, 2008). In the antigen-independent stage the B cell repertoire is built by V(D)J rearrangement. B cells from this stage can react against virtually any possible antigen that they could encounter and that is why they need to be re-tuned by central tolerance to avoid auto reactivity. The central tolerance is achieved by B cell receptor (BCR) editing and clonal deletion (Menard et al., 2013).

The B cell leaves the BM and travel to the PLO through the blood where it reaches maturity and expresses IgD too. It is then faces the second Check-point for auto reactivity where failed cells are eliminated by apoptosis or anergy (Isnardi et al., 2008). B cell activation may occur as a result of interaction with T cells (T cell dependent activation) or in absence of any signals from T cells (T cell independent activation). In the T cell dependent activation, the B cells encounter the antigen peripherally then migrate to the PLO where they interact with T cells that were exposed to the same antigen and the immunological synapse results in a full blown B cell differentiation cascade specific for this antigen. In T cell independent activation the secondary activation may come from TLR (Type 1) or from a multivalent binding of BCR, that could happen with some bacterial carbohydrate antigens (Type 2) (Briney and Jr, 2013).

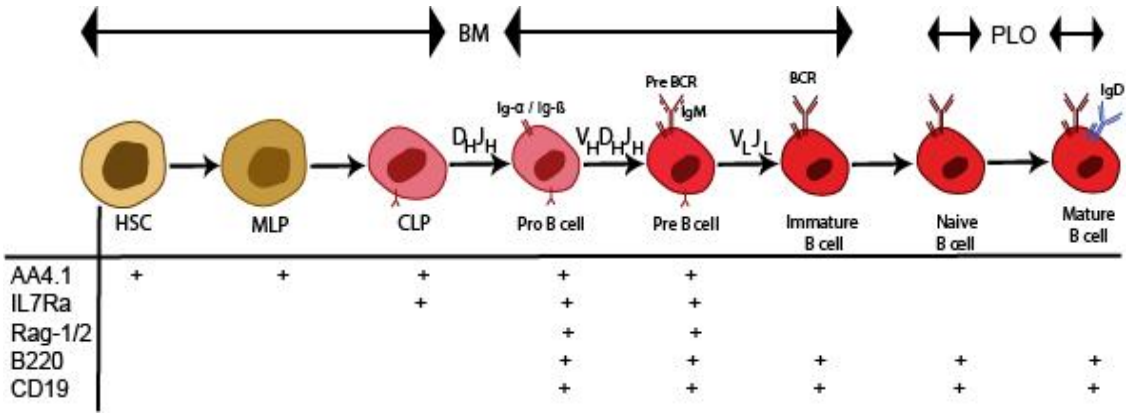

Figure 1.6: Stages of B cell development.
Diagram of B lineage development from hematopoietic stem cells (HSC) in mouse bone marrow through multilineage progenitor (MLP) and common lymphoid progenitor (CLP) to B cell committed stages showing cell surface phenotype, expression of B-lineage genes and of mu heavy chain and kappa light chain. Based on (Hardy and Hayakawa, 2001).

1.3.2. B cell types

B cells could be classified according to their role in immunity into B1 and B2. B1 cells are part of the innate immune system. They are less common, do not form memory cells and found mainly in the serous cavities like the peritoneum and the pleura (Ghosh et al., 2012). B2 cells are the more common type, sharing in adaptive immunity through their high diversity coming from their ability to undergo somatic hyper-mutation and class switching. B2 cells are found mainly in the peripheral lymphoid organs and can be differentiated mainly from B1 cells by lack of surface expression of CD5 and the higher expression of IgD, IgG and IgA (Suzuki et al., 2010).

The germinal centers of peripheral lymphoid organs are the site of the T cell dependent B cell activation. They are delineated into dark and light zones. In the PLO two distinct populations of B cells could be recognized. The Follicular B cells (FO) which is the dominant population (95%) with a $CD23^{hi}$ $CD21^{low}$ pattern (McHeyzer-Williams and McHeyzer-Williams, 2005). They are freely circulating with a higher stimulation threshold. On the other hand, the marginal zone B cells (MZ) are a small population of residential B cells characterized by their $CD23^{low}$ $CD21^{hi}$ pattern (Pillai et al., 2005).

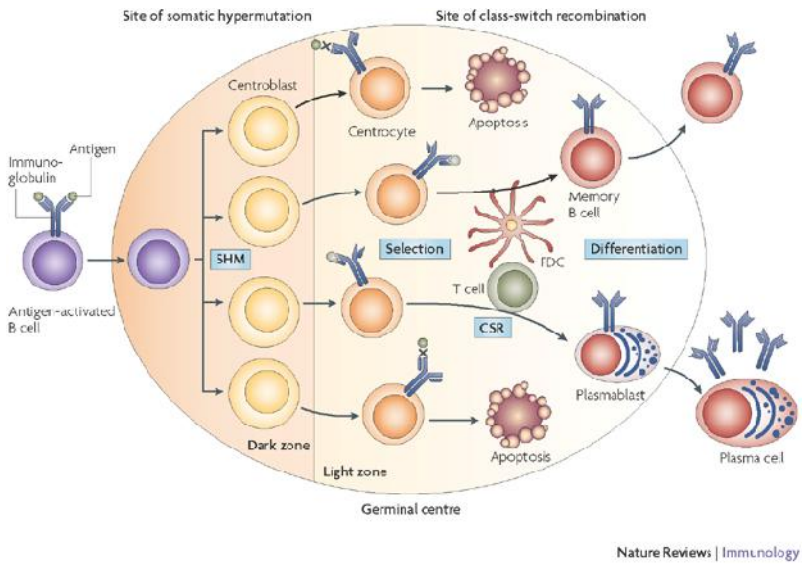

Figure 1.7: The germinal center.
B cells activated by antigens are transformed to centroblasts. These centroplast prolifrate , expand and undergo somatic hypermutation (SHM). The centroblasts moves into the light zone and transform to centrocytes. T cells and follicular dendritic cells (FDCs) select the most competent of the centrocytes which differentiate into memory B cells or plasma cells, while the centrocytes that have an unfavourable antibody are deleted by apoptosis. Adapted from (Klein and Dalla-Favera, 2008)

1.3.3. B cell functions

B cells share directly in the immune response by differentiating into Ag-specific antibody producing cells (plasma cells) (LeBien and Tedder, 2008). They become part of the memory immune response because they also differentiate to memory B cells which ensures a more efficient and faster secondary immune response (Price and Luftig, 2014). They can indirectly share in the immune reaction either positively by serving as a professional antigen presenting cells to CD8+ T cells or negatively through producing IL-10 (DiLillo et al., 2010; Salerno-Goncalves et al., 2014). Moreover, B cells serve as a co-activator of T cells during immune response through CD80, CD86 and OX40L interactions (O'Neill et al., 2007).

1.3.4. Regulatory B cells (Bregs)

Bregs are one of the newly introduced subtypes of B2 cells. They are a small population of $CD5^{+}CD1d^{hi}$ B cells that are able to express and excrete IL-10 when stimulated (Yanaba et al., 2008). The development of these Tregs are dependent on BCR, TLR and CD22 signals (Tedder et al., 2005). They are believed to have a regulating

influence on other B cells and T cells; tuning the immunological response in a concept similar to Tregs but exploiting other immunomodulatory cytokines (Yanaba et al., 2009). They serve to keep the immune response in check in case of auto immune diseases and in case of fulminate inflammatory conditions. Their effects are reported on Th1, Th17, $CD4^+$ T cells and Monocytes (Mauri and Bosma, 2012).

1.3.5. Role of interferon regulatory factor 4 (IRF4) in B-cell development

IRF4 plays a critical and non-redundant role in the adaptive immune responses of mature B cells. Without IRF4, mature B cells accumulate in increased numbers in the spleen and lymph node, although there is a quantitative defect in the percentage of IgM^{hi}, IgD^{lo}, $CD23^{lo}$ mature B cells (Shaffer et al., 2009).

IRF4 is up-modulated by CD40 engagement, and down-modulated by apoptotic and anti-proliferative signals, suggesting involvement of IRF4 in Hodgkin lymphoma pathobiology (Aldinucci et al., 2010).

IRF4 inhibits cell cycle progression of germinal center B cell-derived Burkitt's lymphoma cells and induces terminal differentiation toward plasma cells through mechanisms independent of BCL6 downregulation (Teng et al., 2007).

1.4. Psoriasis

1.4.1. Burden of Psoriasis

The area of the skin is about 1.8 square meters in total making it the largest organ of the human body. It is part of the immune system and considered as the first line of protection against microbes and foreign agents. It consists of two main layers: the epidermis (the upper layer) and the dermis (the lower layer). The hypodermis may refer to a third layer of of subcutaneous fat and connective tissue lying even deeper to the previous layers.

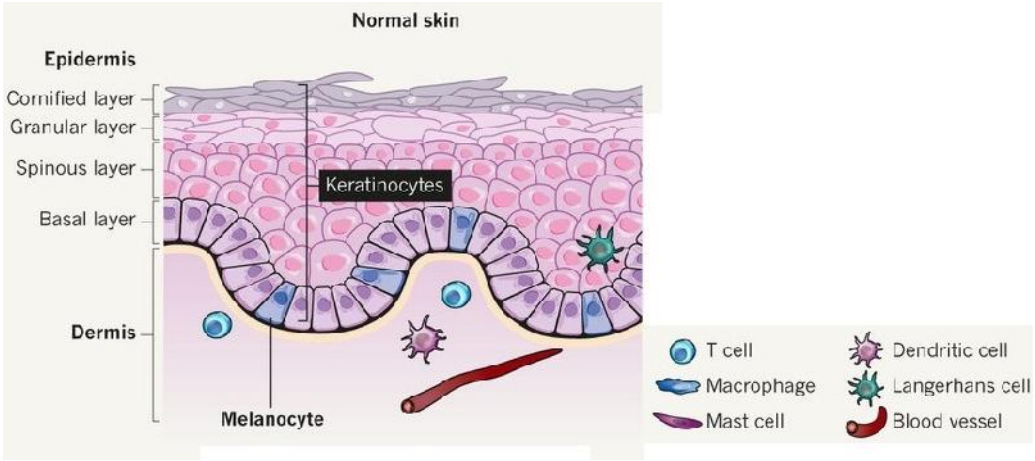

Figure 1.8: Normal skin
The normal skin of human consists of two main layers. The epidermis is the upper layer of the skin and it consists mainly of keratinocytes. The basal layer of epidermis is the one responsible of division and regeneration of all the upper cells. The spinous layer lies above the basal layer. Keratinocytes in the spinous layer are polygonal and held together by desmosomes. The granular layer is the last living layer of the keratinocytes lying above the spinous layer and below cornified layer. It is a thin layer of cells that contain keratohyalin granules, which are filled with proteins that promote hydration and cross-linking of keratin. The cornified layer is a layer of dead and hardened remnants of the keratinocytes after losing most of their nuclei. The dermis is the lower layer of the skin. It is a layer of connective tissue consisting of a mixture of collagen fibers and elastic fibers, embedded in proteoglycans. It contains hair follicles, vessels (blood and lymphatic) and glands (sweat and sebaceous). Small numbers of antigen presenting cells (dendritic cells or macrophages) and lymphocytes (T or B cells) is present in the epidermis and the dermis adapted from (Crow, 2012).

Psoriasis is a systemic chronic immunological disease characterized primarily by abnormal accelerated proliferation of the keratinocytes in the epidermal layer of the skin. Although the main feature of the psoriasis is the pathognomonic silver, scaly, raised and inflamed skin patches, the disease is connected to a number of complications related to other organs such as the joints, heart, liver and lungs.

In the United States the incidence of psoriasis is 200,000 cases each year. The majority of these cases present before the age of thirty five (Enamandram and Kimball, 2013). In European children the prevalence of psoriasis is 0.71% (Augustin et al., 2010a) while its almost absent in Asian children (Chen et al., 2008).

In relation to the age group prevalence, there are two age peaks, the first around twenty five and the other around thirty five in many European countries (Falk and Vandbakk, 1993; Ferrandiz et al., 2001; Simpson et al., 2002). Studies from the United Kingdom, Germany, Russia, and United States showed an additional prevalence peak

around the age of sixty (Gelfand et al., 2005; Javitz et al., 2002; Schmitt and Ford, 2010; Seminara et al., 2011; Stern et al., 2004).

Regarding the gender there is a discrepancy in studies done in different countries. While in Germany (Augustin et al., 2010b), UK (Gelfand et al., 2005) and Norway (Falk and Vandbakk, 1993) there is a slight increase in the incidence in females than males, the opposite is reported in Denmark (Brandrup and Green, 1981) and Australia (Plunkett et al., 1999).

The Psoriasis Disability Index (PDI) is a clinical tool to assess the impact of psoriasis on patients' quality of life. From this it was obvious that psoriasis decreases the quality of life and that this impact is directly proportional to the extent of skin involvement (Gelfand et al., 2004). The more severe the disease is and the more the joints are involved (PsA: Psoriatic Arthritis); the more the direct (e.g. Hospitalization) and indirect medical costs (e.g. Lost productivity) per patient are. In a study of PsA patients in the UK, annual costs per patient ranged from £548 to £4,832 according to the severity of the disease (Poole et al., 2010).

1.4.2. Presentation of Psoriasis

One of the most commonly used grading systems in clinics is the Psoriasis Area and Severity Index (PASI). To classify psoriasis patients, it uses the severity of the lesions in combination to the area affected (Langley and Ellis, 2004). In clinical management it is important to classify the psoriasis according to the different clinical varieties it presents with. Psoriasis present in patients in many degrees and forms. Even in a single patient the severity of the psoriasis vary during the course of the disease. The presentation could include itchiness and/or pain, or maybe totally devoid of them. In clinical practice 80% of cases are mild (PASI index) plaque psoriasis. In plaque psoriasis the patches are distributed symmetrically and commonly seen on the scalp. Other less common forms of psoriasis include guttate psoriasis, inverse/flexural psoriasis, pustular psoriasis and erythrodermic/exfoliative psoriasis (see figure 7) (Crow, 2012).

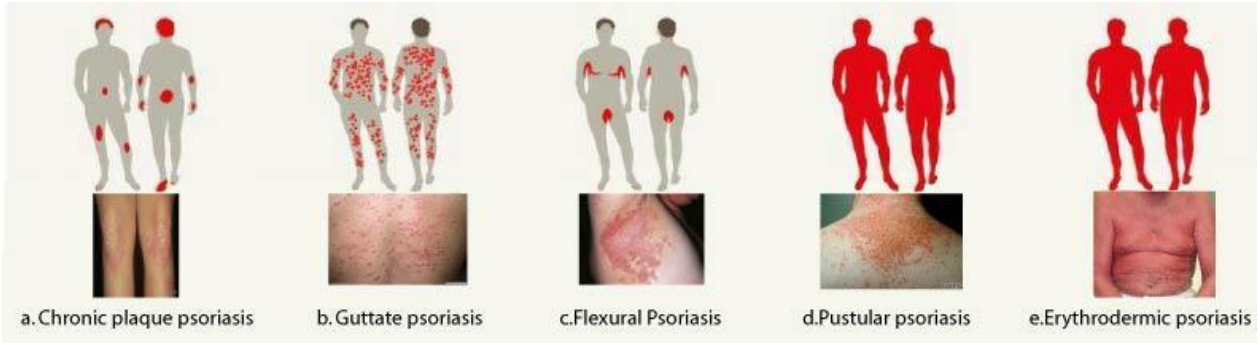

Figure 1.9: Clinical patterns of Psoriasis.
In this figure the red color on the human figures illustrate the distribution of each of the main clinical patterns of psoriasis. The photograph under each human figure shows an example of the NE of each of the listed clinical patterns. Modified from (Crow, 2012).

The connection between the development of psoriasis and other system affection is an idea that is becoming popular, as evidence on psoriasis related non skin diseases are increasing. PsA has become a separate type of arthritis with direct connection to the pathology of psoriasis. The prevalence of PsA in psoriatic patients is 18% in average (Lloyd et al., 2012). The clinical symptoms of PsA vary and are not always correlated with the severity of psoriasis of the skin (Gottlieb et al., 2008). In most of cases, PsA appears in psoriasis patients about ten years after the skin manifestations (Prey et al., 2010).

Table 1: Method for calculating the Psoriasis Area and Severity Index (PASI). Shown is the original description of the PASI which involves the assessment over 4 body regions (head [h], trunk [t], upper [u] and lower [l] extremities) of erythema (E), infiltration (I), and desquamation (D), and body surface area involvement (A). Because the head, upper extremities, trunk, and lower extremities correspond to approximately 10%, 20%, 30%, and 40% of body surface area, respectively, the PASI score is calculated by the formula: $PASI = 0.1(E_h + I_h + D_h)A_h + 0.2(E_u + I_u + D_u)A_u + 0.3(E_t + I_t + D_t)A_t + 0.4(E_l + I_l + D_l)A_l$.
(Langley and Ellis, 2004)

(a)

Degree of Severity (per body region)	**Value given**
No symptoms	0
Slight	1
Moderate	2
Marked	3
Very marked	4

(b)

Surface involved (per body region)	Value given
<10%	1
10%-29%	2
30%-49%	3
50%-69%	4
70%-89%	5
90%-100%	6

1.4.3. Co-morbidities of Psoriasis

The epidemiological risk factors of Psoriasis are shared with the risk factors of cardiovascular diseases (Kimball et al., 2012). Several studies point to an increasing statistical correlation between moderate to severe psoriasis and the development of cardiovascular conditions (Ahlehoff et al., 2011). The association between psoriasis and cancer arises from the side effects of immunosuppressive drugs used for its treatment (Shu et al., 2011). There is a proven positive correlation between psoriasis and depression (Dowlatshahi et al., 2013). Cytokines that are involved in the pathogenesis of psoriasis are also connected with depression (Kurd et al., 2010). Other co-morbidities associated with psoriasis include type 2 diabetes, hypertension and obesity (Naldi and Mercuri, 2010).

1.4.4. Molecular Aspects of Psoriasis

Psoriasis was found to be linked to 36 genomic regions (psoriasis susceptibility loci, PSORS) through several genome-wide association studies (GWAS). The most important genes identified within these regions are genes on the chromosome 17q25 (PSORS2): SLC9A3R (solute carrier family 9, isoform 3 regulatory factor), NAT9 (N-acetyltransferase superfamily), and RAPTOR (rapamycin (TOR); and CARD15 on the chromosome 16q (PSORS8) (Filer et al., 2009; Samuelsson et al., 1999). SLC9A3R and NAT9 susceptibility to psoriasis is related to mutations of the RUNX1 binding site within these genes (Helms et al., 2003). RUNX1 is a gene involved in the development of haemopiotic cells. Also, mutations in the SLC9A3R include ones that lead to functional changes in the immune synapse that is believed to increase in the stimulatory effect on the T lymphocytes giving more chronicity to the inflammation (Itoh et al., 2002). CARD15 is a component of the activation cascade leading to of NF-κB activation and is involved in the innate immune response (Li et al., 2012). Other GWAS draw attention to other members of the NF-κB signaling pathway involved in psoriasis: TNFAIP3 (TNF-inducible protein 3), TNIP1 (TNF-inducible protein 1), NFKBIA (NF-κB inhibitoty protein α), and TRAF3IP2 (TRAF3 interacting protein 2) (Nair et al., 2009; Strange et al., 2010).

The skin is not a mere physical barrier against harmful environment, rather an active component of the immune system. In healthy individuals the injury of the skin leads usually

to a limited inflammation and regeneration of the epidermal layer. On the other hand, in a genetically predisposed individual, the precipitating event (Trauma, Infection, Drugs, UV …etc.) leads to keratinocytes activation followed by immune cell activation. Further on, the immune activation in these patients leads to a loop of exaggerated regeneration and chronic inflammation characteristic to psoriasis. Because of the evident role of the T cells in the pathogenesis, the early trials to investigate psoriasis declared the adaptive immunity as the main perpetrator in psoriasis. More recent studies, including GWAS, presented evidence that innate immunity is another accomplice in the process of psoriasis development (Tsoi et al., 2012). Also, there is recent evidence that in psoriasis the tolerance towards self antigens is defective. The immune cells react towards RNA and DNA released from the keratinocytes in the process of inflammation (Lande et al., 2007). The up to date cellular picture of psoriasis include keratinocytes (KCs), dendritic cells (DCs), T cells , B cells, natural killer cells (NKs), macrophages and mast cells .

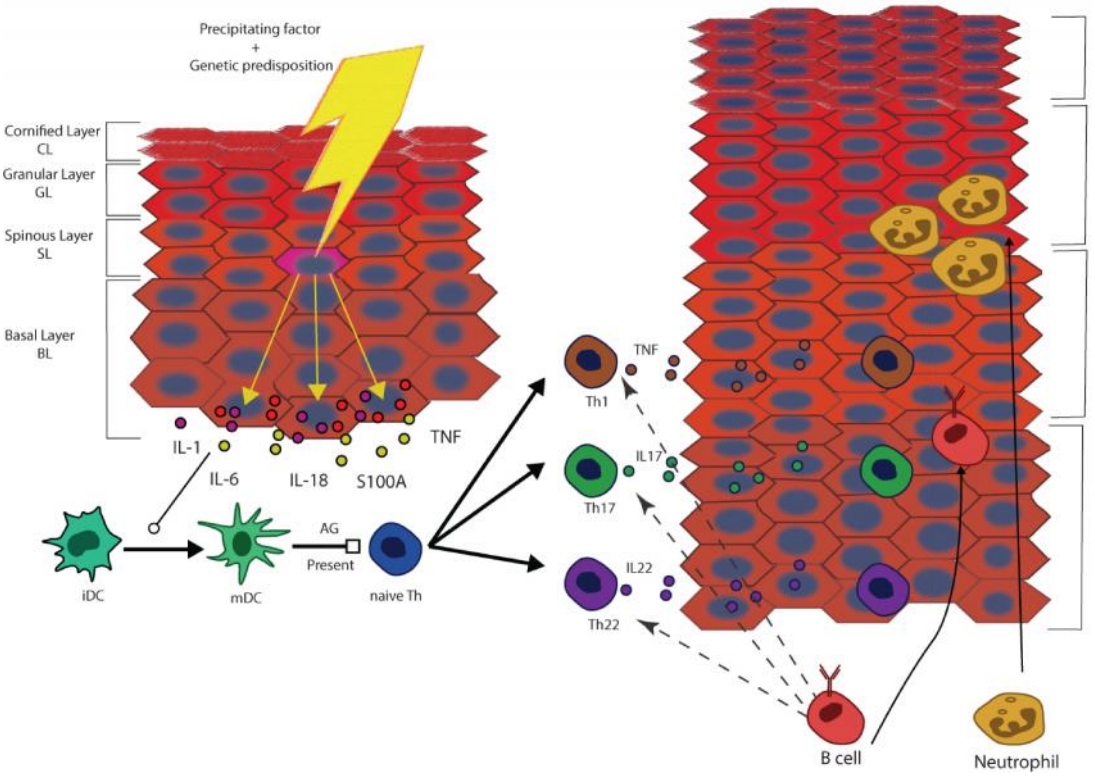

Figure 1.10: Immunological events in psoriasis.
The figure illustrates a scheme of the epidermis with the different layers of keratinocytes. The skin on the left side represents the normal skin. The skin on the right represents skin in a psoriasis patient. Different cells and molecules that share in the pathogenesis of psoriasis. Th: T hepler cell, iDC: immature dendritic cell, mDC: mature dendritic cell.

The skin injury drives stress and activation in KCs which produce cytokines (eg. IL-1, IL-6, IL-18 and TNF-α) and antimicrobial peptides (AMPs: eg. S100A and C-type lectins). AMPs act as opsonins attracting macrophages and neutrophils to the site of inflammation. The cytokines lead to further KC maturation and activation of DCs (Johnston et al., 2011). Important DCs that are involved in the psoriatic reaction are the plasmacytoid DCs (pDCs) that are involved in antiviral response through endosomal Toll-like receptor 7 (TLR-7) and TLR-9. The mDCs activate different subsets of T cells, most importantly Th1, Th17 and Th22 (Skrzeczynska-Moncznik et al., 2012). These cells close the viscous loop of the psoriasis reaction in psoriasis patients through releasing TNF , IL-17 and IL-22 respectively; and affecting the KCs and other cells in the skin (Blumberg et al., 2007; Chung et al., 2009; Guilloteau et al., 2010).

1.4.5. Treatment of Psoriasis

The treatment options of psoriasis include local (topical), systemic and phototherapy. They are used as a monotherpay, combination therapy, rotation therapy or sequential therapy according to the patient and the presentation of the disease. Topical agents include: tar, anthralin, retinoic acid, Vitamin D, corticosteroids and topical immunomodulators. Systemic treatment include: cyclosporin, methotrexate, retinoids and targeted immunotherapy. Phototherapy can be done using ultraviolet rays (UV) or excimer laser; which is also a form of ultraviolet laser. UV maybe broad band, narrow band or PUVA (psoralen with ultraviolet A rays) (Papoutsaki and Costanzo, 2013).

2. Aim of the Work

2.1.1. The Role of NFATc1 in Normal lymphocyte physiology and pathological conditions.

2.1.1.1. Investigate whether NFATc1/αA acts as an oncogene for the development of lymphoid tumors.

2.1.1.2. Investigate molecular mechanisms through which constitutive NFATc1/αA may alter the program of normal lymphocyte development?

2.1.1.3. Investigate the role of NFATc1 in Autoimmunity (IMQ-Induced Psoriasis Model in Mice)

2.1.2. Elucidate the points of interactions between the NFAT and the NF-kB pathways in activated B-cell fate.

2.1.3. IRF4 role in lymphocytic transformation.

3. Material and Methods

3.1.Materials

3.1.1. Antibodies

3.1.1.1. Primary antibodies for FACS analysis (anti-mouse)

AnnexinV	APC	BD Pharmingen
B220	Biotin	BD Pharmingen
B220	FITC	eBioscience
B220	PE	eBioscience
AA4.1	Biotin	BD Pharmingen
CD3	PE	eBioscience
CD19	PE	eBioscience
CD19	FITC	BD Pharmingen
CD16/CD32 (Fc-Block)	-	eBioscience
CD138	FITC	BD Pharmingen
CD23	FITC	BD Pharmingen
CD1d	PE	BD Pharmingen
CD21	PE	BD Pharmingen
CD43	FITC	eBioscience
CD4	FITC	BD Pharmingen
CD5	PerCP-Cy5.5	eBioscience
CD5	PE	eBioscience
CD8a	APC-eFlour 780	eBioscience
IgM	APC	BD Pharmingen
IgM	FITC	eBioscience
IgD	PE	eBioscience
Streptavidin	APC	eBioscience
Streptavidin	eFluor 450	eBioscience

3.1.1.2. Primary antibodies for Western Blot and immunofluorescence analysis (anti-mouse)

Mouse	anti-NFATc1 (clone 7A6)	BD Pharmingen
Rabbit	anti-NFATc1α (polyclonal)	Immunoglobe
Rabbit	anti-NFATc2 (polyclonal)	CellSignaling
Rabbit	anti-NF-κB p65 (D14E12)	CellSignaling
Rabbit	anti- NF-κB p52 (polyclonal)	Abcam
Rat	anti-F4/80 Biotin (clone CI:A3-1)	BioLegend

3.1.1.3. HRP-coupled secondary antibodies for Western Blot analysis

Goat	anti-mouse HRP	Sigma-Aldrich
Goat	anti-rabbit HRP	Sigma-Aldrich

3.1.1.4. Fluorescent-coupled secondary antibodies and reagents for immunofluorescence

Donkey	anti-mouse Alexa 555	Molecular Probes
Donkey	anti-rabbit Alexa 488	Molecular Probes
Donkey	anti-rat Alexa 488	Elita Avota, Uni. Wü

3.1.2. Antibiotics and inhibitors

FK506 (Tacrolimus)	Calbiochem
GolgiStop (Monensin)	Sigma-Aldrich
HALT protease inhibitor cocktail	BD Bioscience

3.1.3. Chemicals

Acetic acid	Roth
Agar	Roth
Agarose	Roth
β-Mercaptoethanol	Roth
Bradford reagent	BioRad
Bromophenol blue	Sigma-Aldrich
[α-P32]-dCTP	Hartmann Analytic
Disodium hydrogen phosphate (Na2HPO4)	Roth
Dimethyl-sulfoxide (DMSO)	Roth, Gibco
Dulbecco's Modified Eagle Medium	Gibco
6x DNA loading Dye	Fermentas
EDTA	Roth
Ethanol (EtOH)	Roth
Ethidium Bromide (EtBr)	Roth
Fetal Bovine Serum, Qualified, US origin	Gibco
Fluoroshield with DAPI	Sigma-Aldrich
Glycine	Roth
Glycerol	Roth
Hydrogen chloride (HCL)	Roth
Isopropanol	Roth
LB medium	Roth
Magnesium chloride	Roth
Magnesium chloride (MgCl2 25mM)	PeqLab

Methanol	Roth
Midori Green	Nippon Genetics
Monosodium phosphate (NaH2PO4)	Roth
Non-fat dried milk powder	AppliChem
2xPCR Mix	Fermentas
Phenol	Roth
Penicillin (10000U)/Streptomycin (10000µg)	Gibco
Ponceou S	Sigma-Aldrich
Power SYBR Green	Sigma-Aldrich
PCR Master Mix	AB
Propidium iodide	Sigma-Aldrich
protein G agarose	Pierce
Rotiphorese®Gel 30	Roth
Sodium citrate	Roth
Sodium chloride (NaCl)	Roth
Sodium dodecyl sulfate (SDS)	Roth
Sodium hydroxide (NaOH)	Roth
Triton-X-100	AppliChem
Tris	Roth
Trypan Blue Solution	Sigma-Aldrich
Trypsin/EDTA	Gibco

dH2O was taken from the “Biocel MilliQ system” (Millipore), if not differently indicated.

3.1.4. Electronic data processing

Data were collected, analyzed and presented using several Microsoft Windows operated computers (Toshiba laptop and Fujitsu-Siemens desktop) and a scanner from HP. Following programs were used:

FlowJo (Version 7.6.2)

BD FACS Diva 5.0

FUSION CAPT

GraphPad Prism 6

Thomson EndNote X3

Image Lab Software

Adobe Photoshop CS6

Adobe Illustrator CS6

Leica Software ImagePro Plus

Microsoft Office Excel 2007

Microsoft Office PowerPoint 2007

Microsoft Office Word 2007

3.1.5. Equipment

Cell culture plates (96 well)	Greiner, Nunc
Cell culture plates (48, 24, 12, 6 well)	Greiner, Nunc
Cell culture plates (6cm, 10cm)	Greiner, Nunc
Cell culture flasks (75cm2 flask)	Greiner
Cell separation columns (LS)	M. Biotech
Cell scraper (24mm)	Hartenstein

Cell strainer (70µm)	BD Bioscience
Cover slips	Marienfeld
Cryo tube (2ml)	Greiner
Cuvette (quartz)	Hellma
Cuvette (plastic)	Braun
Erlenmeyer flasks (1000ml, 500ml, 100ml)	Schot
FACS tubes	BD Bioscience
50ml & 15ml falcon tubes	Greiner
Forceps for animal preparation	Hartenstein
Hybridization mesh	Thermo Fisher
Hybridization bottle	Thermo Fisher
Hyperfilm ECL	Amersham
Freezing container	Nalgene
Microcentrifuge tubes (1.5ml, 2ml)	Eppendorf
Object slides	Hartenstein
Parafilm	Pechiney
Pasteur-pipettes	Hartenstein
PCR plates, white (96 well)	Thermo Fisher
Pipette tips (1000µl, 100µl, 10µl)	Sarstedt
Razor blades	Hartenstein
Scissor for animal preparation	Hartenstein
Serological pipette (25ml, 10ml, 5ml, 2ml)	Greiner
Sterile filters (0.2µm, 0.45µm)	Sartorius
Syringe (2ml, 5ml, 10ml)	Braun Syringe

Needle (23GA, 20GA)	Hartenstein
Tuberculin syringe (26 GA 3/8")	Braun
Protran BA 85 Nitrocellulose	GE Healthcare
Wathman 3MM filter paper	Hartenstein
X-ray cassette	Hartenstein

3.1.6. Instruments

Autoclave	Systec
Balance FCB	Kern
Biofuge 15R	Heraeus
Confocal microscope TCS SP5 II	Leica
Gel DocTM XR+	BioRad
Electrophoresis chamber	CTI
Electrophoresis Power Supply	Micro-Bio-Tec
FACS Canto II	BD
Fridge (4-10°C, -20°C, -70°C)	Siemens
Fusion SL	V. Lourmat
Ice machine	Genheimer
In vivo imaging system (Maestro EX)	CRI
Light microscope CK2	Olympus
LUMIstar Omega	BMG labtech
Centrifuge 5418	Eppendorf
Humidified tissue culture incubators	Heraeus
instruments Hybridization oven	Bachofer
Thermomixer compact	Eppendorf

7000 Sequence Detection System	Applied BioS.
Shaker C40	GLW
Waterbath	Hartenstein
T100 Thermocycler	BioRad
Tank Blot	Hoefer
PCR machine	Biometra
Photometer	Pharmacia
pH-meter	WTW
Vertical electrophoresis unit	Hoefer
Vortex mixer	RA

3.1.7. Ligands and stimulants

Anti-IgM µ-chain F(ab)2	Jackson ImmunoResearch
Ionomycin	Sigma-Aldrich
LPS, ultra-pure	Sigma-Aldrich
TPA (PMA)	Merck

3.1.8. Kits

B cell Isolation Kit, mouse	Miltenyi Biotech
CellTrace™ Kit	Molecular Probes
DecaLabel™ DNA Labeling Kit	Fermentas
First Strand cDNA Synthesis Kit	Fermentas
Intracellular Fixation & Permeabilization	eBiosciene
Long PCR Enzyme Mix	Fermentas
NucleoBond Xtra Maxi	Mach.-Nagel

2x PCR Mix	Fermentas
SuperSignal West Pico ECL Substrate	Pierce

3.1.9. Mice

All mice were kept in a species appropriate environment at 22°C with a 12 hours circadian rhythm in the animal facilities of the Institute of Pathology, the Institute of Microbiology & Hygiene and at the Center of Experimental Molecular Medicine (ZEMM) of the University of Würzburg.

All offspring were genotyped around the fourth week after birth. The used experimental animals were 8-18 weeks old gender-matched littermates. For some experiments age- and gender-matched wild type mice were used as control. All used mouse lines were maintained on C57BL/6 background.

3.1.10. Reverse Transcriptase (RT) and Real-Time PCR Primer

P2 (Ex2/3-Ex3) fwd	aggacccggagttcgacttc
P2 (Ex2/3-Ex3) rev	gcagggtcgaggtgacactag
P1 promoter fwd	gggagcggagaaactttgc
P1 promoter rev	cagggtcgaggtgacactagg
qRT *NFATc1* fwd	gatccgaagctcgtatggac
qRT *NFATc1* rev	agtctctttccccgacatca
Actin fwd	gacggccaggtcatcactattg
Actin rev	aggaaggctggaaaagagcc

2.1.14 Size standards

DNA ladder (Fermentas):	GeneRuler 100 bp
Protein ladder (Fermentas):	PageRuler prestained

3.2.Methods

3.2.1. Generation and maintenance of genetically modified mice

3.2.1.1. *Irf4* $^{flx/flx}$ x mb1-cre mice

mb1-cre transgenic mice were created in M. Reth's laboratory by inserting hCre into the mb-1 WT locus between the exons 2 and 3 (Hobeika et al., 2006). They allow the inactivation of "floxed" genes in bone marrow B cells. *Irf4* floxed mice were created in the Dalla-Favera laboratory by flanking the chromosomal murine *Irf4* gene with loxP sites which are targets of Cre recombinase of bacteriophage P1. These two lines were crossed to produce the *Irf4* $^{flx/flx}$ x mb1-cre mice line that have the *Irf4* gene floxed and express mb1-cre. Therefore, having B-cells lacking IRF4 expression start as early as the bone marrow.

3.2.1.2. caNFATc1/αA x *Irf4* $^{flx/flx}$ x mb1-cre mice.

In the laboratory of Prof. Volker Ellenrieder (Department of Gastroenterology, Univ. Marburg) a transgenic mouse line was created expressing a constitutive active version of the NFATc1/αA isoform under the control of a "floxed" Stop cassette from the ROSA26 (R26) locus (which is an "open" locus that is broadly used for expressing transgenes in mice). These mice we refer to by, caNFATc1/αA. When this cassette is deleted by Cre, the caNFATc1/αA version is expressed. By crossing this line with the *Irf4* $^{flx/flx}$ x mb1-cre line, we got mice having B-cells that (over-) express NFATc1/αA (from the ROSA26 locus) and lack IRF4 expression starting as early as the bone marrow.

3.2.1.3. *caNFATc1/αA X NFATc1* $^{flx/flx}$ *X cd23-cre* mice.

Cd23-cre transgenic mice were created in M. Busslinger`s laboratory by inserting a Cre-IRES-hCd5t expression cassette into exon 2 of a Cd23 BAC construct (Kwon et al., 2008). Those mice were crossed with the *Nfatc1* $^{flx/flx}$ *mice in which the Nfatc1* gene is flanked with loxP sites then crossed with the *caNFATc1/αA* mice to give a line in which splenic B-cells do not have any NFATc1 expression **except** the (over-)expression of NFATc1/αA from the ROSA26 locus.

3.2.1.4. c-RelKo mice.

c-Rel knockout mice where originally created by the Kontagen group (Kontgen et al., 1995) and used in our experiments.

3.2.2. Genotyping of mice

Genotyping was done with 4 weeks old mice. The tip of the tail was cut using a scalpel and put in an eppendrof tube. 30 µl of proteinase K (Fermentas; #EO0491) were added per 1 ml genomic lysis buffer and 20 µl of the cocktail were added to each tail sample following overnight incubation at 56°C. The next day 480 µl of water was added to each sample and incubated for another 10 min at 95°C. Following centrifugation, 3 µl of DNA sample was used to run PCR assays using the following primer pairs:

Detection of caNFATc1/αA gene

caNFAT for	5'-cat gtc tgg gag atg gaa gc-3'
NFAT rev	5'-tct cga gct act tgt cat cg-3'

Detection of Rosa26 wild type gene

Rosa26 for	5'-ggc gga tca caa gca ata at-3'
Rosa26 rev	5'-gag tct tct ggg cag gct ta-3'

Detection of mb1 wild type gene

Mb1 for	5’-CTGCGGGTAGAAGGGGGT-3’
Mb1 rev	5’-CCTTGCGAGGTCAGGGAGCC-3’

Detection of cre gene

iCre for	5’-ACCTCTGATGAAGTCAGGAAGAAC-3’
iCre rev	5’-GGAGATGTCCTTCACTCTGATTCT-3’

Detection of the NFATc1 floxed gene

NFATc1 $^{flx}/_{flx}$ for	5'-CCTATTTAAACACCTGGCTCCCTGCG-3'
NFATc1 $^{flx}/_{flx}$ rev	5'-CCATCTCTCTGACCAACAGAAGCCAG-3'

Detection of the IRF4 floxed and wild type genes

IRF4 $^{flx}/_{flx}$ for	5'-TGC CTT TGG GAC GGA TGC TC-3'
IRF4 $^{flx}/_{flx}$ wt rev	5'-CTT CTA GCT GAC CAC TAA GAA C-3'
IRF4 $^{flx}/_{flx}$ flx rev	5'-GAC CAC TAC CAG CAG AAC AC-3'

Detection of the c-Rel knock out and wild type genes

c-Rel WT for	5'-GTA CTG CAT CAA CTG CAT GAC-3'
c-Rel WT rev	5'-CAG AGA CTA ACA AGT GGT A-3'
c-Rel Ko rev	5'-CTT CCT CTT CTC TGC CAG AC-3'

Genomic lysis buffer:

300mM	NaCl
25mM	EDTA
50mM	Tris (pH 8.0)
0.2%	SDS

3.2.3. Lymphocyte isolation

Age (8-10 weeks old) and sex matched animals were sacrificed and dissected followed by the removal of spleen and BM and LNs. BM cells were flushed out using a syringe and PBS.

To obtain peritoneal cells, glass pipettes and PBS were used. Single cell populations were obtained from all specimens using a cell strainer (Hartenstein). Erythrocytes were lysed with TAC buffer. B cell isolation was done using Miltenyi's B cell isolation kit (#130-090-862) according to manufacturer's instructions with a yield of 95-98% pure B cell population.

TAC buffer

8.26 g NHCl
1 g KHCO
0.037 g EDTA
Dissolved in 1000 ml ddH_2O; Mix well and autoclave

3.2.4. Cell counting

To determine cell numbers cells were diluted with Trypan Blue to exclude dead cells and filled under a cover slid on a Neubauer counting chamber. Four fields were counted (≥ 10 cells) and the cell number was calculated according the mean of four and the dilution factor of the chamber ($1x10^4$) per ml

3.2.5. Cell culture

$5x10^6$ cells were cultured in 1 ml X-vivo 15 medium (BE04-418Q; Lonza). Incubations were done for periods ranging from 15 minutes to 72 hours. Stimulations were done by LPS (10 µg/ml; Sigma, #L5293), α-IgM (10 µg/ml; Jackson Lab., #115-006-020), α-CD40 (2 µg/ml; R&D, #MAB440) or TPA (Sigma, #79346) and ionomycin (Invitrogen, #I24222) or combinations of them. For harvesting, the cells were sucked from the wells and then washed twice with cold PBS.

PBS

8 g NaCl
0.2 g KCl
1.44 g Na_2HPO_4
0.24 g KH_2PO_4
Dissolved in 800 ml ddH_2O; adjust pH to 7.4 with HCl, add ddH_2O to 1 Liter.

3.2.6. Protein extraction

3.2.6.1. Whole cell protein extraction

Whole protein extract was prepared by incubation of cells on ice with modified RIPA buffer for 15 minutes followed by hard vortexing at 4°C for 30 minutes followed by centrifugation and sucking the supernatent.

Modified RIPA buffer

150 mM	NaCl
1.0%	NP-40 (Sigma)
0.5%	sodium deoxycholate
0.1%	SDS
50 mM	Tris, pH 8.0

3.2.6.2. Nuclear and/or cytoplasmic protein extraction

All steps are done in the cold room. The amounts are adjusted to 5-10 X 10^6 cells. The cells are washed twice with 1 ml ice cold PBS (2000 rpm for 3 minutes.). After the second wash 120 µl of ice cold buffer A is added and let sit on ice for 15 minutes. Then, 25 ul 10% NP-40 is added and vortexed for 30 seconds then let sit 30 seconds. The nuclei are pelleted by centrifugation at 9000 rpm for 60 seconds. After that, the supernatant (cytoplasmic proteins) was carefully remove from the pellet and discarded or put in pre-chilled microcentrifuge tubes. 52 µl of ice cold buffer B is added to resuspend the nuclear pellet followed by vigorous agitation (vortex) for 30 minutes. Nuclear extracts (supernatants) are recovered after centrifugation for 15 minutes at 12000 rpm and put in pre-chilled microcentrifuge tubes. Both cytoplasmic and nuclear proteins contained in the buffers were stored at -70º.

Buffer A (Hypotonic):

10 mM	HEPES pH 7.9
10 mM	Kcl
0.1 mM	EDTA
0.1 mM	EGTA

Buffer B (High salt):

20 mM	HEPES pH 7.9
0.4 M	NaCl
1 mM	EDTA
1 mM	EGTA
20%	Glycerol

For each buffer just before extraction add:

2 mM	DTT
0.5 mM	PMSF
10µl/ml	Halt Protease Inhibitor Cocktail (Pierce biotechnology)

3.2.6.3. Bradford assay

The Bradford assay kit from BIORAD was used to estimate the protein concentration according to manufacturer's protocol. This assay is based on complexes built between the Bradford reagent (Coomassie-Brilliant-Blue G-250) and proteins under acidic conditions, leading to different absorption characteristics at 595 nm wave length. The standard curve was prepared with BSA solution at serial concentrations covering the estimated sample concentration range.

3.2.7. Expression analysis

3.2.7.1. Western blot

Equal amounts of protein were loaded for each sample per lane (minimum of 30 µg) for the separation on SDS-PAGE gels. Nitrocellulose membranes (WHATMAN, #BA 85) were used for protein transfer. Membranes were blocked using 4% non-fat dry milk in TBS-Tween buffer for 1 hour on shaker. The membranes were incubated with primary antibodies in TBS-Tween buffer over night at 4°C on a shaker. Then secondary antibodies (α-mouse or α-rabbit) were used in TBS-Tween buffer according to the source of primary antibodies for 1 hour on a shaker. Signals were developed using Super SignalTM kit (Pierce Chemical Company, CA) and imaged using Fusion-SL system (Vilber Lourmat) or with an X-ray film (Hyperfilm ECL, Amersham). To confirm equal loading, the membranes were re-blotted with β-actin (AC-15mAb; Sigma, #A1978).

10% Resolving gel (10 ml)

H_2O	4.0 ml
30% Polyacrylamide (Applichem)	3.3 ml
1.5 M Tris (pH 8.8)	2.5 ml
10% Ammonium persulfate (APS) (Sigma)	0.1 ml
10% Sodiumdodecyl sulfate (SDS) (Roth)	0.1 ml
TEMED (Sigma)	0.004 ml

Stacking gel (3 ml)

H_2O	2.1ml
30% Polyacrylamide (Applichem)	0.5 ml
1.5 M Tris (pH 6.8)	0.25 ml
10% Ammonium persulfate (APS) (Sigma)	0.3 ml
10% Sodiumdodecyl sulfate (SDS) (Roth)	0.3 ml
TEMED (Sigma)	0.003 ml

Running buffer (TG Buffer)

3.02 g	Tris
18.8 g	Glycine (Roth)
10 ml	10% SDS

ddH2O added to 1 Liter

Transfer buffer

72.5 g	Glycine
14.5 g	Tris
1 liter	methanol

ddH2O added to 5 Liter

Wash buffer (TBS Tween)

2.42 g	Tris
8 g	NaCl

ddH2O added to 1 Liter and add 450µl of Tween.

3.2.7.2. RT-PCR

Cells were suspended in 1 mL Trizol and stored at -70°C. Prior to RNA extraction, the tubes were allowed to thaw at room temperature and 200 µl of chloroform (Roth) was added to the samples. After 5 minutes incubation at room temperature, the tubes were vortexed for 10 seconds and then centrifuged at 4°C and 12000 rpm for 10 minutes. Then, the aqueous upper phase was transferred into a new autoclaved (RNase free) microcentrifuge tube and 500 µL of isopropanol (Roth) were added. After a short vortex, the cells were incubated at room temperature for 10 minutes and centrifuged at the 12000 rpm for 30 minutes. The supernatant was discarded and the pellet was washed with 1 ml of 75% Ethanol (Roth), then air-dried before re-dissolving in 10 µL of DEPC water (Roth). The newly extracted RNA was mixed with 1 µl of 6x loading dye and run on a 1% agarose gel to check for degradation.

1 µg of total RNA was used to synthesize cDNA using the iScript™ cDNA Synthesis Kit (BIO-RAD). cDNA preparation was done using Titan One Tube RT-PCR System (Roche Diagnostics). 2XPCR Master Mix (Thermo Scientific) and Gene Ruler™ 100bp (Thermo Scientific) ladder were used.

1% Agarose gel

1 g Agarose (Applichem)
100 ml TAE Buffer (1x)
10 µl Ethidium bromide (Roth)

50x TAE buffer

242 g Tris base
57.1 ml Acetic Acid
100 ml 0.5 M EDTA
ddH2O added to 1 Liter

6x DNA loading dye

3 ml glycerol (30%)
25 mg bromophenol blue (Roth)
ddH2O added to 10 ml

3.2.7.3. Electrophoretic mobility shift assay (EMSA)

EMSA is an electrophoresis technique used to study protein–nucleic acid interactions. Using a radioactive labeled oligonucleotide probe mixed with the protein extracts of cells the binding is determined by the higher position shifting of the complex (or part of the complex) when running on polyacrylamide gel in comparison to the free running probes. The higher position is due to the slower mobility through the gel due to the larger size of protein + nucleic acid complex. The specificity of this binding is determined by either competition by an excess of a known factor binding probe or by adding an antibody specific for a transcription factor to the mix producing a supershift. The position of the complexes and the upper shifting are detected by the radioactive impression of the complex on an X-ray film (Hyperfilm ECL, Amersham).

We prepared radioactive labeled double-stranded probe that were approximately 25 bp in length corresponding to NFATc1 and NF-κB binding sites. After extraction of nuclear proteins from cells, the protein concentration of extracts was measured. Equal amounts of nuclear proteins were incubated with a mixture of the radioactively labeled double-stranded probe, 3xBi-Buffer and Poly(deoxyinosinic-deoxycytidylic) acid sodium salt (Poly dI-dC) at -4 °C for 30 minutes. The mixture was loaded on a 6% non-

denaturing polyacrylamide gel and fractionated for about 3 hours using 0.5X TAE as running buffer. After the run, the gel was fixed using 10% acetic acid, dried on a vacuum gel dryer for 1 hour, then exposed to an X-ray film in a well sealed X-ray cassette overnight at -70° C. Longer exposure periods up to 72 hours were often needed.

3x Binding buffer

HEPES 7.9 pH	60 mM
DTT	3 mM
EDTA	3 mM
KCL	150 mM
Ficoll	12 %

50X TAE Stock Solution

For each litre of solution:

242 g	Tris Base
57.1 ml	Glacial Acetic Acid
100 ml	0.5 M EDTA

Mix Tris with stir bar to dissolve in about 600 ml of ddH2O, then add the EDTA and acetic acid. Finally, bring final volume to 1 l with ddH2O and store at room temperature.

3.2.8. Cell staining and sorting

3.2.8.1. Flow-assisted cytometric analysis (FACS)

The principle of FACS is based on the passage of cells in a single cell flow across a beam of laser. According to the interaction of the laser with the cells (native) or fluorescence-labeled antibodies they carry, the cells are measured and analyzed. Information gathered from these events include their numbers (events), their size (forward), granularity (side scatter) and fluorescent properties. Cells could be analyzed for structure and expression of surface molecules and intracellular proteins. We used the FACS Canto II (BD).

3.2.8.2. Surface marker staining

To stain cells with fluorescent labeled antibodies 0.5-1x10^6 cells were transferred into 1.5 ml reaction tubes and washed twice with FACS-Buffer

(PBS/0.1%BSA) and suspended in a total volume of 50 µl FACS-Buffer. A master mix of the fluorescent antibodies (0.25 µl antibody/sample) and the Fc-Block (1:250) was prepared in 50 µl FACS-Buffer per sample. 50 µl of the master mix was added to each sample tube. Samples were incubated with antibodies for 15 minutes at room temperature in the dark. After two more washing steps the cells were directly measured, continued for intracellular marker staining or fixed in 4% formaldehyde.

3.2.8.3. Intracellular marker staining

Cells were stimulated in culture with different stimuli for different time periods. TPA (Sigma), ionomycin (Invitrogen) and Golgi-plug (BD) were added to the culture for the final 6 hours. The cells were harvested, washed then stained for the surface markers according to the previous protocol. After that, cells were fixed and permeabilized using eBioscience fixing and permeablizing kit according to manufacturers recommendations, then stained with anti-mouse IL-10 APC antibody (eBioscience). Prior to FACS measurement, they were re-washed and re-suspended in FACS buffer.

3.2.8.4. Proliferation assay

Carboxyfluorescein diacetate succinimidyl ester (CFDA-SE) is colorless and nonfluorescent until the acetate groups are cleaved by intracellular esterases to yield highly fluorescent carboxyfluorescein succinimidyl ester (CFSE). The succinimidyl ester group reacts with intracellular amines, forming fluorescent conjugates that are well stable for long times (up to 8 weeks). Due to the acetate groups CFDA-SE diffuses freely into cells equally and are retained there, passing only through cell divisions. Due to the progressive halving of CFSE fluorescence within daughter cells following each cell division, FACS could be used to measure this decrease in the concentration of the dye in cell populations indicating the frequency and efficiency of cell proliferation. Purified cells were incubated with CFDA-SE (Invitrogen, #C34554) at 37 °C for 3 minutes. The cells were then washed with RPMI 1640 (Invitrogen), re-suspended in X-vivo medium (BioWhittaker) and cultured in a 96-well plate with various stimuli. At various time points the cells were harvested, washed then

suspended in 200 µL FACS-Buffer. The approximate excitation and emission peaks of CFSE are 492 nm and 517 nm, respectively.

3.2.8.5. Apoptosis assay

To investigate apoptosis in our cells we used annexin-V and propidium iodide (PI). Annexin-V is a protein, which binds to phosphatidylserine on the cell surface of apoptotic cells. PI is membrane impermeable and therefore intercalates only into the DNA of dead cells. Two stock aliquots of 100µl/sample of Annexin-binding buffer (ABB) were prepared in 2 microcentrifuge tubes. To either one of them annexin-V (APC or FITC) was added with a 1/100 concentration. To the other PI [1mg/ml] was added in the same concentration. Cells were washed twice using FACS-Buffer, then 100 µl of the annexin-V stock aliquot was added to each sample tube and incubated for 15 minutes at room temperature in the dark. Just before measuring the samples on the FACS device 100 µl of the PI stock aliquot was added individually to the sample tubes. The sample was measured on the FACS within one hour of the beginning of the staining and each sample was vortexed well before measurment.

Annexin-Binding Buffer:

10 mM	HEPES
149 mM	NaCl2
2.5 mM	CaCl2

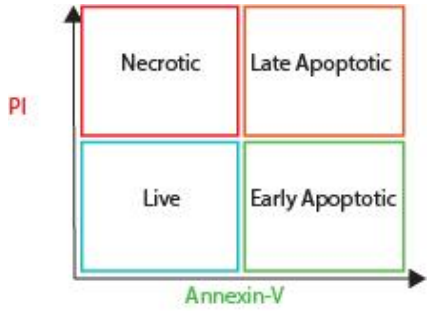

3.2.9. Psoriasis Induction in mice

After anesthesia of the mouse using intraperitoneal (IP) injection of anesthetic cocktail Ketamine/Xylazine (50-100 mg/kg of Ketamine-HCl and 5-10mg/kg Xylazine-HCl), shave 2 x 3 Centimeters of upper back hair carefully. 4.166mg of IMQ cream (Aldara 5%, 3M Pharmaceuticals) is applied to the shaved back of the each mouse daily for a period of 6-8 days.

3.2.10. ELISA

Samples were either serum from mice at specified time points of immunization or supernatant of media where cells were stimulated and incubated for specific time periods. NUNC Maxisorb 96-well plates (eBioscience) were used to detect the secretion of mouse IL-10. Samples were serially diluted using dilution buffer and incubated for 2 hours at 37°C. The plates were coated with coating solution and kept at 4°C overnight. Followed by 2 hours incubation at 37°C with blocking solution and 3 times washing with wash buffer, samples were added to the plates. Secondary antibodies were then added to the plates and left overnight at 4°C. Next day, substrate was added to each plate and allowed to develop color. The plates were read using a plate reader (Molecular Devices) and quantifications were done against a standard curve.

Coating solution Anti-mouse IL-10 antibody (Biolegend) in PBS(8 µg/ml)

Blocking solution 1% BSA (Sigma) in PBS + 0.05% sodium azide (Sigma)

Dilution buffer 0.1% BSA in PBS + 0.05% sodium azide

Wash buffer PBS+0.05% Tween 20

Substrate p-Nitrophenylphosphate (Sigma)/1 ml diethanolamine buffer

Diethanolamine buffer (pH 9.8)
0.1 g MgCl2
0.2 g NaAzide
97 ml Diethanolamine ddH_2O added to 1 liter

3.2.11. Tissue staining and microscopy

3.2.11.1. Haematoxylin and eosin staining (H & E)

Stain the slides with haematoxylin for 4 minutes, followed by washing under running tap water for 15 minutes. After that differentiate with 0.3% acid alcohol, followed by washing under running tap water for 15 minutes. Then stain with eosin for 2 minutes, followed by washing under running tap water for 15 minutes. Finally, tissues were dehydrated by shortly dipping them in ethanol 100%, then left to dry for 60 minutes at 37 °C and then mounted with cover slip.

0.3% acid alcohol

Commercial grade ethanol	2800 ml
Distilled water	1200 ml
Conc. hydrochloric acid	12 ml

3.2.11.2. Cytospins and Immunocytochemistry

This is a method to investigate protein expression in fixed single cells. The visualization of the stained cells is done with several types of microscopes according to the type of staining. The confocal microscope enables visualization of emitted light of fluorochrome based stains after excitation with laser light.

After harvesting and washing the cells we repeatedly pipeted and vortexed the cells to remove any clumps and assure single cell suspension 1x cold RPMI. The cells where fixed on slides using a cytospin centrifuge with a speed of 350 rpm for 3 minutes. Each sample had a concentration of 70 - 80x10^3 cells/slide. Slides were dried at RT for 3-4 hours then they were fixed with 4% paraformaldehyde for 20 min (filtered). After 3 washes with PBS^{--}, cells were permeabilized by 0.1% Trinton-X in PBS^{--} (phosphate buffered saline without supplementation with $CaCl_2$ or $MgCl_2$) for 5 minutes at RT. After 3 washes with PBS^{--}, cells were blocked for 20 minutes using PBS/0.1% BSA. After a single wash cells were incubated with the primary antibody for 60 minutes at RT in humid chamber. After 3 washes with PBS^{--}, cells were blocked for 20 minutes using PBS/0.1% BSA. After a single wash cells were incubated with the secondary antibody 60 minutes at RT in the humid chamber. After 3 washes with PBS^{--}, cells were mounted with fluorochrome and DAPI (Fluoroshield, Sigma-Aldrich). PBS^{--} means that the phosphate buffered saline buffer does not contain calcium or magnesium.

3.2.11.3. Immunohistochemistry

We performed peroxidase based staining and fluorochrome based staining. In peroxidas based stainings the detection of the investigated antigen is done by antibodies labeled with peroxidase and the positive colour (brown) could be detected by light microscopy on a background tissue stained with haematoxilin (blue). Fluorochrome-

based staining allows multiple antigen differentiation which help in distinguishing co-expression and cell specific expression of target proteins. Fluorochrome-based staining is visualized using confocal microscope of emitted light from the fluorochrome after excitation with laser light.

After de-paraffinisation of the tissues, antigen retrieval protocols were applied to the tissues according the primary antibody that would be used. Then, the slides were left to dry at RT for 15 minutes. The internal peroxidase activity of the tissues was blocked using peroxidase blocking solution (DAKO s2023 RTU.) for 5 minutes. After 3 washes, tissues were blocked using Ab-diluent (DAKO s2022 RTU.) for 20 minutes. After that, tissues were incubated with the primary antibody (diluted in proper Ab-diluent) for 60 minutes. After a single wash, tissues were incubated with the secondary biotinylated antibody (DAKO 5001 RTU.) for 20 minutes. After a single wash, tissues were incubated with the the streptavidin-HRP-link (DAKO 5001 RTU.) for 20 minutes. After a single wash, tissues were dipped in haematoxylin for background staining, followed by running water for 10 minutes to remove any extra dye. Finally, tissues were dehydrated by shortly dipping them in 100% ethanol, then left to dry for 60 minutes at 37 °C and mounted with cover slip. All washings were done by TBS-buffer. All incubations were done at RT in humid chamber.

TBS:

50 mM Tris
150 mM NaCl
Adjust pH with HCl to pH 7.6

3.2.11.4. Confocal microscopy

A confocal microscope detects the emitted light of fluorochrome after excitation with laser light. Major advantages of confocal scanning microscopy are its higher resolution by the usage of two pinholes to blind out diffused light and the possibility to scan through a whole cell. The pictures were taken with a Leica Confocal microscope (TCS SP5 II) and analyzed with the Leica Software Image Pro Plus.

3.2.12. Statistical analysis

The statistical analysis was performed using GraphPad (Prism) software, version 6.0. Data were presented as mean and error bars in figures represent ±SEM (standard error of mean). Unpaired t-test was performed to evaluate the statistical significance of the data set. A value of $p<0.001$(***) is considered highly significant, while $p<0.05$(*) as well as $p<0.005$(**) are known to be statistically significant.

4. Results

4.1. Expression of a constitutive active version of NFATc1 (caNFATc1/αA) with ablated IRF4 in B cells from mice.

The role of NFATc1 in the development of B cells was investigated in our group and other groups in several previous studies (Muller and Rao, 2010; Serfling et al., 2012). We studied this by inactivating the Nfatc1 gene at different levels of B cell development by using different types of mouse cre-lines. For example, the mb1cre line (starting expression in BM) and CD23cre line (starting expression in spleen) with the floxed version of the Nfatc1 gene were used. We showed that the knock out of NFATc1 does not alter B cell compartment in BM or spleen regarding numbers. However, it impairs the development of peritoneal B1a cells (Bhattacharyya et al., 2011). In this work we wanted to further investigate (i) NFATc1 role in B cell development deploying a constitutive active version of the short NFATc1 isoform NFATc1/αA, designated as caNFATc1/αA, and (ii) the interplay between NFATc1 and IRF4 in this process. The constitutive active version of NFATc1 is expressed from the ROSA 26 locus under the control of a STOP sequence which is 'floxed' and, therefore, can be expressed by crossing theses mice with mouse lines expressing cre. For studying the role of IRF4 we used mice that bear a 'floxed' IRF4 allele for its conditional inactivation.

4.1.1. Mice with a constitutive active version of NFATc1/αA show expression of NFATc1 in splenic B cells without any stimulation.

In order to check the constitutive activity of NFAT in B cells from the caNFATc1/αA x mb1cre mice we performed a WB with a whole protein from B cells extracted from them without any stimulation, with α-IgM stimulation and without and with CsA. The results show a strong expression of NFATc1, even stronger than in stimulated B cells from WT mice. In both WT and caNFATc1/αA x mb1cre mice the expression was abolished by CsA (Fig. 4.1).

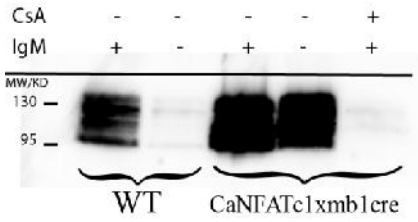

Figure 4.1: Expression of NFATc1 in splenic B-cells from caNFATc1/αA x mb1cre mice
WB using total protein extract from splenic B cells from caNFATc1/αA x mb1cre and WT mice. The cells were either left unstimulated or stimulated with α-IgM for 24 hours. The last lane shows protein extract from cells stimulated with α-IgM and also CsA was added.

4.1.2. Increased numbers of splenic B cells in mice expressing a constitutive active version of NFATc1 with a knocked out IRF4

In order to examine the results of constitutive activity of the NFATc1 and/or the knock out of the IRF4 specifically in B cells, we used FACS analysis of the surface markers of splenocytes to examine the relative numbers of B and T cells from spleens of caNFATc1/αA x mb1cre, IRF4 $^{f/f}$ x mb1cre and caNFATc1/αA x IRF4 $^{f/f}$ x mb1cre mice, in comparison to WT mice. The results showed no significant difference in B-cell counts from spleens of the controls (WT) and mice with over-expression of a constitutive active version of NFATc1 (caNFATc1/αA x mb1cre mice), or mice lacking the Irf4 gene (IRF4 Ko mice). But the results showed a significant increase in B-cells from spleens of mice with both over-expression of NFATc1 and inactivation of the Irf4 gene (caNFATc1/αA x mb1cre x IRF4 Ko) (Fig. 4.2).

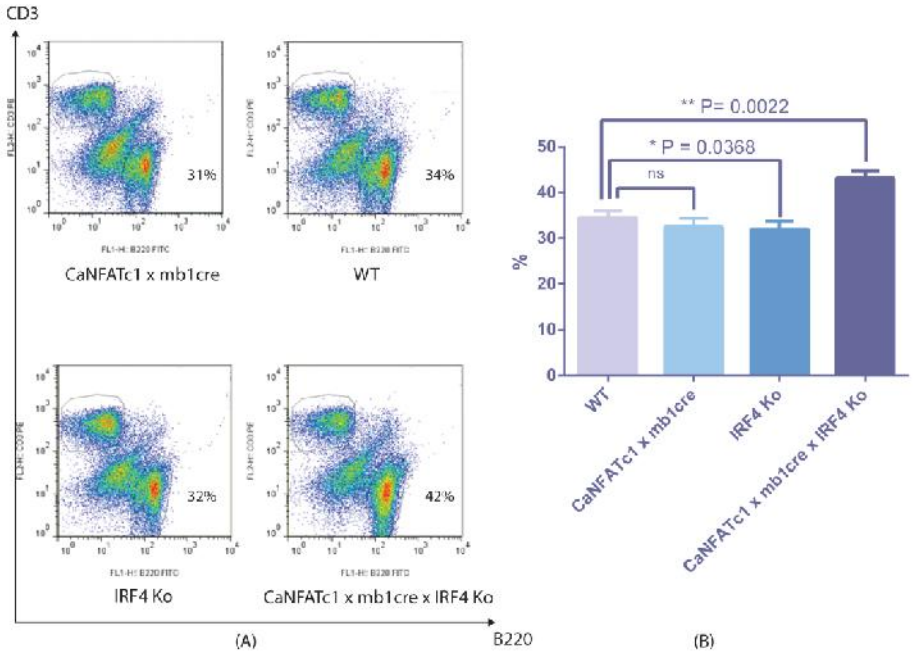

Figure 4.2: Lymphocytic counts using Flow cytometry.
Lymphocytes were isolated from spleens of WT, caNFATc1/αA x mb1cre, IRF4 $^{f/f}$ x mb1cre and caNFATc1/αA x IRF4 $^{f/f}$ x mb1cre mice. The cells were stained against the surface marker B220 (B cell marker) and CD3 (T cell marker). The B220 antibody was labeled with FITC (X axis) and CD3 with PE (Y axis). (A) FACS generated dot blots. (B) Diagram representing data from four experiments.

4.1.3. Decreased AICD (Activation induced cell death) of B cells in IRF4 Knockout mice and caNFATc1/αA x mb1cre x IRF4 Ko mice, compared to wild type mice

To explore the effect of NFATc1 and IRF4 on B cell survival, we conducted annexin-V based apoptosis assays. In these experiments we observed a

significant decrease in living cells from wild type mice when stimulated with α-IgM in comparison to non stimulated cells. Also, there was a significant decrease in the live cells from caNFATc1/αA x IRF4$^{f/f}$ x mb1cre and IRF4 Ko x mb1cre mice in comparison to cells coming from WT mice. This was found to be more significant in stimulated cells (AICD) than non stimulated cells. However, there is no significant difference between the number of living cells in Irf4Ko and caNFATc1/αA x IRF4$^{f/f}$ x mb1cre mice in both cases of IgM stimulation or non stimulation (Fig. 4.3).

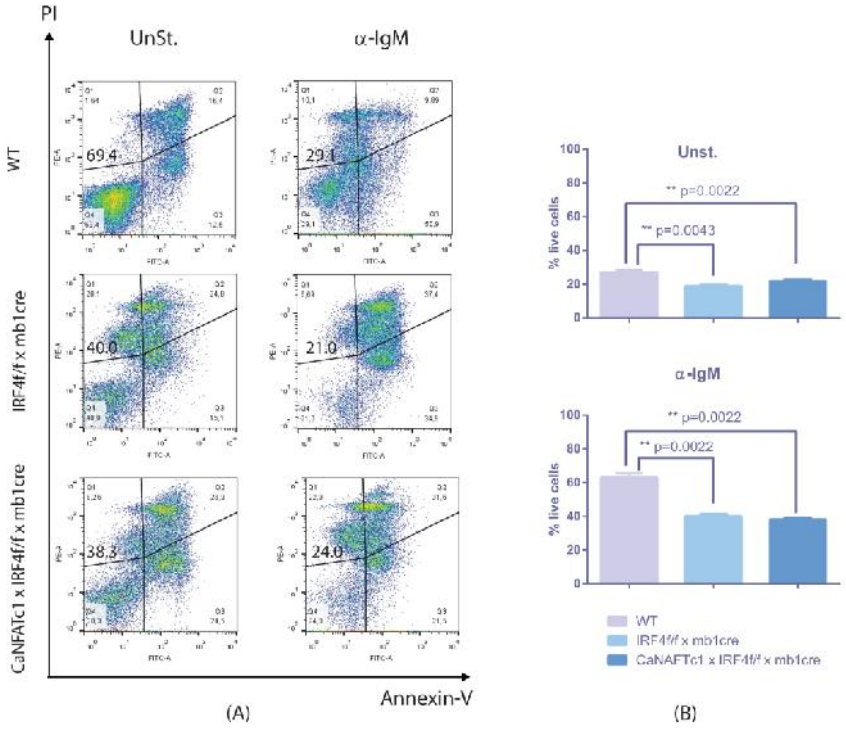

Figure 4.3: Activation Induced Cell Death (AICD) of splenic B-cells from caNFATc1/αA x IRF4$^{f/f}$ x mb1cre and IRF4$^{f/f}$ x mb1cre mice, after 48 hour incubation
Isolated B cells from WT , IRF4 $^{f/f}$ x mb1cre and caNFATc1/αA x IRF4 $^{f/f}$ x mb1cre mice/; were cultured with or without α-IgM for 48 hr. Cells were stained with Annexin-V (X axis) and propidium iodide (PI, Y axis). (A) FACs generated dot blots for numbers of apoptotic/live cells. (B) Diagram representing percentage of live cells from data of four experiments.

4.1.4. Increase in the proliferative capacity of the B cells from IRF4 knockout and caNFATc1/αA x mb1cre x IRF4 Ko mice compared to wild type mice

Using CFSE staining and the Flowjo software we wanted to examine the effect of NFATc1 and IRF4 on B cell proliferation. Data from these experiments show that with stimulation by α-IgM and LPS; the numbers of cells going into maximum number of division cycles are higher in caNFATc1/αA x IRF4$^{f/f}$ x mb1cre

than IRF4$^{f/f}$ x mb1cre which are higher than the cells from wild type mice. With α-CD40 stimulations, only the numbers of cells going into maximum number of division cycles from caNFATc1/αA x IRF4$^{f/f}$ x mb1cre mice are significantly higher than cells coming from both wild type and IRF4$^{f/f}$ x mb1cre (Fig. 4.4).

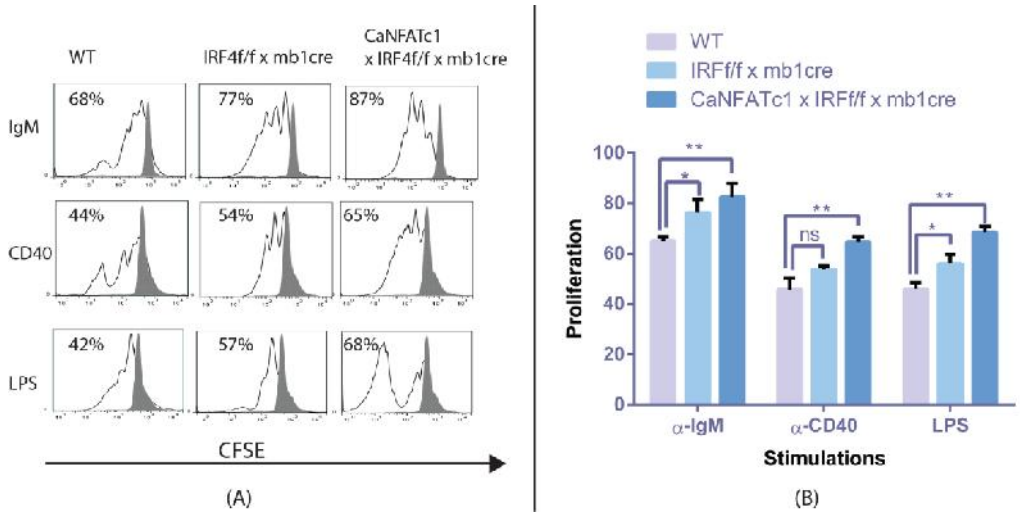

Figure 4.4: Proliferation studies of splenic B-cells from caNFATc1/αA x IRF4$^{f/f}$ x mb1cre and IRF4$^{f/f}$ x mb1cre

Isolated B cells from WT, IRF4 $^{f/f}$ x mb1cre and caNFATc1/αA x IRF4 $^{f/f}$ x mb1cre were shortly incubated with CFSE, then divided and cultured for 48h without stimulation. The stimulations included α-IgM (10µg/ml), with α-CD40 (5µg/ml) or LPS (10µg/ml). Using the Flowjo software, analysis of the proliferation based on the CFSE dilution was done. (A)FACS generated histograms demonstrating the pattern of proliferation of cells. (B) Quantative representation of data from three experiments of CFSE-based proliferation analysis.

4.1.5. In B cells the expression of RelB is affected by defects in IRF4.

To investigate the effect of the IRF4 on the NF-κB factors, the expression of Rel-B in B cells using WB was investigated. The experiments showed that upon stimulations (α-IgM, α-CD40 and LPS) for 48h, Rel-B expression was lower in IRF4$^{f/f}$ x mb1cre mice than in B-cells from wild type mice (Fig. 4.5).

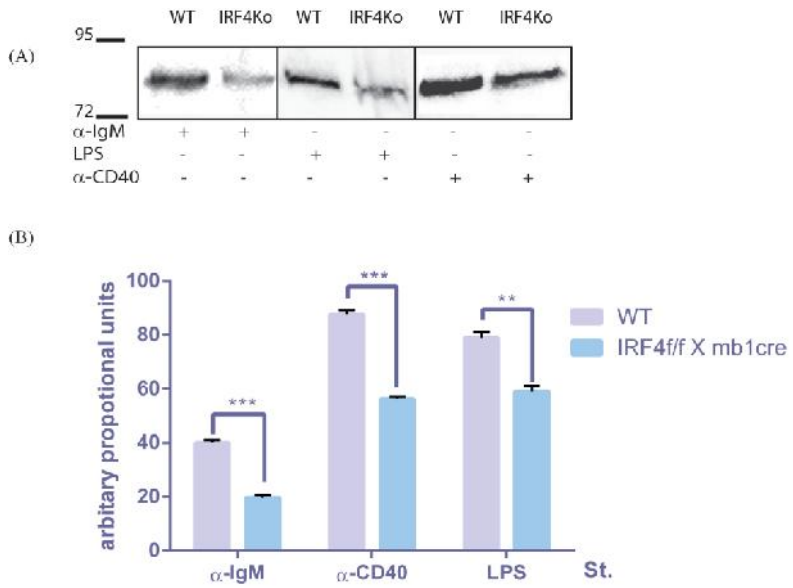

Figure 4.5: Expression of Rel-B in B-cells from IRF4Ko.
(A) The WB of the NFATc1 using whole protein extracts from splenic B cells. (B) Quantative representation of Western blot based on band intensity measurement by fusion software.

4.2. The NFAT - NF-κB connection

4.2.1. Increase in BCR-induced AICD in B cells lacking NFATc1 and/or c-Rel

To explore the interaction between the NF-κB and NFAT pathways on B cell survival, we determined by FACS using annexin-V the apoptosis rate of B cells from spleens of c-RelKo, NFATc1$^{f/f}$ x mb1cre and NFATc1$^{f/f}$ x c-RelKo x mb1cre mice, upon stimulation with α-IgM, α-CD40 and LPS for 48h. Our data did not show a significant change in live cells in the population of splenic B-cells for all gene-deficient mice (NFATc1 knock-out, c-Rel Knock-out and double knock-out) after stimulations with LPS or α-CD40, in comparison to splenic cells B cells from wild type mice and in comparison to the same type of B cells without stimulation. However, only with α-IgM there was a decrease in live cells in all gene-deficient mice in comparison to the unstimulated cells. Also, the B cells coming from double knock-out mice showed a significant decrease in the live cells, in comparison to the WT cells upon α-IgM stimulation (Fig. 4.6).

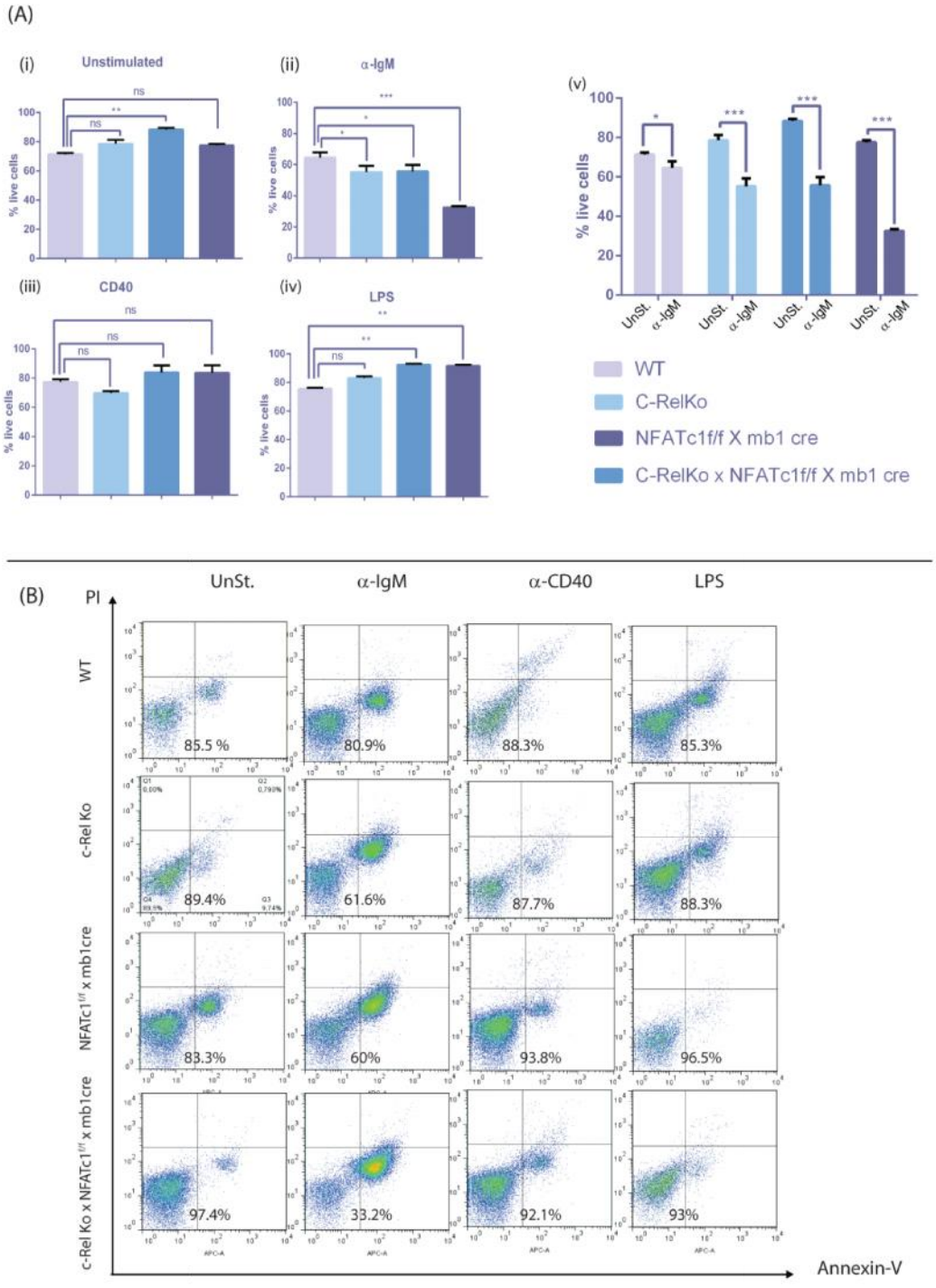

Figure 4.6: Activation Induced Cell Death (AICD) in splenic B-cells after incubation for 48 hours in c-RelKo mice.

Isolated B cells from WT, c-RelKo, NFATc1$^{f/f}$ x mb1cre and NFATc1$^{f/f}$ x c-RelKo x mb1cre mice were cultured with or without stimulation for 48h. Stimulations included α-IgM (10µg/ml), α-CD40 (5µg/ml) and LPS (10µg/ml). Cells were stained with annexin-V (X axis) and propidium iodide (PI, Y axis). (A) Diagram representing percentage of live cells from data of four experiments. (B) FACs generated dot blots for numbers of live cells from one of the experiments.

4.2.2. More defects in proliferation of DKO B cells than of B cells from single NFATc1 knock-out and c-Rel knock-out

In order to investigate the role of NF-κB and NFAT pathways on B cell proliferation, we conducted FACS-based analysis of CFSE staining and dilution for determining the proliferation of splenic B cells from c-RelKo, NFATc1$^{f/f}$ x mb1cre and NFATc1$^{f/f}$ x c-RelKo x mb1cre, in comparison to B cells from WT mice. These in vitro experiments showed that B cells from NFATc1 knock-out and c-Rel Knock-out mice exhibit a proliferative defect towards various stimulation schemes (α-IgM, LPS and α-CD40), in comparison to B cells from WT mice. This defect is even more significant in B cells coming from Double knock-out mice, deficient for both c-Rel and NFATc1 (Fig. 4.7).

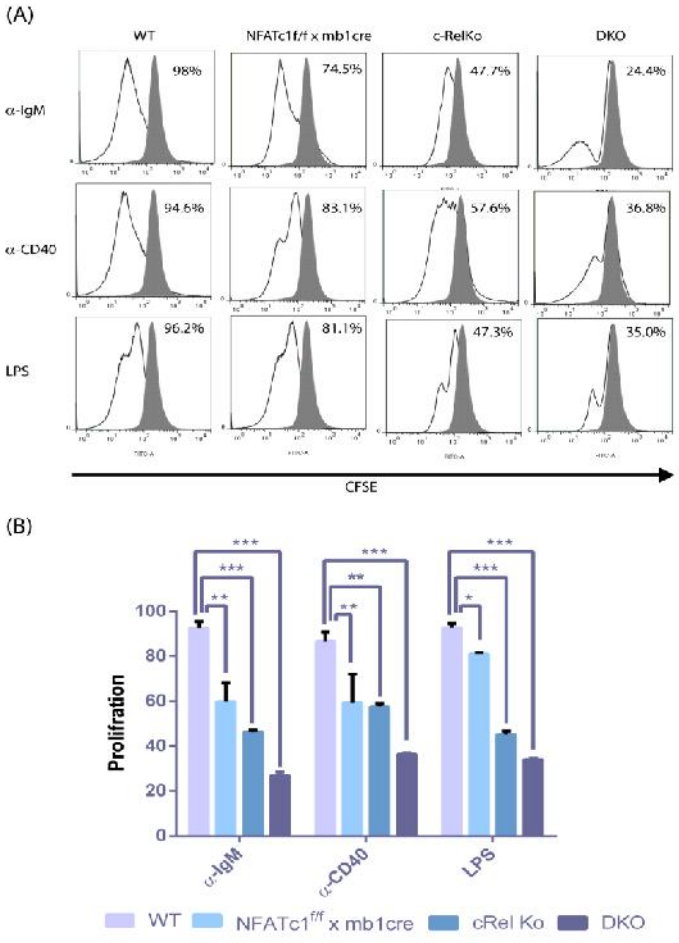

Figure 4.7: Proliferation studies of splenic B-cells deficient for NFATc1, c-Rel or both factors (DKO).
B cells isolated from WT, c-Rel Ko, NFATc1$^{f/f}$ x mb1cre and NFATc1$^{f/f}$ x c-Rel Ko x mb1cre mice were shortly incubated with CFSE, then divided and cultured without stimulation, with α-IgM for 48h, with α-CD40 for 72h or with LPS for 72h. Using Flowjo we analyzed the proliferation based on the CFSE dilution. (A) FACs generated histograms demonstrating the proliferation of cells. The grey overlay is the non-proliferating unstimulated cells (B) Quantative representation of data from three experiments of CFSE based proliferation analysis.

4.2.3. In B cells the expression of RelB is affected by NFATc1 expression

To investigate the effect of NFATc1on the expression of NF-κB members we performed several WBs. We used protein extracts of B cells from NFATc1$^{f/f}$ x CD23cre, caNFATc1/αA x CD23cre and NFATc1$^{f/f}$ x caNFATc1/αA x CD23cre mice. The WBs showed that most of the members of NF-κB remained unaffected by changes in the NFATc1 levels in B cells (Results not shown). However, in figure 4.8 we show that Rel-B (a member of the non-canonical NF-κB pathway) was affected. We demonstrate that all the α-IgM stimulated samples (last four columns) show a higher expression of Rel-B than the non-stimulated samples (first four columns). With α-IgM stimulation for 48 h, the expression from the NFATc1$^{f/f}$ x CD23cre B cells (6th column) are higher than the wild type (5th column) and the expression from the NFATc1$^{f/f}$ x caNFATc1/αA x CD23cre (7th column) are even higher than the NFATc1$^{f/f}$ x CD23cre. However, the expression in B cells from caNFATc1/αA x CD23cre (last column) is surprisingly lower than all other samples (5th, 6th and 7th).

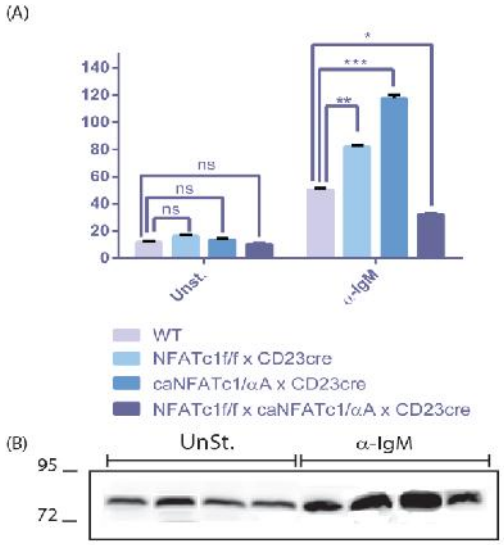

Figure 4.8: Expression of Rel-B in B-cells from NFATc1$^{f/f}$ x CD23cre, caNFATc1 xCD23cre and caNFATc1 x NFATc1$^{f/f}$ x CD23cre mice
(A) Quantative representation of the Western blot in (A) based on band intensity measurement by fusion software. (B) Western blot showing the expression of Rel-B in whole protein extracts from splenic B-cells from NFATc1$^{f/f}$ x CD23cre (NFATc1 is knocked out in splenic B cells), caNFATc1/αA x CD23cre (NFATc1/αA is over expressed in splenic B cells) and NFATc1$^{f/f}$ x caNFATc1/αA x CD23cre (NFATc1 is knocked and NFATc1/αA is over expressed in B cells) mice.

4.2.4. In B cells the expression of NFATc1 is affected by c-Rel ablation.

To investigate the effect of c-Rel ablation (a member of the canonical NF-κB pathway) on the expression of NFATc1 we performed several WBs. We used

protein extracted from B cells from wild type and c-Rel knock-out mice. As Figure 4.9 demonstrates, the WBs showed that α-IgM-induced expression of NFATc1 is strongly decreased in B-cells from c-Rel Knock-out mice, in comparison to B cells from wild type mice as early as 2 hours stimulation. This defect is even more evident over longer stimulation periods (4-24 hours).

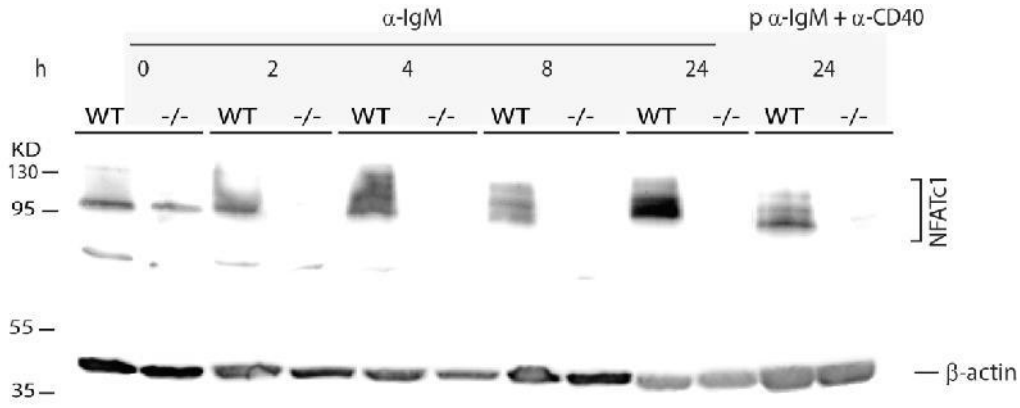

Figure 4.9: Expression of NFATc1 in B cells from c-Rel Knock-out mice.
Western blot using whole protein extracts from splenic B-cells. Cells were either left unstimulated (0h) or stimulated for 2-24h by 10µg/ml α-IgM or by 10µg/ml α-IgM for 30min followed by 5 µg/ml α-CD40 for 24h.

In these EMSAs ('Electrophoretic Mobility Shift Assays') we analyzed the DNA binding of NFAT and NF-κB factors in primary splenic B cells from wild type and c-Rel-deficient mice. Figure 4.10.A illustrates that the generation of NF-κB complexes in the absence of c-Rel was strongly impaired (lanes 9-12), in comparison to their formation in wild type extracts (lanes 1-8). More precisely, after 2 h stimulation by α-IgM a strong defect in NF-κB complex formation can be seen in wild type extracts (lanes 3 and 6). Under the same stimulation conditions no complex formation can be observed for nuclear protein extractions from B cells of c-Rel-deficient mice (lanes 11 and 12). Interestingly, a very similar effect of c-Rel ablation was observed for the appearance of nuclear NFAT complexes (see lanes 23 and 24). In agreement with the western blot data (from figure 19) these finding suggests that c-Rel exerts a strong effect on the expression and nuclear localization of NFAT factors.

In super-shift EMSA experiments we analyzed which NF-kB and NFAT proteins are affected by the missing c-Rel. The data of the super-shift EMSA experiment (figure 4.10.B) show that the α-IgM induction of NFATc1 is strongly

affected by the c-Rel ablation. In Figure 4.10.C a replication of the same experiment that emphasizes on the same results, where the NFAT complexes can be seen in the after 2 hours in the WT (lane 2) and a further supershift of the complexes that show that NFATc1(lane 3) is more expressed than NFATc2 (lane 4). On the other hand, there is lack of the NFAT complexes formation and subsequently the shifted complexes in lanes of the c-Rel knock-out (lanes 5-8). Using the κB probe we could clearly see that the c-Rel is not part of the complex (lane 15) and the main contributors are p50, p65 and RelB (lanes 13, 14 and 16) and therefore, the absence of the c-Rell is the main reason of the NFAT complex formation defects.

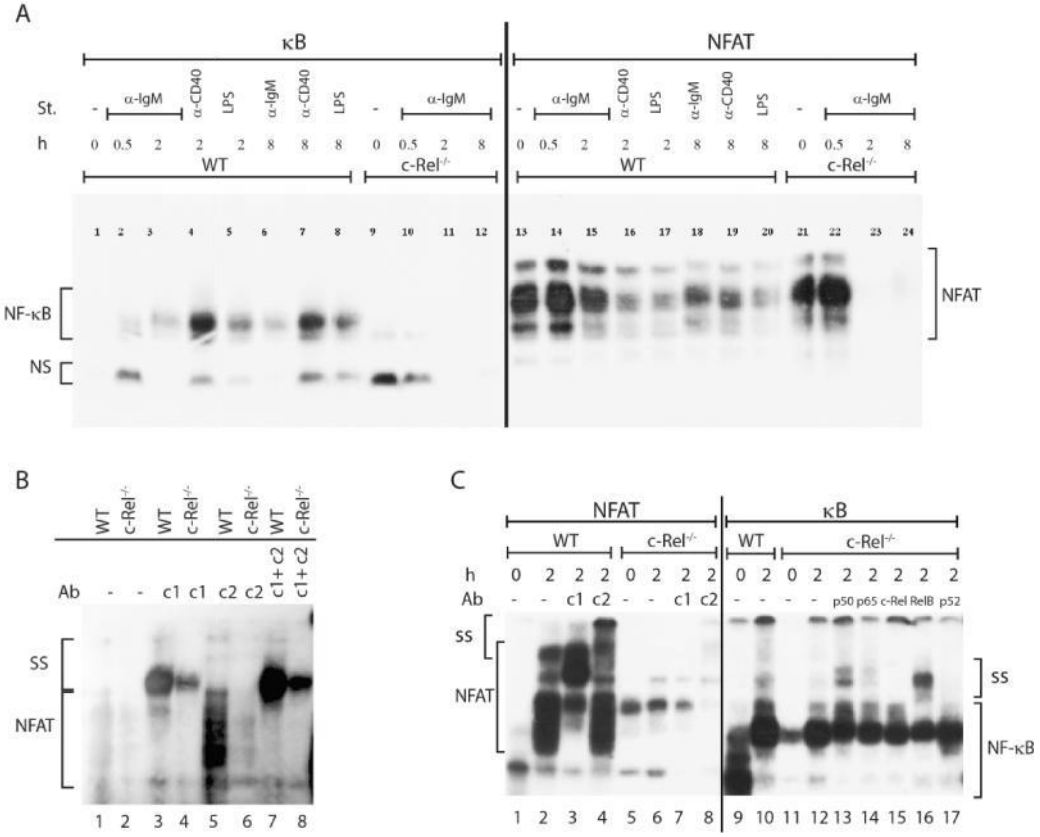

Figure 4.10: EMSA and super shift EMSA for detecting NFAT and NF-κB factors in primary splenic B cells from wild type and c-Rel-deficient mice

WT: protein extracts from wild type mice B-cells , c-Rel$^{-/-}$: protein extracts from c-Rel deficient mice B-cells. St.: the type of stimulation used. h: duration of stimulation. c1: NFATc1 antibody. c2: NFATc2 antibody. Splenic B-cells were either left untreated or treated by α-IgM, α-CD40 or LPS. The stimulations was for variable time durations as indicated. Cells were harvested, then nuclear proteins were extracted. The protein content of extracts was measured, and equal amounts of nuclear proteins were incubated – under EMSA conditions – with a radioactively labeled double-stranded probe of approximately 25 bp. Upon incubation of probe with 2.5 μg nuclear protein for 30 min on ice, the incubation mixture was loaded on a 6% non-denaturing polyacrylamide gel and fractionated for about 3 hrs. After the run, the gel was dried on a gel dryer and exposed overnight (or longer) at -70° C. A and B is from one experiment, where A is the EMSA and B is the supershift from sample 18 and sample 24 of A. C is an independent experiment with the EMSA and supershift EMSA together.

In the results from these experiments (Fig. 4.11) we could see that the c-Rel Knock-out mice has a defect of the expression of NFATc as early as the RNA synthesis with different stimulation durations (0.5, 1, 6, and 24 hours) in comparison to the RNA synthesis in case of the wild type mice. This is all in agreement with the EMSA experiments (Fig. 4.10) and the WB results (Fig. 4.9) previously presented.

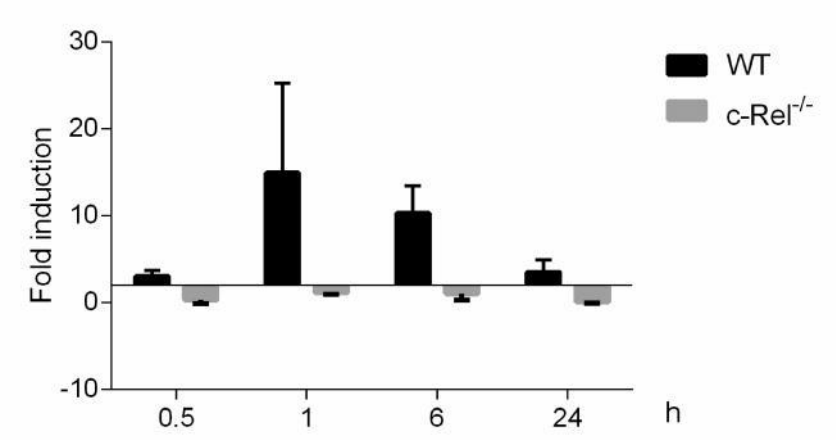

Figure 4.11: RT-PCR assay showing the generation of NFATc1 RNA from p1 in primary splenic B cells from wild type and c-Rel-deficient mice
Experiments were done three times and in each time a triplicate of the sample were used for the measurements. Stimulations used were 0.5, 1, 6, and 24 hours.

4.2.5. Plasma cells development is impaired in mice with c-Rel defect

To identify how the c-Rel abolishment may interfere with the B cell development we performed extracted B cells from spleens of WT and c-Rel knock-out mice. Stimulated them for 48 hours with different stimuli as shown in figure 4.12 and examined the formation of plasma cells using FACs and surface marker staining of B220 and CD138. The results showed that wild type mice all stimulations produce increase in plasma cell numbers that is higher from the non stimulated samples and the corresponding samples from the c-Rel Ko mice (Fig. 4.12).

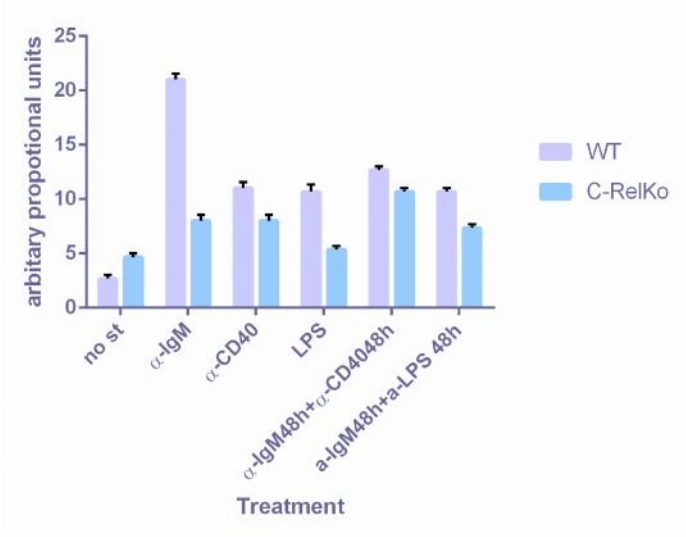

Figure 4.12: Plasma cells in c-Rel Ko mice.
Quantative representation of percentage of plasma cells in splenic B-cells from c-Rel Ko mice after different stimulation schemes. Plasma cells were identified by the surface expression of B220 and CD138.

4.3. IMQ- induced skin inflammation - a mouse model for human psoriasis

Cyclosporin A (CsA) application is one of the treatments that is included in several psoriasis management protocols. It was found that CsA modulates the immune reaction that is supposed to be part of the pathogenesis of psoriasis. Also, CsA is a known inhibitor of NFATc activation pathway by inhibiting the dephosphorylation of cytoplasmic NFATc by blocking the activity of the Ca++-dependent Ser/Thr-phosphatases calcinurine (CN). To investigate the link between psoriasis and NFAT in general and NFAT in B cells in particular the following experiments were performed.

4.3.1. IMQ induces a psoriasis-like inflammation in mice

To examine how IMQ does affect the mouse skin we applied IMQ (or a vehicle in the control group) to the shaved backs of the WT mice for 7 successive days. We observed a clear cut inflammation that started after 3 days and reached maximum after 6 days that shows many features similar to human psoriasis. By naked eye we observed erythema, scaling and thickening (Fig. 4.13.A), That we analyzed according to the modified PASI scoring system (Fig. 4.13.B). H.&E. stainings and microscopy examinations confirmed the characteristics of human psoriasis in skin sections including parakeratosis, acanthosis and elongation of the dermal papillae in the IMQ-treated mouse skin (Fig. 4.13.C: 2), in comparison to the apparently healthy skin in the vehicle-treated mouse skin (Fig. 4.13.C: 1).

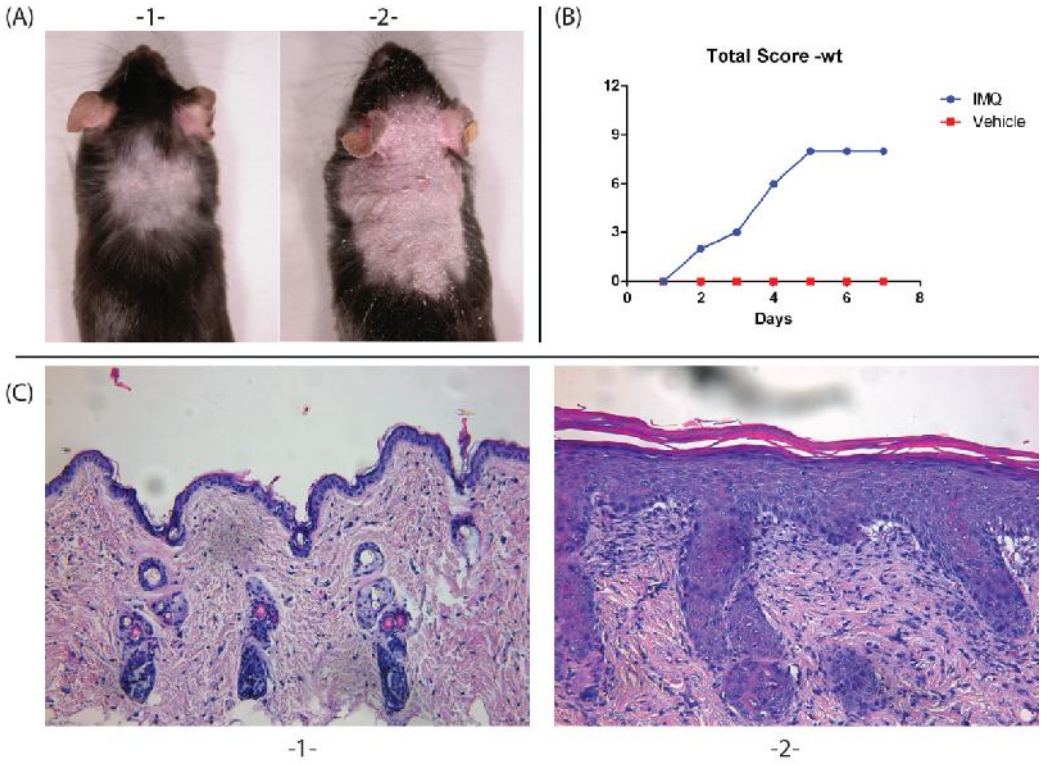

Figure 4.13: IMQ-induced psoriasis-like inflammation in WT mice.
(A) Naked eye picture examination (NE) of psoriasis like skin reaction (erythema, scaling and thickening) in wild type mice treated with IMQ -2- compared to a healthy looking skin in WT mice treated with a vehicle -1-. (B) modified psoriasis area and severity Index (mPASI). (C) Light microscopy examination (LM) of skin sections from mice after 7 days of treatment stained with H. &E. showing parakeratosis (retention of nuclei in the stratum corneum), acanthosis (thikening of the stratum basale and spinosum) and elongation of the dermal papillae in the IMQ-treated -2- in comparison to the vehicle-treated -1-.

4.3.2. The IMQ-induced psoriasis is attenuated upon NFATc1 ablation in B cells

To see if the ablation of NFATc1 from B cells may have an effect on the clinical picture of the IMQ-induced psoriasis in mice, we used IMQ on NFATc1$^{f/f}$ x mb1cre mice and WT mice in the same way as in the previous experiment. By naked eye examination the wild type mouse showed the same picture, mPASI score and H. & E. stainings as the in previous experiment (Fig. 4.14.A: 2 , Fig. 4.14.B: blue and Fig. 4.14.C: 2) of the psoriasis-like inflammation. In contrast, the clinical picture of NFATc1$^{f/f}$ x mb1cre mice showed minor -if any- alterations, in comparison WT mice (Fig. 4.14.A: 1 , Fig. 4.14.B: red and Fig. 4.14.C: 1).

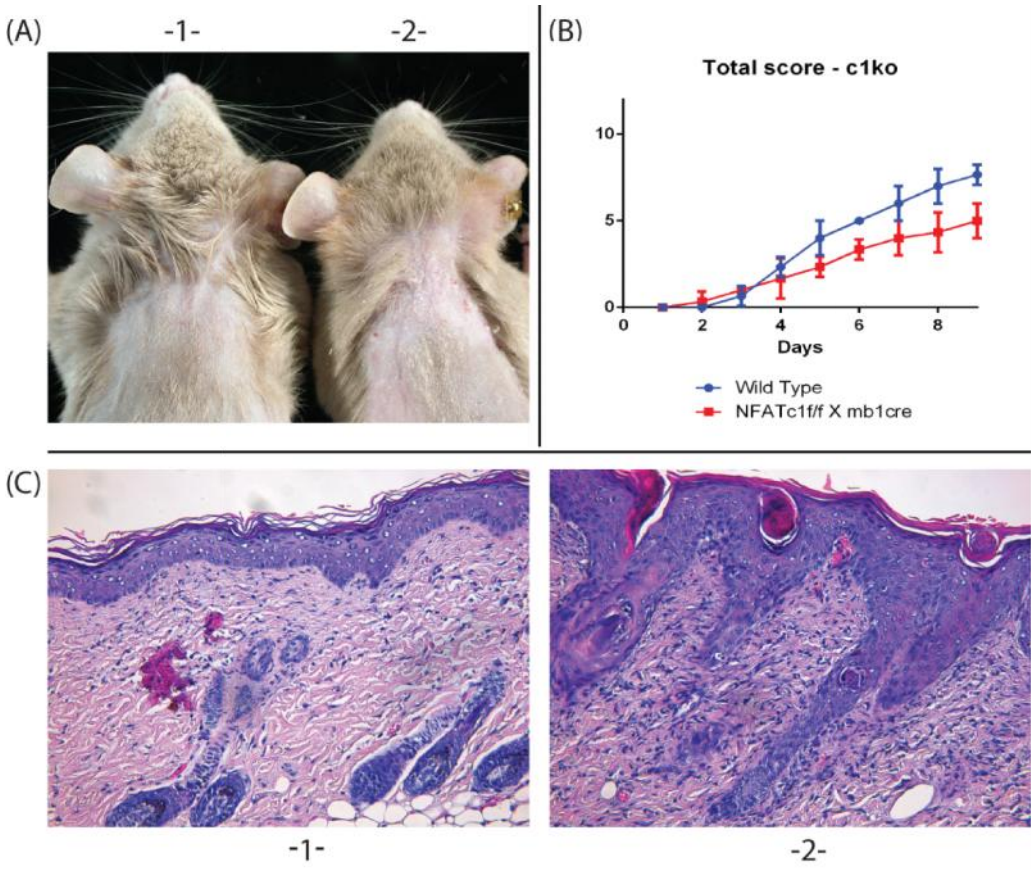

Figure 4.14: IMQ induced psoriasis-like inflammation in WT and NFATc1$^{f/f}$ x mb1cre mice.
(A) Naked eye picture examination (NE) of psoriasis like skin reaction (erythema, scaling and thickening) in wild type mice treated with IMQ -2- compared to a healthy looking skin in NFATc1$^{f/f}$ x mb1cre mice treated also with IMQ -1-. (B) modified psoriasis area and severity Index (mPASI). (C) light microscopy examination (LM) of skin sections from mice after 9 days of treatment stained with H. &E. showing parakeratosis (retention of nuclei in the stratum corneum), acanthosis (thikening of the stratum basale and spinosum) and elongation of the dermal papillae.

4.3.3. The IMQ-induced psoriasis is more severe in mice lacking B cells and the inflammation decreases upon adoptive transfer of B cells from WT mice and is nearly abolished upon transfer of B cells lacking NFATc1

To further investigate the role of B cells in psoriasis-like autoimmune pathogenesis, we explored the effect of IMQ on homozygous mb1cre mice. These mice bear two mutated mb1/Cd79a alleles that code for the α-chain of BCR. Due to this signaling defect these mice posses very low B cell numbers in periphery. Our first set of experiments showed that IMQ application on homozygous mb1cre mice produce an exaggerated psoriasis-like inflammation seen by NE (Fig. 4.15.A) that was confirmed by modified PASI scoring (Fig. 4.15.B) and H.&E. staining (Fig. 4.15.C), in comparison to the IMQ-induced psoriasis-like inflammation in WT mice. Moreover, our second set of experiments showed that the adoptive transfer of B cells from WT mice 5 days before the IMQ application decreased the psoriasis-like inflammation. More interestingly, adoptive transfer using B cells lacking NFATc1 (from NFATc1$^{f/f}$ x mb1cre mice) lead to minimal inflammation (Fig. 4.15.D and .E) indicating an important role of NFATc1 expression in B cells for the generation of psoriasis-like inflammation.

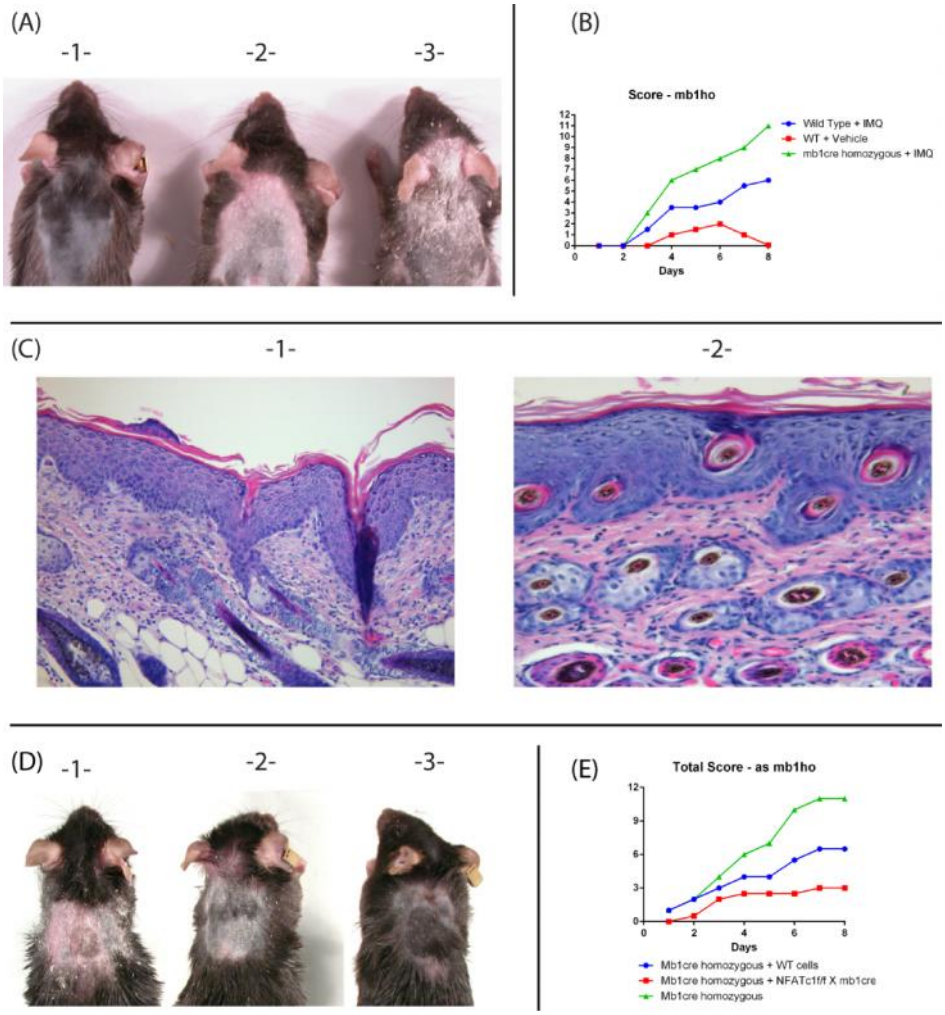

Figure 4.15: IMQ induced psoriasis-like inflammation in mice bearing two inactivated mb1/Cd79a alleles (mb1cre homozygous)

(A) Naked eye picture examination (NE) of psoriasis like skin reaction (erythema, scaling and thickening) in wild type mice treated with IMQ -2- compared to a healthy looking skin in WT mice treated with a vehicle -1-, compared to severe skin inflammation and scaling in mb1cre homozygous mice treated with IMQ -3-. (B) modified Psoriasis Area and Severity Index (mPASI). (C) Light microscopy examination (LM) of skin sections from mice after 9 days of treatment stained with H. &E. (D) -1- Naked eye examination in skin of mb1cre homozygous mice after induction of severe psoriasis-like inflammation by IMQ. -2- B cells from WT mice were adoptively transferred to the mb1cre homozygous mouse 5 days before the IMQ treatment. This mouse is showing less inflammation. -3- B cells from NFATc1$^{f/f}$ x mb1cre mouse were adoptively transferred to the mb1cre homozygous mouse 5 days before the IMQ treatment. This mouse is showing slight inflammation. (E) modified Psoriasis Area and Severity Index (mPASI) of the (D) mice.

4.3.4. Decreased Ig-class switch in IMQ-induced psoriasis-like inflammation in mice with ablated NFATc1 in B cells

To investigate the B cell compartment changes that may have a role in the differential response towards the IMQ-induced psoriasis-like inflammation, we examined surface immunoglobulin expression in B cells using FACS. We found a decrease in the B cells expressing IgG1 in mice with knocked-out NFATc1 in comparison to B cells from WT mice (Fig. 4.16).

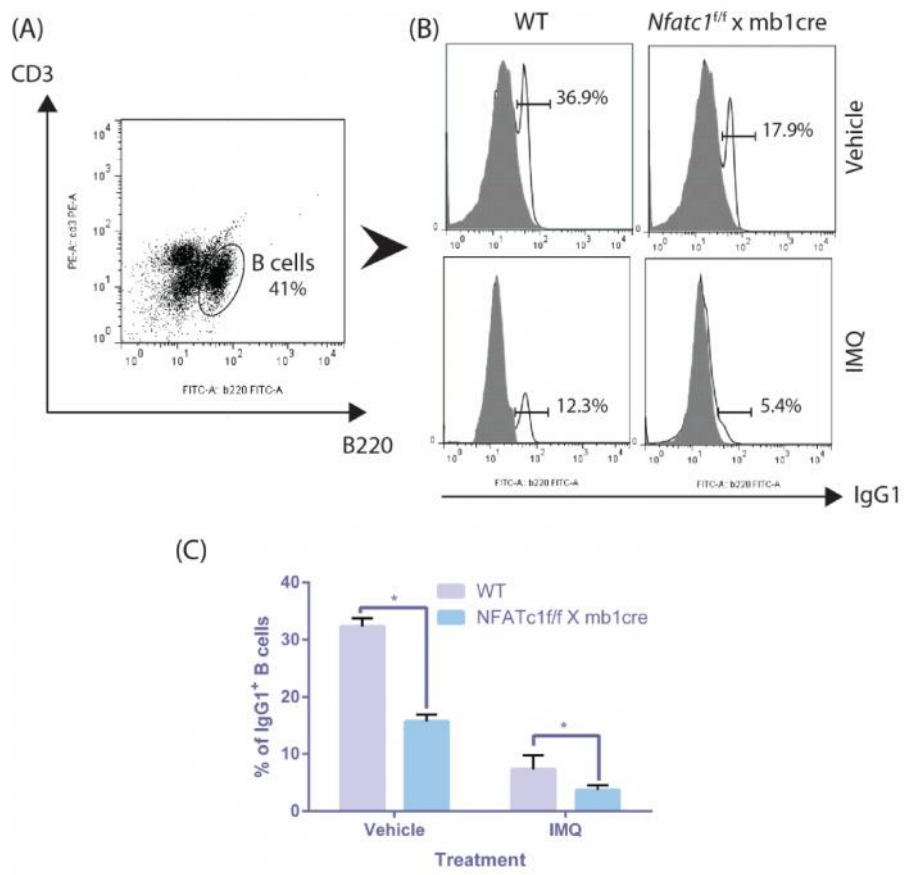

Figure 4.16: IgG1 expressing B cells from LN in IMQ induced psoriasis-like inflammation. Mice back skin was shaved then were treated by IMQ or vehicle for 8 days. Spleenocytes where isolated and stained for B220 (in FITC – horizontal axis) and IgG1 (in PE – vertical axis). (A) FACS generated dot blot demonstrating the gating protocol on the B cells using B220 and CD3 staining. B cells are $B220^{+}CD3^{-}$ (B) FACS generated histograms demonstrating the percentage of $IgG1^{+}$ B cells. The solid grey histogram is an overlay of an isotype control. (C) Quantative representation of data from four different experiments.

4.3.5. Increased numbers of Bregs in IMQ-induced psoriasis-like inflammation in mice with ablated NFATc1 in B cells

To investigate the role of Bregs in the IMQ-induced psoriasis-like inflammation, we used surface staining of B cells to analyze their numbers in the NFATc1$^{f/f}$ x mb1cre mice. After gating on B cells (B220+) the percentage of Bregs (CD5^{+} CD1d^{hi}) were found to be significantly increased in NFATc1$^{f/f}$ x mb1cre mice, compared to WT mice both with the vehicle or the IMQ application. With IMQ application the numbers of Bregs significantly increase in both WT and NFATc1$^{f/f}$ x mb1cre mice (Fig. 4.17).

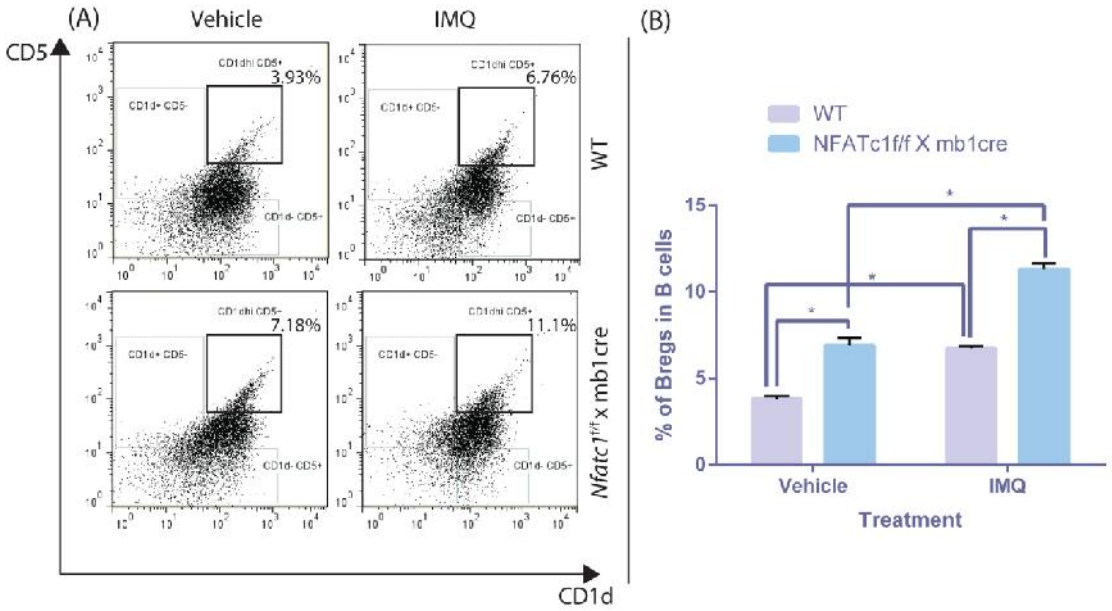

Figure 4.17: Bregs in LN in IMQ-induced psoriasis-like inflammation.
Mice back skin was shaved then were treated by IMQ or vehicle for 8 days. Spleenocytes where extracted and stained for B220 (FITC), CD1d (PE) and CD5 (PerCP). After gating on B220^{+} cells (B cells), cells were blotted using CD1d (horizontal axis) and CD5 (vertical axis). (A) FACS generated dot blot demonstrating the numbers or Bregs. The Bregs are the CD5^{+} CD1d^{hi} cells (top right gate of each blot). (B) Bar figure representing data from four different experiments.

4.3.6. Increased IL-10 expression in Bregs in IMQ-induced psoriasis in mice with ablated NFATc1 in B cells

To investigate the actual effect of the Bregs that is increased in NFATc1$^{f/f}$ x mb1cre mice in response to the IMQ-treatments, we used intracellular FACS staining to analyze the expression of IL-10 in Bregs cells. Our data showed a significant increase in IL-10 expression in NFATc1$^{f/f}$ x mb1cre mice, compared the

IL-10 expression of the Bregs cells from WT with vehicle application to the mice. Additionally, this significance is increased in response to IMQ treatment (Fig. 4.18)

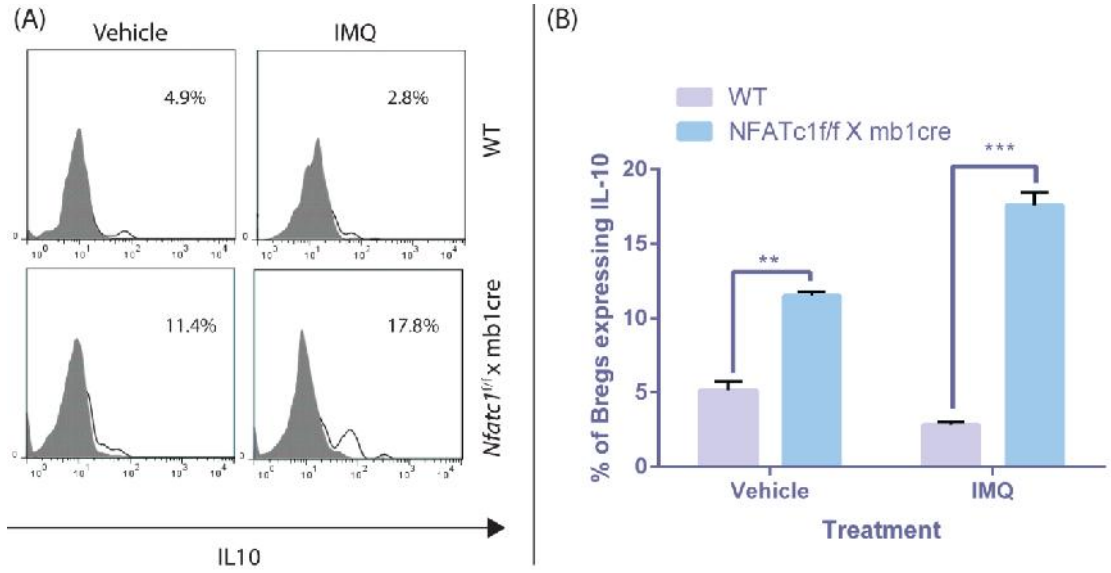

Figure 4.18: IL-10 expression from Bregs in LN in IMQ induced psoriasis-like inflammation. Mice back skin was shaved, then were treated by IMQ or vehicle for 8 days. Spleenocytes where isolated and stained for B220 (FITC), CD1d (PE), CD5 (PerCP) and IL-10 (APC). After gating on B220+ cells (B cells), cells were blotted using CD1d and CD5. After that, we re-gated on Bregs (CD5+ CD1dhi cells). (A) FACS generated histogram of the IL-10 expression showing the expression of IL10. The solid grey histogram is an overlay of an isotype control. (B) Bar figure representing data from four different experiments.

5. Discussion

5.1. Expression of a constitutive active version of NFATc1 (caNFATc1/αA) with ablated IRF4 in B cells from mice.

The NFAT factors NFATc1, NFATc2 and NFATc3 are expressed in immune cells, especially B and T cells, and regulate their development and function through regulating gene expression. The Ca^{++}-calcineurin axis in general and the NFATc factors in particular are induced through the immune receptors and regulate transcriptional states of important genes of lymphokine production (IL-2) (Nguyen et al., 2010), proliferation (CDK4) (Baksh et al., 2002) and apoptosis (Fas ligand, FASLG) (Lee et al., 2002). Retroviral tagging experiments provided data that proves that most of the oncogenic virus binding sites lies in close vicinity of the murine NFATc1 promoter indicating that its part of the modulatory effect of the virus in the infected cell (Serfling et al., 2006a).

To test the effect of over expression of NFATc1/αA on B cells we generated the caNFATc1/αA x mb1cre mice which over express the NFATc1/αA in B cells and we proved that the expression of the NFATc1 is high even without any stimulation (Fig. 4.1). We also generated an IRF4 $^{f/f}$ x mb1cre mouse to be crossed with the caNFATc1/αA x mb1cre producing an effect that includes disruption of the late stages of B cell development as occurring in lymphoid tumors (Calado et al., 2010). Our experiments showed that the isolated effect of constitutive NFAtc1 or knocked out IRF4 does not cause any effect in the development and hence the numbers of B cells. However, we found increased numbers of splenic B cells in mice with both constitutive NFATc1 and a knocked out IRF4 (Fig. 4.2), indicating that a ‘double hit’ in factors affecting B cell activation (NFATc1 in this case) and late B cell differentiation (IRF4 in this case) is needed to alter the development of the B cells and lead to increase in their numbers above normal. Also there was increased stimulation induced proliferation of the B cells from either the mice with the missing IRF4 alone or together with the over expressed NFATc1 pointing to a state of uncontrolled proliferation (Fig. 4.4). This is similar to previous cell line transfection studies which revealed that over-expression of NFATc1/αA leads to increased

proliferation and cell transformation marking it as a potential oncogene in lymphocytes (Robbs et al., 2008). Also in line with Pham's group, which proved that NFATc1 recruit chromatin remodeling complexes to targeted gene promoters leading to alteration of gene expression in DLBCL cells (diffuse large B cell lymphoma) (Pham et al., 2010). Nevertheless, in our experiments the cell survival of the transgenic mice was less than the wild type mice (Fig. 4.3), implying that NFATc1 over expression and/or IRF4 Knock out may not predispose to tumorogenesis in a direct explicit mechanism. However, the overall picture of a 'double hit' effect could be related to the work from Rajewsky's group that addresses the NF-κB over-expression together with the BLIMP-1 disruption (Calado et al., 2010). Putting in mind the data of Lu et al. which suggest that IRF4 controls the expression of BLIMP-1, we can assume that the effect of IRF4 knock out will have a similar effect as the BLIMP-1 (Lu, 2008). The provisional experiments to identify the molecular interaction of IRF4 that leads to such changes in B cell physiology showed affection of the Rel-B of the non canonical NF-κB pathway.

5.2. The NFAT - NF-κB connection

5.2.1. Increase in BCR-induced AICD in B cells lacking NFATc1 and c-Rel

Our data showed that ablation of NFATc1 or c-Rel alone in B cells does not impair apoptosis. However, the BCR induced AICD (upon α-IgM stimulation) is significantly increased in DKO B cells, in comparison to WT or to single knock-out of NFATc1 or c-Rel (Fig. 4.6). This may point that defects in either single members of the pathway does not affect cell survival. Nevertheless, the activation of the BCR signals in the absence of NFATc1 or c-Rel impairs cell survival by inducing more AICD especially with defects in both pathways (DKO mice). That may indicate that both of these members play a co-operative role in B cell survival. This is in accordance with previous results from our laboratory that states that the BCR induced AICD is increased in NFATc1 knock-out B cells (Bhattacharyya et al., 2011), but this increase is dependent on the strength of the α-IgM mediated BCR signals. High concentrations of α-IgM, such as 10μg/ml and more, could 'overplay' the defect in the BCR-mediated AICD. The c-Rel knock out effect is also fitting well with the findings of Gerondakis that proved that A1 induction through c-Rel signals

protect B cells from BCR-induced AICD (Grumont et al., 1999). The absence of such profound effect with the stimulation of other B cell receptors (Toll-like receptor or CD40) is probably due to the intact functions of other members of the NF-κB family, as the original producers of the c-Rel Knock-out mice states (Kontgen et al., 1995). Our other results show that other members of the canonical pathway are intact and remained unchanged in expression in NFATc1 knock-out mice (unbuplished data, Serfling et al). Also, our results could be understood in the light of data demonstrating that the molecular interaction of c-Rel with Bim (Bcl-2 member) leading to neutralization of specific phosphorylation pro-apoptotic signals which support B cell survival (Banerjee et al., 2008).

5.2.2. More defects in proliferation of DKO B cells than of B cells from single NFATc1 knock-out and c-Rel knock-out

Our experiments showed a cumulative negative effect in proliferation of B cells from the double knock out of NFATc1 and c-Rel, compared to the B cells from single knock-out of NFATc1 or c-Rel (Fig. 4.7). The proliferative defect in NFATc1 deficient mice is in accordance to previous results of our laboratory (Bhattacharyya et al., 2011). These results may be explained by the interaction of NFATc1 with STAT-3 as previously proposed by Kundumani-Sridharan (Kundumani-Sridharan et al., 2012). On the other hand, the proliferative defect of B cells from c-Rel knock-out mice goes well with other data from the Gerondakis group (Kontgen et al., 1995). It could be accounted by the effect on Cyclin E and Bcl-xL explained by Cheng (Cheng et al., 2003). Taken together these data with our findings indicate that the cumulative effect observed from the DKO B cells is due to a complimentary effect of both TFs on B cell proliferation.

5.2.3. In B cells the expression of RelB is affected by NFATc1 expression whereas the expression of NFATc1 is affected by c-Rel.

The link between the members of NFAT and NF-κB families has always been rooted to the RHD that represents the DNA binding domain of both factors. RHD mediates most of the NFAT interactions with the DNA binding motifs of both

transcription factors. In our hands (Fig. 4.8) we could show that RelB expression in B cells is increased in mice lacking NFATc1 in B cells ($NFATc1^{f/f}$ x CD23cre mice) and decreased in the mice with the overexpressed NFATc1 (caNFATc1/αA x CD23cre mice). This inverse connection between NFATc1 expression and RelB expression points to an opposing interplay between the NFAT pathway and the non-canonical NF-κB pathway. However, this observation is not supported by data showing the inhibition of NFAT-affected gene expression using VIVIT and not genes affected by NF-κB (Aramburu et al., 1999). But it might be in line with data from the group of Cai et al. who proved that activation of NFAT and NF-κB dependens on each other (Cai et al., 2011).

On the other hand, our WB experiments showed that at the protein level the expression of NFATc1 is defective in c-Rel Knock-out mice (Fig. 4.9). In addition, the RNA transcripts of P1-directed NFATc1/α were also severely impaired in c-Rel knock-out mice, as shown in our RT-PCR experiments (Fig. 4.11). Moreover, the EMSA and super shift EMSA data support these findings by the lack of NFAT complexes in nucleoprotein extracts of B cells from c-Rel knock-out mice after 2 hours of B cell stimulation (Fig. 4.10). This points to a role of c-Rel (as a member of the canonical NF-κB pathway) in sustaining NFATc1 expression. This finding - together with the previously suggested RelB role- indicate a double edged relationship of the NFAT pathway with the two sides of the NF-κB pathway (i.e. the canonical and the non-canonical pathways). This is supported by research findings from cancer fields that suggests a close association between NFAT and NF-κB regarding co-expression and constitutive expression. One of these findings comes from studies of pancereatic cancer cells. Kalthoff and colleagues showed that both NFAT and NF-κB factors are crucial for tumor development and chemotherapy resistance in pancreatic cancer (Arlt et al., 2012). Furthermore, it is worth to notice that DNA binding motifs that are bound by both NF-κB and NFAT members are found in the promoters of many inducible genes (eg. Nfatc1 P1 promoter) and are also considered as optimal c-Rel binding sites. Accordingly, we could infer that both c-Rel or NFATc affect the fate of peripheral B cells through theses motifs (Kunsch et al., 1992).

Two studies report on a direct interaction between NF-κB and NFAT proteins under over-expression conditions. One of these investigates deals with the CD154/CD40LG promoter in human LBCL lymphoma cells. The other investigates the function of NFATc1 in neonatal cardiomyocytes. In both of them, they use super-shift EMSA to suggest a co-operative hetero-dimer formation between NFATc1 and c-Rel. Conversely, they do not show any prove of interaction between NFAT and NF-κB without over-expression (physiological conditions) and they do not investigate how the protein-protein interactions between the two factors affect their DNA binding and, thereby, the activity of genes.

My data on the role of c-Rel on NFATc1 expresion (shown in figures 4.8, 4.9, 4.10 and 4.11) and other data from our group (not shown here) indicate that the induction of NFATc1 is supported by c-Rel expression. c-Rel binds to the P1 promoter of Nfatc1 in which two composite κB/NFAT sites for the binding of both c-Rel/p50 and NFATc1 are situated. The data propose that according to the predominating levels of these factors during physiological or pathological conditions (eg. cancer), they bound independently to the composite κB/NFAT binding sites found in the promoters of many inducible genes.

5.2.4. Plasma cells development is impaired in mice with c-Rel defect

Our flow-cytometry analysis of B cell surface markers showed a defect in B cell development towards plasma cells in c-Rel knock-out mice (Fig. 4.12). This is consistent with the results of Kontgen et al. who showed a defect in antibody production in B cells from c-Rel knock-out mice (Kontgen et al., 1995). The work of other laboratories confirmed that c-Rel activation is important for the generation of GC B cells and plasma cells (Klein and Dalla-Favera, 2008).

5.3. IMQ-induced skin inflammation - a mouse model for human psoriasis

5.3.1. IMQ induces a psoriasis-like inflammation in mice

The development of inflammation in the skin of mice following the application of IMQ was first reported by Gilliet in 2004. The study concluded the important role of innate immunity in the development of a psoriasis-like inflammation (Gilliet et al., 2004). In order to test the model, we applied IMQ in Aldara creme (or a vehicle in the control group) to the shaved backs of WT mice for 7 successive days, and observed a clear cut inflammation that started after 3 days and reached maximum after 6 days. The inflammatory reaction was very similar to psoriasis by naked eye inspection: erythema, scaling and thickeningof the skin was observed (Fig. 4.13.A). We analyzed these alterations according to the modified PASI scoring system (Fig. 4.13.B). H.&E. staining and microscope examination confirmed the characteristics of the psoriasis generation in skin sections, including parakeratosis, acanthosis and elongation of the dermal papillae (Fig. 4.13.C). This is in accordance to previous results of the Burkhard Becher group. However, these sceintists investigated the pathogenesis of inflamation from the T cells side and found that IL17 in the psoriasis-like inflamation does not come only from Th17 cells but also from Rorγt+ and γδ T cells (Pantelyushin et al., 2012).

5.3.2. The IMQ-induced psoriasis is attenuated upon NFATc1 ablation in B cells

The treatment regimens of psoriasis included cyclosporin A application, as early as the autoimmune background of the disease was recognized. Cyclosporin A inhibits the immune reaction through suppression of the Ca^{++}-calcinurine pathway. Because NFAT is activated through signals of the Ca^{++}-calcinurine pathway upon de-phosphorylation by the phosphatase calcinurine, we wanted to investigate the probability of NFAT involvement in the IMQ-induced psoriasis-like inflammation. When we used IMQ application on $NFATc1^{f/f}$ x mb1cre mice, we found a dramatic decrease in the psoriasis-like inflammation, in comparison to WT mice. This clearly points that NFATc1 is part of the signaling pathway that contributes to psoriasis development. Additionally, it also points that B cells are important in the protection from the psoriasis as NFATc1 in these mice was missing only in B cells (Fig. 4.14).

This is well understood in the light of the various data that incorporate NFAT with most of lymphocyte functions (Serfling et al., 2007). On their work on the CNS, the laboratory of Lodygin et al. presented data that considered NFAT activation as a crucial initiating step in autoimmunity (Lodygin et al., 2013). Moreover, it was suggested that NFATc1 is important in regulating the proliferation and differentiation of keratinocytes, based on its expression in normal and pathogenic human keratinocytes (Al-Daraji et al., 2009). However, some data presented by Ghosh et al. seem to disagree, indicating that hyperactive NFAT maybe a 'muffler' for development of the murine autoimmune encephalomyelitis. These authors are actually describing a picture for the T cell compartment and incorporating a status of increased IL-10 expression from CD4 T cells (Ghosh et al., 2010).

5.3.3. The IMQ-induced psoriasis is more severe in mice lacking B cells and the inflammation decreases upon adoptive transfer of B cells from WT mice and is nearly abolished upon transfer of B cells lacking NFATc1

In order to delineate the actual role of B cell involvement in the IMQ-induced psoriasis-like inflammation we used mb1cre homozygous mice which due to the inactivation of the BCR-α-chain have a minimal number of B cells. With IMQ application on these mice we observed an exaggerated psoriasis-like inflammation by naked eye examination (Fig. 4.15.A). This is also reflected on scores using the modified PASI scoring system (Fig. 4.15.B). The H.&E. stained skin sections showed a severe picture of hyperproliferative inflammation (Fig. 4.15.C). Moreover, the adoptive transfer of B cells from WT mice 5 days before the IMQ application decreased psoriasis-like inflammation, but more interestingly, using B cells lacking NFATc1 (from $NFATc1^{f/f}$ x mb1cre mice) lead to a less profound inflammation (Fig. 4.15.D and .E). This shows that the ablation of NFATc1 in B cells is important for protection from IMQ-induced psoriasis-like inflammation. The results of Sato's group agree with our view of the importance of B cells in psoriasis. They used $CD19^{-/-}$ mice, another model of B cell-deficiency in mice. They showed a similar increase in the severity of the IMQ-induced psoriasis-like inflammation as in our mb1-cre homozygous mouse model (Yanaba et al., 2013).

5.3.4. Decreased class switching in IMQ-induced psoriasis-like inflammation in mice with ablated NFATc1 in B cells

To examine the effect of the lack of NFATc1 in B cells that lead to the dampening effect on IMQ-induced psoriasis-like inflammation we studied the surface immunoglobulin expression in B cells using FACS. We found a decrease in the B cells expressing IgG1 in mice with knocked-out NFATc1 in comparison to B cells from WT mice (Fig. 4.16), indicating a decrease in Ig class switch. The lack of class switch points to less reactive B cells towards antigens. This may be in agreement with results by Wang's laboratory, that suggest that psoriasis pathogesis is in part due to loss of tolerance towards self antigens which leads to reaction of the immune cells towards RNA and DNA released from the keratinocytes in the process of inflammation (Lande et al., 2007). In our NFATc1 x mb1cre mice, the decreased reactivity of B cells due to less class switching leads to decrease in immune reactions towards the keratinocytes, subsequently, to a decrease in psoriasis-like inflammation in response to IMQ treatment. This is also compatible to data published from our laboratory that show that in NFATc1$^{f/f}$ x CD23-cre mice due to the ablation of NFATc1, Ig class switch is strongly impaired upon T cell–independent immune reactions (Bhattacharyya et al., 2011).

5.3.5. Increased numbers of Bregs in IMQ-induced psoriasis in mice with ablated NFATc1 in B cells

Further analysis of the NFATc1$^{f/f}$ x mb1cre mice showed an increase in the percentage of Bregs upon the IMQ treatment (Fig. 4.17). This indicates that the inactivation of NFATc1 on bone marrow B cells leads to more Breg numbers in periphery. Subsequently, this causes an inhibitory effect on the psoriasis-like inflammation. This scenario fits well to the role of Bregs in psoriasis-like inflammation proposed by Sato's group. Their data also identified IL-17 and IFN-γ as central players in the Bregs mediated suppression of psoriasis (Yanaba et al., 2013).

5.3.6. Increased IL-10 expression from Bregs in IMQ-induced psoriasis in mice with ablated NFATc1 in B cells

The analysis of Bregs showed more IL-10 expression by these cells in NFATc1$^{f/f}$ x mb1cre mice, compared to the IL-10 expression of the same Bregs in WT mice in response to IMQ treatment (Fig. 4.18). This suggests that IL-10 maybe one of the players that mediates the B cell dampening effect on IMQ-induced psoriasis-like inflammation in NFATc1$^{f/f}$ x mb1cre mice. These findings are in agreement with previous data from our laboratory that could explain the role of NFATc1 in murine autoimmune encephalomyelitis, a mouse model of human multiple sclerosis (MS). NFATc1$^{f/f}$ x CD23-cre mice showed also decreased levels of IL-10 from B cells which is concomitant with the less severe form of EAE in these mice (Bhattacharyya et al., 2011). These EAE data are in agreement with the data from Sato's group on the role of Bregs in the generation of psoriasis-like inflammation (Yanaba et al., 2013).

6. References

Ahlehoff, O., G.H. Gislason, M. Charlot, C.H. Jorgensen, J. Lindhardsen, J.B. Olesen, S.Z. Abildstrom, L. Skov, C. Torp-Pedersen, and P.R. Hansen. 2011. Psoriasis is associated with clinically significant cardiovascular risk: a Danish nationwide cohort study. *J Intern Med* 270:147-157.

Al-Daraji, W.I., T.T. Malak, R.J. Prescott, A. Abdellaoui, M.M. Ali, T. Dabash, B.G. Zelger, and B. Zelger. 2009. Expression, localisation and functional activation of NFAT-2 in normal human skin, psoriasis, and cultured keratocytes. *Int J Clin Exp Med* 2:176-192.

Aldinucci, D., B. Rapana, K. Olivo, D. Lorenzon, A. Gloghini, A. Colombatti, and A. Carbone. 2010. IRF4 is modulated by CD40L and by apoptotic and anti-proliferative signals in Hodgkin lymphoma. *Br J Haematol* 148:115-118.

Aramburu, J., M.B. Yaffe, C. Lopez-Rodriguez, L.C. Cantley, P.G. Hogan, and A. Rao. 1999. Affinity-driven peptide selection of an NFAT inhibitor more selective than cyclosporin A. *Science* 285:2129-2133.

Arlt, A., H. Schafer, and H. Kalthoff. 2012. The 'N-factors' in pancreatic cancer: functional relevance of NF-kappaB, NFAT and Nrf2 in pancreatic cancer. *Oncogenesis* 1:e35.

Augustin, M., G. Glaeske, M.A. Radtke, E. Christophers, K. Reich, and I. Schafer. 2010a. Epidemiology and comorbidity of psoriasis in children. *Br J Dermatol* 162:633-636.

Augustin, M., K. Reich, G. Glaeske, I. Schaefer, and M. Radtke. 2010b. Co-morbidity and age-related prevalence of psoriasis: Analysis of health insurance data in Germany. *Acta Derm Venereol* 90:147-151.

Baksh, S., H.R. Widlund, A.A. Frazer-Abel, J. Du, S. Fosmire, D.E. Fisher, J.A. DeCaprio, J.F. Modiano, and S.J. Burakoff. 2002. NFATc2-mediated repression of cyclin-dependent kinase 4 expression. *Mol Cell* 10:1071-1081.

Balkhi, M.Y., J. Willette-Brown, F. Zhu, Z. Chen, S. Liu, D.C. Guttridge, M. Karin, and Y. Hu. 2012. IKKalpha-mediated signaling circuitry regulates early B lymphopoiesis during hematopoiesis. *Blood* 119:5467-5477.

Banerjee, A., R. Grumont, R. Gugasyan, C. White, A. Strasser, and S. Gerondakis. 2008. NF-kappaB1 and c-Rel cooperate to promote the survival of TLR4-activated B cells by neutralizing Bim via distinct mechanisms. *Blood* 112:5063-5073.

Berland, R., and H.H. Wortis. 2003. Normal B-1a cell development requires B cell-intrinsic NFATc1 activity. *Proc Natl Acad Sci U S A* 100:13459-13464.

Bhattacharyya, S., J. Deb, A.K. Patra, D.A. Thuy Pham, W. Chen, M. Vaeth, F. Berberich-Siebelt, S. Klein-Hessling, E.D. Lamperti, K. Reifenberg, J. Jellusova, A. Schweizer, L. Nitschke, E. Leich, A. Rosenwald, C. Brunner, S. Engelmann, U. Bommhardt, A. Avots, M.R. Muller, E. Kondo, and E. Serfling. 2011. NFATc1 affects mouse splenic B cell function by controlling the calcineurin--NFAT signaling network. *J Exp Med* 208:823-839.

Blumberg, H., H. Dinh, E.S. Trueblood, J. Pretorius, D. Kugler, N. Weng, S.T. Kanaly, J.E. Towne, C.R. Willis, M.K. Kuechle, J.E. Sims, and J.J. Peschon. 2007. Opposing activities of two novel members of the IL-1 ligand family regulate skin inflammation. *J Exp Med* 204:2603-2614.

Brandrup, F., and A. Green. 1981. The prevalence of psoriasis in Denmark. *Acta Derm Venereol* 61:344-346.

Briney, B.S., and J.E. Jr. 2013. Secondary mechanisms of diversification in the human antibody repertoire. *Front Immunol* 4:42.

Cai, T., X. Li, J. Ding, W. Luo, J. Li, and C. Huang. 2011. A cross-talk between NFAT and NF-kappaB pathways is crucial for nickel-induced COX-2 expression in Beas-2B cells. *Curr Cancer Drug Targets* 11:548-559.

Calado, D.P., B. Zhang, L. Srinivasan, Y. Sasaki, J. Seagal, C. Unitt, S. Rodig, J. Kutok, A. Tarakhovsky, M. Schmidt-Supprian, and K. Rajewsky. 2010. Constitutive canonical NF-kappaB activation cooperates

with disruption of BLIMP1 in the pathogenesis of activated B cell-like diffuse large cell lymphoma. *Cancer Cell* 18:580-589.

Carrasco, D., F. Weih, and R. Bravo. 1994. Developmental expression of the mouse c-rel proto-oncogene in hematopoietic organs. *Development* 120:2991-3004.

Chen, G.Y., Y.W. Cheng, C.Y. Wang, T.J. Hsu, M.M. Hsu, P.T. Yang, and W.C. Chen. 2008. Prevalence of skin diseases among schoolchildren in Magong, Penghu, Taiwan: a community-based clinical survey. *J Formos Med Assoc* 107:21-29.

Chen, L., J.N. Glover, P.G. Hogan, A. Rao, and S.C. Harrison. 1998. Structure of the DNA-binding domains from NFAT, Fos and Jun bound specifically to DNA. *Nature* 392:42-48.

Cheng, S., C.Y. Hsia, G. Leone, and H.C. Liou. 2003. Cyclin E and Bcl-xL cooperatively induce cell cycle progression in c-Rel-/- B cells. *Oncogene* 22:8472-8486.

Chung, Y., S.H. Chang, G.J. Martinez, X.O. Yang, R. Nurieva, H.S. Kang, L. Ma, S.S. Watowich, A.M. Jetten, Q. Tian, and C. Dong. 2009. Critical regulation of early Th17 cell differentiation by interleukin-1 signaling. *Immunity* 30:576-587.

Chuvpilo, S., A. Avots, F. Berberich-Siebelt, J. Glockner, C. Fischer, A. Kerstan, C. Escher, I. Inashkina, F. Hlubek, E. Jankevics, T. Brabletz, and E. Serfling. 1999. Multiple NF-ATc isoforms with individual transcriptional properties are synthesized in T lymphocytes. *J Immunol* 162:7294-7301.

Chuvpilo, S., E. Jankevics, D. Tyrsin, A. Akimzhanov, D. Moroz, M.K. Jha, J. Schulze-Luehrmann, B. Santner-Nanan, E. Feoktistova, T. Konig, A. Avots, E. Schmitt, F. Berberich-Siebelt, A. Schimpl, and E. Serfling. 2002. Autoregulation of NFATc1/A expression facilitates effector T cells to escape from rapid apoptosis. *Immunity* 16:881-895.

Crist, S.A., D.L. Sprague, and T.L. Ratliff. 2008. Nuclear factor of activated T cells (NFAT) mediates CD154 expression in megakaryocytes. *Blood* 111:3553-3561.

Crow, J.M. 2012. Psoriasis uncovered. *Nature* 492:S50-51.

DiLillo, D.J., T. Matsushita, and T.F. Tedder. 2010. B10 cells and regulatory B cells balance immune responses during inflammation, autoimmunity, and cancer. *Ann N Y Acad Sci* 1183:38-57.

Dowlatshahi, E.A., M. Wakkee, L.R. Arends, and T. Nijsten. 2013. The Prevalence and Odds of Depressive Symptoms and Clinical Depression in Psoriasis Patients: A Systematic Review and Meta-Analysis. *J Invest Dermatol*

Enamandram, M., and A.B. Kimball. 2013. Psoriasis epidemiology: the interplay of genes and the environment. *J Invest Dermatol* 133:287-289.

Falk, E.S., and O. Vandbakk. 1993. Prevalence of psoriasis in a Norwegian Lapp population. *Acta Derm Venereol Suppl (Stockh)* 182:6-9.

Fehr, T., C.L. Lucas, J. Kurtz, T. Onoe, G. Zhao, T. Hogan, C. Vallot, A. Rao, and M. Sykes. 2010. A CD8 T cell-intrinsic role for the calcineurin-NFAT pathway for tolerance induction in vivo. *Blood* 115:1280-1287.

Ferrandiz, C., X. Bordas, V. Garcia-Patos, S. Puig, R. Pujol, and A. Smandia. 2001. Prevalence of psoriasis in Spain (Epiderma Project: phase I). *J Eur Acad Dermatol Venereol* 15:20-23.

Filer, C.E., P. Ho, I.N. Bruce, J. Worthington, and A. Barton. 2009. Investigation of association of genes NAT9, SLC9A3R1 and RAPTOR on chromosome 17q25 with psoriatic arthritis. *Ann Rheum Dis* 68:292-293.

Gelfand, J.M., S.R. Feldman, R.S. Stern, J. Thomas, T. Rolstad, and D.J. Margolis. 2004. Determinants of quality of life in patients with psoriasis: a study from the US population. *J Am Acad Dermatol* 51:704-708.

Gelfand, J.M., R. Weinstein, S.B. Porter, A.L. Neimann, J.A. Berlin, and D.J. Margolis. 2005. Prevalence and treatment of psoriasis in the United Kingdom: a population-based study. *Arch Dermatol* 141:1537-1541.

Ghosh, S., S.A. Hoselton, and J.M. Schuh. 2012. mu-chain-deficient mice possess B-1 cells and produce IgG and IgE, but not IgA, following systemic sensitization and inhalational challenge in a fungal asthma model. *J Immunol* 189:1322-1329.

Ghosh, S., S.B. Koralov, I. Stevanovic, M.S. Sundrud, Y. Sasaki, K. Rajewsky, A. Rao, and M.R. Muller. 2010. Hyperactivation of nuclear factor of activated T cells 1 (NFAT1) in T cells attenuates severity of murine autoimmune encephalomyelitis. *Proc Natl Acad Sci U S A* 107:15169-15174.

Ghosh, S., M.J. May, and E.B. Kopp. 1998. NF-kappa B and Rel proteins: evolutionarily conserved mediators of immune responses. *Annu Rev Immunol* 16:225-260.

Gilliet, M., C. Conrad, M. Geiges, A. Cozzio, W. Thurlimann, G. Burg, F.O. Nestle, and R. Dummer. 2004. Psoriasis triggered by toll-like receptor 7 agonist imiquimod in the presence of dermal plasmacytoid dendritic cell precursors. *Arch Dermatol* 140:1490-1495.

Gomez-Rodriguez, J., N. Sahu, R. Handon, T.S. Davidson, S.M. Anderson, M.R. Kirby, A. August, and P.L. Schwartzberg. 2009. Differential expression of interleukin-17A and -17F is coupled to T cell receptor signaling via inducible T cell kinase. *Immunity* 31:587-597.

Gottlieb, A., N.J. Korman, K.B. Gordon, S.R. Feldman, M. Lebwohl, J.Y. Koo, A.S. Van Voorhees, C.A. Elmets, C.L. Leonardi, K.R. Beutner, R. Bhushan, and A. Menter. 2008. Guidelines of care for the management of psoriasis and psoriatic arthritis: Section 2. Psoriatic arthritis: overview and guidelines of care for treatment with an emphasis on the biologics. *J Am Acad Dermatol* 58:851-864.

Greene, M.W., M.S. Ruhoff, C.M. Burrington, R.S. Garofalo, and S.J. Orena. 2010. TNFalpha activation of PKCdelta, mediated by NFkappaB and ER stress, cross-talks with the insulin signaling cascade. *Cell Signal* 22:274-284.

Grumont, R.J., I.J. Rourke, and S. Gerondakis. 1999. Rel-dependent induction of A1 transcription is required to protect B cells from antigen receptor ligation-induced apoptosis. *Genes Dev* 13:400-411.

Guilloteau, K., I. Paris, N. Pedretti, K. Boniface, F. Juchaux, V. Huguier, G. Guillet, F.X. Bernard, J.C. Lecron, and F. Morel. 2010. Skin Inflammation Induced by the Synergistic Action of IL-17A, IL-22, Oncostatin M, IL-1{alpha}, and TNF-{alpha} Recapitulates Some Features of Psoriasis. *J Immunol*

Hardy, R.R., and K. Hayakawa. 2001. B cell development pathways. *Annu Rev Immunol* 19:595-621.

Haylett, R.S., N. Koch, and L. Rink. 2009. MHC class II molecules activate NFAT and the ERK group of MAPK through distinct signaling pathways in B cells. *Eur J Immunol* 39:1947-1955.

Helms, C., L. Cao, J.G. Krueger, E.M. Wijsman, F. Chamian, D. Gordon, M. Heffernan, J.A. Daw, J. Robarge, J. Ott, P.Y. Kwok, A. Menter, and A.M. Bowcock. 2003. A putative RUNX1 binding site variant between SLC9A3R1 and NAT9 is associated with susceptibility to psoriasis. *Nat Genet* 35:349-356.

Heyne, K., C. Winter, F. Gerten, C. Schmidt, and K. Roemer. 2013. A novel mechanism of crosstalk between the p53 and NFkappaB pathways: MDM2 binds and inhibits p65RelA. *Cell Cycle* 12:2479-2492.

Hobeika, E., S. Thiemann, B. Storch, H. Jumaa, P.J. Nielsen, R. Pelanda, and M. Reth. 2006. Testing gene function early in the B cell lineage in mb1-cre mice. *Proceedings of the National Academy of Sciences of the United States of America* 103:13789-13794.

Hogan, P.G., L. Chen, J. Nardone, and A. Rao. 2003. Transcriptional regulation by calcium, calcineurin, and NFAT. *Genes Dev* 17:2205-2232.

Hogan, P.G., R.S. Lewis, and A. Rao. 2010. Molecular basis of calcium signaling in lymphocytes: STIM and ORAI. *Annu Rev Immunol* 28:491-533.

Horsley, V., A.O. Aliprantis, L. Polak, L.H. Glimcher, and E. Fuchs. 2008. NFATc1 balances quiescence and proliferation of skin stem cells. *Cell* 132:299-310.

Isnardi, I., Y.S. Ng, I. Srdanovic, R. Motaghedi, S. Rudchenko, H. von Bernuth, S.Y. Zhang, A. Puel, E. Jouanguy, C. Picard, B.Z. Garty, Y. Camcioglu, R. Doffinger, D. Kumararatne, G. Davies, J.I. Gallin, S. Haraguchi, N.K. Day, J.L. Casanova, and E. Meffre. 2008. IRAK-4- and MyD88-dependent pathways are essential for the removal of developing autoreactive B cells in humans. *Immunity* 29:746-757.

Itoh, K., M. Sakakibara, S. Yamasaki, A. Takeuchi, H. Arase, M. Miyazaki, N. Nakajima, M. Okada, and T. Saito. 2002. Cutting edge: negative regulation of immune synapse formation by anchoring lipid raft to cytoskeleton through Cbp-EBP50-ERM assembly. *J Immunol* 168:541-544.

Javitz, H.S., M.M. Ward, E. Farber, L. Nail, and S.G. Vallow. 2002. The direct cost of care for psoriasis and psoriatic arthritis in the United States. *J Am Acad Dermatol* 46:850-860.

Johnston, A., X. Xing, A.M. Guzman, M. Riblett, C.M. Loyd, N.L. Ward, C. Wohn, E.P. Prens, F. Wang, L.E. Maier, S. Kang, J.J. Voorhees, J.T. Elder, and J.E. Gudjonsson. 2011. IL-1F5, -F6, -F8, and -F9: a novel IL-1 family signaling system that is active in psoriasis and promotes keratinocyte antimicrobial peptide expression. *J Immunol* 186:2613-2622.

Kim, S.Y., J.C. Kim, J.K. Kim, H.J. Kim, H.M. Lee, M.S. Choi, P.J. Maeng, and J.K. Ahn. 2008. Hepatitis B virus X protein enhances NFkappaB activity through cooperating with VBP1. *BMB Rep* 41:158-163.

Kimball, A.B., P. Szapary, U. Mrowietz, K. Reich, R.G. Langley, Y. You, M.C. Hsu, N. Yeilding, D.J. Rader, and N.N. Mehta. 2012. Underdiagnosis and undertreatment of cardiovascular risk factors in patients with moderate to severe psoriasis. *J Am Acad Dermatol* 67:76-85.

Klein, U., and R. Dalla-Favera. 2008. Germinal centres: role in B-cell physiology and malignancy. *Nat Rev Immunol* 8:22-33.

Kontgen, F., R.J. Grumont, A. Strasser, D. Metcalf, R. Li, D. Tarlinton, and S. Gerondakis. 1995. Mice lacking the c-rel proto-oncogene exhibit defects in lymphocyte proliferation, humoral immunity, and interleukin-2 expression. *Genes Dev* 9:1965-1977.

Krappmann, D., and C. Scheidereit. 2005. A pervasive role of ubiquitin conjugation in activation and termination of IkappaB kinase pathways. *EMBO Rep* 6:321-326.

Kundumani-Sridharan, V., D. Van Quyen, J. Subramani, N.K. Singh, Y.E. Chin, and G.N. Rao. 2012. Novel interactions between NFATc1 (Nuclear Factor of Activated T cells c1) and STAT-3 (Signal Transducer and Activator of Transcription-3) mediate G protein-coupled receptor agonist, thrombin-induced biphasic expression of cyclin D1, with first phase influencing cell migration and second phase directing cell proliferation. *J Biol Chem* 287:22463-22482.

Kunsch, C., S.M. Ruben, and C.A. Rosen. 1992. Selection of optimal kappa B/Rel DNA-binding motifs: interaction of both subunits of NF-kappa B with DNA is required for transcriptional activation. *Mol Cell Biol* 12:4412-4421.

Kurd, S.K., A.B. Troxel, P. Crits-Christoph, and J.M. Gelfand. 2010. The risk of depression, anxiety, and suicidality in patients with psoriasis: a population-based cohort study. *Arch Dermatol* 146:891-895.

Kwon, K., C. Hutter, Q. Sun, I. Bilic, C. Cobaleda, S. Malin, and M. Busslinger. 2008. Instructive role of the transcription factor E2A in early B lymphopoiesis and germinal center B cell development. *Immunity* 28:751-762.

Lai, J.F., C.L. Zindl, L.B. Duffy, T.P. Atkinson, Y.W. Jung, N. van Rooijen, K.B. Waites, D.C. Krause, and D.D. Chaplin. 2010. Critical role of macrophages and their activation via MyD88-NFkappaB signaling in lung innate immunity to Mycoplasma pneumoniae. *PLoS One* 5:e14417.

Lande, R., J. Gregorio, V. Facchinetti, B. Chatterjee, Y.H. Wang, B. Homey, W. Cao, B. Su, F.O. Nestle, T. Zal, I. Mellman, J.M. Schroder, Y.J. Liu, and M. Gilliet. 2007. Plasmacytoid dendritic cells sense self-DNA coupled with antimicrobial peptide. *Nature* 449:564-569.

Langley, R.G., and C.N. Ellis. 2004. Evaluating psoriasis with Psoriasis Area and Severity Index, Psoriasis Global Assessment, and Lattice System Physician's Global Assessment. *J Am Acad Dermatol* 51:563-569.

LeBien, T.W. 2000. Fates of human B-cell precursors. *Blood* 96:9-23.

LeBien, T.W., and T.F. Tedder. 2008. B lymphocytes: how they develop and function. *Blood* 112:1570-1580.

Lee, M.O., H.J. Kang, Y.M. Kim, J.H. Oum, and J. Park. 2002. Repression of FasL expression by retinoic acid involves a novel mechanism of inhibition of transactivation function of the nuclear factors of activated T-cells. *Eur J Biochem* 269:1162-1170.

Li, H., A. Rao, and P.G. Hogan. 2011. Interaction of calcineurin with substrates and targeting proteins. *Trends Cell Biol* 21:91-103.

Li, Q., and I.M. Verma. 2002. NF-kappaB regulation in the immune system. *Nat Rev Immunol* 2:725-734.

Li, Z.Z., L.L. Tao, J. Zhang, H.J. Zhang, and J.M. Qu. 2012. Role of NOD2 in regulating the immune response to Aspergillus fumigatus. *Inflamm Res* 61:643-648.

Lloyd, P., C. Ryan, and A. Menter. 2012. Psoriatic arthritis: an update. *Arthritis* 2012:176298.

Lodygin, D., F. Odoardi, C. Schlager, H. Korner, A. Kitz, M. Nosov, J. van den Brandt, H.M. Reichardt, M. Haberl, and A. Flugel. 2013. A combination of fluorescent NFAT and H2B sensors uncovers dynamics of T cell activation in real time during CNS autoimmunity. *Nat Med* 19:784-790.

Lopez-Rodriguez, C., J. Aramburu, A.S. Rakeman, and A. Rao. 1999. NFAT5, a constitutively nuclear NFAT protein that does not cooperate with Fos and Jun. *Proc Natl Acad Sci U S A* 96:7214-7219.

Lu, R. 2008. Interferon regulatory factor 4 and 8 in B-cell development. *Trends Immunol* 29:487-492.

Mao, X.R., A.M. Moerman-Herzog, Y. Chen, and S.W. Barger. 2009. Unique aspects of transcriptional regulation in neurons--nuances in NFkappaB and Sp1-related factors. *J Neuroinflammation* 6:16.

Mauri, C., and A. Bosma. 2012. Immune regulatory function of B cells. *Annu Rev Immunol* 30:221-241.

McHeyzer-Williams, L.J., and M.G. McHeyzer-Williams. 2005. Antigen-specific memory B cell development. *Annu Rev Immunol* 23:487-513.

Menard, L., T. Cantaert, N. Chamberlain, S.G. Tangye, S. Riminton, J.A. Church, A. Klion, C. Cunningham-Rundles, K.E. Nichols, and E. Meffre. 2013. Signaling lymphocytic activation molecule (SLAM)/SLAM-associated protein pathway regulates human B-cell tolerance. *J Allergy Clin Immunol*

Moorthy, A., O. Savinova, J. Ho, V. Wang, D. Vu, and G. Ghosh. 2006. The 20S proteasome processes NF-kappaB1 p105 into p50 in a translation-independent manner. *The EMBO journal* 25:1945-1956.

Muller, M.R., and A. Rao. 2010. NFAT, immunity and cancer: a transcription factor comes of age. *Nat Rev Immunol* 10:645-656.

Murley, J.S., Y. Kataoka, D.E. Hallahan, J.C. Roberts, and D.J. Grdina. 2001. Activation of NFkappaB and MnSOD gene expression by free radical scavengers in human microvascular endothelial cells. *Free Radic Biol Med* 30:1426-1439.

Muthusamy, V., and T.J. Piva. 2010. The UV response of the skin: a review of the MAPK, NFkappaB and TNFalpha signal transduction pathways. *Arch Dermatol Res* 302:5-17.

Nabel, G.J., and I.M. Verma. 1993. Proposed NF-kappa B/I kappa B family nomenclature. *Genes Dev* 7:2063.

Nair, R.P., K.C. Duffin, C. Helms, J. Ding, P.E. Stuart, D. Goldgar, J.E. Gudjonsson, Y. Li, T. Tejasvi, B.J. Feng, A. Ruether, S. Schreiber, M. Weichenthal, D. Gladman, P. Rahman, S.J. Schrodi, S. Prahalad, S.L. Guthery, J. Fischer, W. Liao, P.Y. Kwok, A. Menter, G.M. Lathrop, C.A. Wise, A.B. Begovich, J.J. Voorhees, J.T. Elder, G.G. Krueger, A.M. Bowcock, and G.R. Abecasis. 2009. Genome-wide scan reveals association of psoriasis with IL-23 and NF-kappaB pathways. *Nat Genet* 41:199-204.

Naldi, L., and S.R. Mercuri. 2010. Epidemiology of comorbidities in psoriasis. *Dermatol Ther* 23:114-118.

Negishi-Koga, T., and H. Takayanagi. 2009. Ca2+-NFATc1 signaling is an essential axis of osteoclast differentiation. *Immunol Rev* 231:241-256.

Nguyen, T.N., L.J. Kim, R.D. Walters, L.F. Drullinger, T.N. Lively, J.F. Kugel, and J.A. Goodrich. 2010. The C-terminal region of human NFATc2 binds cJun to synergistically activate interleukin-2 transcription. *Mol Immunol* 47:2314-2322.

O'Neill, S.K., Y. Cao, K.M. Hamel, P.D. Doodes, G. Hutas, and A. Finnegan. 2007. Expression of CD80/86 on B cells is essential for autoreactive T cell activation and the development of arthritis. *J Immunol* 179:5109-5116.

Pantelyushin, S., S. Haak, B. Ingold, P. Kulig, F.L. Heppner, A.A. Navarini, and B. Becher. 2012. Rorgammat+ innate lymphocytes and gammadelta T cells initiate psoriasiform plaque formation in mice. *J Clin Invest* 122:2252-2256.

Papoutsaki, M., and A. Costanzo. 2013. Treatment of psoriasis and psoriatic arthritis. *BioDrugs* 27 Suppl 1:3-12.

Perkins, N. 2006. Post-translational modifications regulating the activity and function of the nuclear factor kappa B pathway. *Oncogene* 25:6717-6730.

Perkins, N.D. 2007. Integrating cell-signalling pathways with NF-kappaB and IKK function. *Nat Rev Mol Cell Biol* 8:49-62.

Pham, L.V., A.T. Tamayo, C. Li, C. Bueso-Ramos, and R.J. Ford. 2010. An epigenetic chromatin remodeling role for NFATc1 in transcriptional regulation of growth and survival genes in diffuse large B-cell lymphomas. *Blood* 116:3899-3906.

Pillai, S., A. Cariappa, and S.T. Moran. 2005. Marginal zone B cells. *Annu Rev Immunol* 23:161-196.

Plunkett, A., K. Merlin, D. Gill, Y. Zuo, D. Jolley, and R. Marks. 1999. The frequency of common nonmalignant skin conditions in adults in central Victoria, Australia. *Int J Dermatol* 38:901-908.

Poole, C.D., M. Lebmeier, R. Ara, R. Rafia, and C.J. Currie. 2010. Estimation of health care costs as a function of disease severity in people with psoriatic arthritis in the UK. *Rheumatology (Oxford)* 49:1949-1956.

Prey, S., C. Paul, V. Bronsard, E. Puzenat, P.A. Gourraud, S. Aractingi, F. Aubin, M. Bagot, B. Cribier, P. Joly, D. Jullien, M.L. Maitre, M.A. Richard-Lallemand, and J.P. Ortonne. 2010. Assessment of risk of psoriatic arthritis in patients with plaque psoriasis: a systematic review of the literature. *J Eur Acad Dermatol Venereol* 24 Suppl 2:31-35.

Price, A.M., and M.A. Luftig. 2014. Dynamic Epstein-Barr virus gene expression on the path to B-cell transformation. *Adv Virus Res* 88:279-313.

Resch, U., Y.M. Schichl, G. Winsauer, R. Gudi, K. Prasad, and R. de Martin. 2009. Siva1 is a XIAP-interacting protein that balances NFkappaB and JNK signalling to promote apoptosis. *J Cell Sci* 122:2651-2661.

Robbs, B.K., A.L. Cruz, M.B. Werneck, G.P. Mognol, and J.P. Viola. 2008. Dual roles for NFAT transcription factor genes as oncogenes and tumor suppressors. *Mol Cell Biol* 28:7168-7181.

Salerno-Goncalves, R., T. Rezwan, and M.B. Sztein. 2014. B cells modulate mucosal associated invariant T cell immune responses. *Front Immunol* 4:511.

Samuelsson, L., F. Enlund, A. Torinsson, M. Yhr, A. Inerot, C. Enerback, J. Wahlstrom, G. Swanbeck, and T. Martinsson. 1999. A genome-wide search for genes predisposing to familial psoriasis by using a stratification approach. *Hum Genet* 105:523-529.

Schmitt, J., and D.E. Ford. 2010. Psoriasis is independently associated with psychiatric morbidity and adverse cardiovascular risk factors, but not with cardiovascular events in a population-based sample. *J Eur Acad Dermatol Venereol* 24:885-892.

Seminara, N.M., K. Abuabara, D.B. Shin, S.M. Langan, S.E. Kimmel, D. Margolis, A.B. Troxel, and J.M. Gelfand. 2011. Validity of The Health Improvement Network (THIN) for the study of psoriasis. *Br J Dermatol* 164:602-609.

Sen, R., and D. Baltimore. 1986. Multiple nuclear factors interact with the immunoglobulin enhancer sequences. *Cell* 46:705-716.

Serfling, E., A. Avots, S. Klein-Hessling, R. Rudolf, M. Vaeth, and F. Berberich-Siebelt. 2012. NFATc1/alphaA: The other Face of NFAT Factors in Lymphocytes. *Cell Commun Signal* 10:16.

Serfling, E., R. Barthelmas, I. Pfeuffer, B. Schenk, S. Zarius, R. Swoboda, F. Mercurio, and M. Karin. 1989. Ubiquitous and lymphocyte-specific factors are involved in the induction of the mouse interleukin 2 gene in T lymphocytes. *EMBO J* 8:465-473.

Serfling, E., F. Berberich-Siebelt, and A. Avots. 2007. NFAT in lymphocytes: a factor for all events? *Sci STKE* 2007:pe42.

Serfling, E., S. Chuvpilo, J. Liu, T. Hofer, and A. Palmetshofer. 2006a. NFATc1 autoregulation: a crucial step for cell-fate determination. *Trends Immunol* 27:461-469.

Serfling, E., S. Klein-Hessling, A. Palmetshofer, T. Bopp, M. Stassen, and E. Schmitt. 2006b. NFAT transcription factors in control of peripheral T cell tolerance. *Eur J Immunol* 36:2837-2843.

Shaffer, A.L., N.C. Emre, P.B. Romesser, and L.M. Staudt. 2009. IRF4: Immunity. Malignancy! Therapy? *Clin Cancer Res* 15:2954-2961.

Shaw, J.P., P.J. Utz, D.B. Durand, J.J. Toole, E.A. Emmel, and G.R. Crabtree. 1988. Identification of a putative regulator of early T cell activation genes. *Science* 241:202-205.

Shu, X., J. Ji, J. Sundquist, K. Sundquist, and K. Hemminki. 2011. Survival in cancer patients hospitalized for psoriasis: a population-based cohort study in Sweden. *Br J Dermatol* 165:129-136.

Simpson, C.R., W.J. Anderson, P.J. Helms, M.W. Taylor, L. Watson, G.J. Prescott, D.J. Godden, and R.N. Barker. 2002. Coincidence of immune-mediated diseases driven by Th1 and Th2 subsets suggests a common aetiology. A population-based study using computerized general practice data. *Clin Exp Allergy* 32:37-42.

Skrzeczynska-Moncznik, J., A. Wlodarczyk, K. Zabieglo, M. Kapinska-Mrowiecka, E. Marewicz, A. Dubin, J. Potempa, and J. Cichy. 2012. Secretory leukocyte proteinase inhibitor-competent DNA deposits are potent stimulators of plasmacytoid dendritic cells: implication for psoriasis. *J Immunol* 189:1611-1617.

Staudt, L.M. 2010. Oncogenic activation of NF-kappaB. *Cold Spring Harb Perspect Biol* 2:a000109.

Stern, R.S., T. Nijsten, S.R. Feldman, D.J. Margolis, and T. Rolstad. 2004. Psoriasis is common, carries a substantial burden even when not extensive, and is associated with widespread treatment dissatisfaction. *J Investig Dermatol Symp Proc* 9:136-139.

Strange, A., F. Capon, C.C. Spencer, J. Knight, M.E. Weale, M.H. Allen, A. Barton, G. Band, C. Bellenguez, J.G. Bergboer, J.M. Blackwell, E. Bramon, S.J. Bumpstead, J.P. Casas, M.J. Cork, A. Corvin, P. Deloukas, A. Dilthey, A. Duncanson, S. Edkins, X. Estivill, O. Fitzgerald, C. Freeman, E. Giardina, E. Gray, A. Hofer, U. Huffmeier, S.E. Hunt, A.D. Irvine, J. Jankowski, B. Kirby, C. Langford, J. Lascorz, J. Leman, S. Leslie, L. Mallbris, H.S. Markus, C.G. Mathew, W.H. McLean, R. McManus, R. Mossner, L. Moutsianas, A.T. Naluai, F.O. Nestle, G. Novelli, A. Onoufriadis, C.N. Palmer, C. Perricone, M. Pirinen, R. Plomin, S.C. Potter, R.M. Pujol, A. Rautanen, E. Riveira-Munoz, A.W. Ryan, W. Salmhofer, L. Samuelsson, S.J. Sawcer, J. Schalkwijk, C.H. Smith, M. Stahle, Z. Su, R. Tazi-Ahnini, H. Traupe, A.C. Viswanathan, R.B. Warren, W. Weger, K. Wolk, N. Wood, J. Worthington, H.S. Young, P.L. Zeeuwen, A. Hayday, A.D. Burden, C.E. Griffiths, J. Kere, A. Reis, G. McVean, D.M. Evans, M.A. Brown, J.N. Barker, L. Peltonen, P. Donnelly, and R.C. Trembath. 2010. A genome-wide association study identifies new psoriasis susceptibility loci and an interaction between HLA-C and ERAP1. *Nat Genet* 42:985-990.

Suzuki, K., M. Maruya, S. Kawamoto, and S. Fagarasan. 2010. Roles of B-1 and B-2 cells in innate and acquired IgA-mediated immunity. *Immunol Rev* 237:180-190.

Tedder, T.F., J.C. Poe, and K.M. Haas. 2005. CD22: a multifunctional receptor that regulates B lymphocyte survival and signal transduction. *Adv Immunol* 88:1-50.

Teng, Y., Y. Takahashi, M. Yamada, T. Kurosu, T. Koyama, O. Miura, and T. Miki. 2007. IRF4 negatively regulates proliferation of germinal center B cell-derived Burkitt's lymphoma cell lines and induces differentiation toward plasma cells. *Eur J Cell Biol* 86:581-589.

Tsoi, L.C., S.L. Spain, J. Knight, E. Ellinghaus, P.E. Stuart, F. Capon, J. Ding, Y. Li, T. Tejasvi, J.E. Gudjonsson, H.M. Kang, M.H. Allen, R. McManus, G. Novelli, L. Samuelsson, J. Schalkwijk, M. Stahle, A.D. Burden, C.H. Smith, M.J. Cork, X. Estivill, A.M. Bowcock, G.G. Krueger, W. Weger, J. Worthington, R. Tazi-Ahnini, F.O. Nestle, A. Hayday, P. Hoffmann, J. Winkelmann, C. Wijmenga, C. Langford, S. Edkins, R. Andrews, H. Blackburn, A. Strange, G. Band, R.D. Pearson, D. Vukcevic, C.C. Spencer, P. Deloukas, U. Mrowietz, S. Schreiber, S. Weidinger, S. Koks, K. Kingo, T. Esko, A. Metspalu, H.W. Lim, J.J. Voorhees, M. Weichenthal, H.E. Wichmann, V. Chandran, C.F. Rosen, P. Rahman, D.D. Gladman, C.E. Griffiths, A. Reis, J. Kere, R.P. Nair, A. Franke, J.N. Barker, G.R. Abecasis, J.T. Elder, and R.C. Trembath. 2012. Identification of 15 new psoriasis susceptibility loci highlights the role of innate immunity. *Nat Genet* 44:1341-1348.

Winslow, M.M., E.M. Gallo, J.R. Neilson, and G.R. Crabtree. 2006. The calcineurin phosphatase complex modulates immunogenic B cell responses. *Immunity* 24:141-152.

Xiao, G., A.B. Rabson, W. Young, G. Qing, and Z. Qu. 2006. Alternative pathways of NF-kappaB activation: a double-edged sword in health and disease. *Cytokine Growth Factor Rev* 17:281-293.

Yanaba, K., J.D. Bouaziz, K.M. Haas, J.C. Poe, M. Fujimoto, and T.F. Tedder. 2008. A regulatory B cell subset with a unique CD1dhiCD5+ phenotype controls T cell-dependent inflammatory responses. *Immunity* 28:639-650.

Yanaba, K., J.D. Bouaziz, T. Matsushita, T. Tsubata, and T.F. Tedder. 2009. The development and function of regulatory B cells expressing IL-10 (B10 cells) requires antigen receptor diversity and TLR signals. *J Immunol* 182:7459-7472.

Yanaba, K., M. Kamata, N. Ishiura, S. Shibata, Y. Asano, Y. Tada, M. Sugaya, T. Kadono, T.F. Tedder, and S. Sato. 2013. Regulatory B cells suppress imiquimod-induced, psoriasis-like skin inflammation. *J Leukoc Biol* 94:563-573.

Zanoni, I., R. Ostuni, G. Capuano, M. Collini, M. Caccia, A.E. Ronchi, M. Rocchetti, F. Mingozzi, M. Foti, G. Chirico, B. Costa, A. Zaza, P. Ricciardi-Castagnoli, and F. Granucci. 2009. CD14 regulates the dendritic cell life cycle after LPS exposure through NFAT activation. *Nature* 460:264-268.

Zheng, Y., S. Josefowicz, A. Chaudhry, X.P. Peng, K. Forbush, and A.Y. Rudensky. 2010. Role of conserved non-coding DNA elements in the Foxp3 gene in regulatory T-cell fate. *Nature* 463:808-812.

Abbreviations

3’	3 prime
5’	5 prime
°C	degree Celsius
ABB	Annexin-Binding Buffer
AICD	activation induced cell death
AP-1	activator-protein 1
APC	antigen presenting cell
-APC	allophycocyanin
(d)ATP	(desoxy)adenosine triphosphate
B6/N	laboratory black inbred mouse line
BCR	B-cell receptor
BM	bone marrow
bp	base pair
BSA	bovine serum albumin
BSS	buffered salt solution
C57/B6	laboratory black inbred mouse line (=B6/N)
Ca^{2+}	calcium
CARD9	caspase recruitment domain containing protein 9
CBP	CREB binding protein
CCL2	chemokine ligand 2
CCR2	chemokine receptor 2
CD	cluster of differentiation
CFSE	carboxyfluorescein diacetate succinimidyl ester
CK1	casein kinase 1
CLP	common lymphoid progenitor
CLR	C-type lectin receptor
CMP	common myeloid progenitor
CN	calcineurin
CO_2	carbon dioxide
CP	crossing point
CsA	cyclosporine A
Ct	threshold cycle
CTL	cytotoxic T-cell
(d)CTP	(desoxy)cytidine triphosphate
CMV	cytomegalovirus
CyCAP	cyclophillin C associated protein
CyPA	cyclophillin A
DAG	diacyl-glycerol
DL	dilution factor
DMEM	Dulbecco's Modified Eagle Medium
DMSO	dimethyl-sulfoxide
DN	double negative
DNA	deoxyribonucleic acid
DP	double positive
dTTP	desoxythymidine triphosphate

DTT	dithiothreitol
DYRK1	dual-specificity-tyrosine-phosphorylation-regulated kinase
ECL	enhanced chemiluminescence
EDTA	ethylenediaminetetraacetic acid
EGF	epidermal growth factor
ELISA	enzyme-linked immunosorbent assay
ER	endoplasmic reticulum
ES(C)	embryonic stem cell
et. al	*et aliter*
EtBr	ethidium Bromide
EtOH	ethanol
FA	formaldehyde
FACS	fluorescence activated cell sorting
FCS	fetal calf (bovine) serum
FITC	fluorescein-isothiocyanat
F	forward
Fig.	figure
FK506	tacrolismus
FKBP	FK506 binding protein
fl	loxP sites (floxed)
for	forward
g	gram
GA	gauge
GADS	GRB2-related adaptor protein
gLB	genomic lysis buffer
GSK3	glycogen synthase kinase 3
(d)GTP	(desoxy)guanine triphosphate
H_2O	water
HCL	hydrogen chloride
HD	high dye (formaldehyde)
hr(s)	hour(s)
HRP	horseradish-peroxidase
HSC	hematopoietic stem cell
I	ionomycin
IFN	interferon
Ig	immunoglobulin
IKK	Iκb kinase
IL	interleukin
IMQ	imiquimod
iNOS	inducible nitric oxide synthase
i.p.	intraperitoneal
IP_3	inositol 1,4,5-trisphosphate
ITAM	immune receptor tyrosine based activation motif
ITK	IL-2-inducible T-cell kinase
kg	kilo-gram
kb	kilo-base pair
l	liter

-L	lower
Lck	lymphocyte-specific protein tyrosine kinase
Lox	loxP sites
KI	knock-in
KO	knock-out
LPS	lipopolysaccharide
LRRK2	leucin rich repeat kinase 2
LSY	lysis
M	molar mass
m	milli-
Malt1	mucosa associated lymphoid tissue lymphoma translocation gene 1
MAPK	mitogen-activated protein kinase
MCP-1	monocyte chemotactic protein-1
MES	2-(N-morpholino)ethanesulfonic acid
mg	milligram
Mg	magnesium
MgCl	magnesium chloride
MHC	major histocompatibility complex
min(‘)	minute
ml	milliliter
MPP	multi-potent progenitor
mol	mole
msec	milliseconds
n	nano-
Na_2HPO_4	disodium hydrogen phosphate
NaCl	sodium chloride
NaH_2PO_4	monosodium phosphate
NaOH	sodium hydroxide
nc	non-coding
NES	nuclear export signal
NEU	neutralization
NFAT	nuclear factor of activated T-cells
NF-κB	nuclear factor kappa-light-chain-enhancer of activated B cells
NHR	NFAT regulatory domain
NIK	NF-κB inducing kinase
NK cells	natural killer cells
NLS	nuclear translocation signal
NO	nitrogen monoxide
NRON	ncRNA repressor of nuclear factor of activated T-cells
NS	non specific
ON	overnight
OVA	ovalbumin
ORAI1	calcium release activated calcium channel
p	pico-
p	peritoneal
P1	promoter 1
P2	promoter 2

P^{32}	radioactive isotope of phosphorus
PAF	platelet activation factor
Pam3Cys	tripalmitoyl-S-glyceryl-cysteine
PAMP	pathogen associate molecule pattern
PBMCs	peripheral blood mononuclear cells
PCR	polymerase chain reaction
PE	phycoerythrin
PEC(s)	peritoneal cell(s)
PGK	phosphoglycerate kinase
PIP_2	phospholipid phosphatidylinositol 4,5-bisphosphate
PLC	phospholipase C
R	reverse
r	resident
RBL	red blood cell lysis
RES	resuspension
rev	reverse
RHD	Rel-homology domain
RNA	ribonucleic acid
ROS	reactive oxygen species
rpm	rounds per minute
RPMI	Roswell Memorial Institute Medium
RSD	Rel-similarity domain
RTK	receptor tyrosine kinase
RT	room temperature
RT-PCR	reverse Transcriptase-PCR
SDS	sodium dodecyl sulfate
sec (’’)	seconds
SLP76	SH2-domain-containing leukocyte protein of 76 kDa
SOC	store operated Ca^{2+} influx
SP	single positive
Src	c-Src tyrosine kinase
SRR	serine rich region
STIM1	stromal interaction molecule 1
Syc	spleen tyrosine kinase
TAD	Transactivation domain
TAE	Tris/Acetate/EDTA
TCR	T-cell receptor
T_h	T-helper cell
TLR	toll-like receptor
T_m	melting temperature
TM	transmembrane
TNF	tumor necrosis factor
TPA (PMA)	tetradecanoylphorbol-acetat (phorbol-12-myristat-13-acetat)
T_{reg}	regulatory T-cell
µ	micro-
U	unit
-U	upper

UDP	uridine diphosphate
wo (w/o)	without
wt	wild type
YPD	yeast Extract Peptone Dextrose
ZAP-70	ζ-chain-associated protein kinase of 70 kDa

Curriculum Vitae

Hani Gouda Alsaid Alrefai

Summary of qualifications

- M.B.B.Ch.
  Mansoura faculty of medicine - 2000 -Very good with honors
- Master of medical biochemistry & molecular biology
  Mansoura faculty of medicine - 2006
- Diploma of total Quality management in health reform
  American university in Cairo - 2008

Positions

- Rotating internship in Mansoura university hospitals (1/3/2001 – 28/2/2002)
- General practitioner in Ministry of Health (1/3/2002 – 1/7/2002)
- Demonstrator of biochemistry & molecular biology (2/7/2002 – 21/10/2006)
- Ass. Lecturer of biochemistry & molecular biology (22/10/2006)

Scholarships and Fellowships

- Scholarship for Diploma in Java2 programming (2001)
  Ministry of telecommunications and Sun Microsystems
- Fellowship for M.Sc. in Biochemistry and Molecular Biology
  Mansoura faculty of medicine – Mansoura University (2002-2006).
- Scholarship for International Bioinformatics Software School IBSS'2008
  The Moroccan Society of bioinformatics & Microsoft research program
- Full PhD from GERLS (German Egyptian Research Long term Scholarships)
  DAAD (Germany) and MEHSR (Egypt) – Graduate School of Life Science – Wuerzburg University (2009 – 2014).

Laboratory experience

- Molecular biology techniques:
  DNA and RNA extraction ; PCR; RT-PCR; Gel electrophoresis; Chromatin immunoprecipitation, EMSA and FISH.
- Biochemical techniques:
  ELISA and HPLC.
- Cell culture techniques:
  Cell culture, cell counting and magnetic cell isolation
- Thymidine incorporation assay
- Flow-cytometry assisted cell sorting techniques
  Cell surface staining, intracellular staining, cell proliferation assay, apoptosis assay …etc.
- Immunohistochemistry.
- Laboratory mice handling:
  breeding; tagging; blood sampling; tissue sampling (Spleen, LN BM) and anathesia.

- Routine Histological Laboratory work
- Routine biochemical Laboratory work:
- Routine parasitological Laboratory work:
- Routine microbiological Laboratory work:
- Routine immunological Laboratory work:
- Routine hematological Laboratory work:

Courses and workshops

- Career workshop 1 day 2011
  McKinsey & Company
- Basic course for laboratory animal handling 7days 2011
  University of Wuerzburg
- LATEX 3 days 2010
  Graduate School of life science - University of Wuerzburg
- Becoming a better academic writer 2 days 2010
  Graduate School of life science - University of Wuerzburg
- How to write a scientific paper and get it published 2 days 2010
  Graduate School of life science - University of Wuerzburg
- International Bioinformatics Software School 6 days 2008
  Moroccan Society of bioinformatics – Morocco, in association with Microsoft research
- International CLL Workshop 3 days 2008
  (Flowcytometry – FISH – PCR – Heteroduplex & gene scan)

  Clinical pathology Dep. of Mansoura faculty of medicine, Mansoura Oncology center in Collaboration with FDA, NCI, NIH, Bethasda, MD, USA
- Hands on HPLC applications 3 days 2008
  Institute of graduate studies – Alexandria university
- People Management in health care organizations 2 months 2008
  Institute of quality management – American university in Cairo
- Information Management in Healthcare 2 months 2008
  Institute of quality management – American university in Cairo
- Biochemical & Molecular Tumor Markers 40 hours 2008
  Cancer biology Dep. – National cancer institute (NCI)
- Six sigma quality improvement in health care 2 months 2007
  Institute of quality management – American university in Cairo
- Spoken English skills 4 weeks 2007
  Fulbright scholarship in Mansoura English for specific purposes unit
- Basics of scientific research 4 days 2006
  Mansoura university Faculty & leadership development project
- Skills of effective communication 3 days 2006
  Mansoura university Faculty & leadership development project
- Skills of creative thinking 3 days 2006
  Mansoura university Faculty & leadership development project
- Skills of time management 3 days 2005
  Mansoura university Faculty & leadership development project

- Introduction to Bioinformatics 2 weeks 2005
  Institute of graduate studies – Alexandria university
- E-learning (E-learning content development) 2 months 2005
  Department of engineering services – American university in Cairo
- English for research & thesis writing 1 month 2004
  English for specific purposes department – faculty of commerce
- Molecular biology & PCR basics 2 weeks 2004
  Institute of graduate studies – Alexandria university
- Java2 programming 8 months 2000
  Graduate development program - Egyption ministry of communication & information

Teaching activities and expierence

- Theoretical:
  - Chemistry & metabolism of carbohydrate
  - Chemistry & metabolism of lipid
  - Chemistry & metabolism of protein
  - Chemistry & metabolism of nucleic acids
  - Enzymology and enzyme kinetics
  - Chemistry & metabolism of vitamins
  - Biological oxidation & bioenergetics
  - Mechanism of hormonal action
  - Introduction to molecular biology.
- Practical:
  - Basic carbohydrate, lipid and protein identification techniques
  - Hb derivatives identification
  - Colorimetery
  - Molecular biology basic techniques.

Languages

- Arabic (mother tongue)
- English: Excellent: TOEFL 110 (IBT)
- German: B2 (Goethe certificate)

Conferences and symposia

- Mansoura faculty of medicine annual congress (2002 – 2003 – 2004 – 2005 – 2006 – 2007)
- Biochemistry & M. biology Egyptian ass. conference (2004 - 2004 – 2005 – 2006 -2007)
- Mansoura Biochemistry & m. biology dep. annual congress – 2008
  (participation and organization)
- 3rd Retreat of Transregio TR52 – Wuerzburg university – 2009
- 4th Retreat of Transregio TR52 – Mainz university – 2010
- Puzzling world of cancer TR17 – Wuerzburg university – 2010
- Regulators of adaptive immunity – Erlangen university – 2010
- 6th international symposium of the GSLS – Würzburg – 2011
- 7th international symposium of the GSLS – Würzburg – 2012
  (participation and organization)
- Ernst Klenk Symposium in Mol. Medicine – Cologne – 2012
- 8th international symposium of the GSLS – Würzburg – 2013

- 9th Spring school on Immunology of DGfI – Ettal – 2013

Professional memberships

- Egyption medical syndicate.
- Egyption Society of medical Biochemistry & molecular biology.
- Moroccan Society of bioinformatics.

Publications

- Risk Stratification of Adhesion molecules with Bronchial asthma and Allergic Rhinitis – Chest Egyption journal – 2005/2006
- NF-κB factors support the induction of NFATc1 in B lymphocytes - in progress
- NFATc1 affects Bregs' role in Imiquimod-Induced Psoriasiform skin inflammation in mice - in progress

References

- Prof. Edgar Serfling
  Molecular Pathology dep. – Institute of Pathology – Wuerzburg university – serfling.e@mail.uni-wuerzburg.de
- Prof. Adel Zalata
  Medical biochemistry department – Mansoura medicine – dradelzalata@gmail.com
- Prof. Dr. Thomas Hünig
  Institut für Virologie und Immunbiologie – Wuerzburg university – huenig@vim.uni-wuerzburg.de
- Prof. Dr. med. Matthias Goebeler
  Director of the Dermatology, Venerology und Allergiology department and clinics – Wuerzburg university – Goebeler_M1@klinik.uni-wuerzburg.de
- Prof. Mohamed Al-Shabrawey, MD, Ph.D - Oral Biology and Anatomy - Medical College of Georgia - Augusta-GA, 30912 – USA - email: malshabrawey@mcg.edu

Extracurricular activities

- FameLab Egypt 2009 – Finalist in Egypt round (2009)
- ICDL 2007
- Sun Microsystems Java2 certified programmer (2001)
- Microsoft office instructor experience (2010)
- Volunteer community service group aiming at supporting the orphans & elderly (1998 – 2000)